DOCTORAL THESIS

Novel Spent Dialysate Based Optical Methods: Towards More Universal Dose Quantification of Haemodialysis

Joosep Paats

TALLINNA TEHNIKAÜLIKOOL
TALLINN UNIVERSITY OF TECHNOLOGY
TALLINN 2025

TALLINN UNIVERSITY OF TECHNOLOGY
DOCTORAL THESIS
49/2025

Novel Spent Dialysate Based Optical Methods: Towards More Universal Dose Quantification of Haemodialysis

JOOSEP PAATS

TAL TECH PRESS

TALLINN UNIVERSITY OF TECHNOLOGY
School of Information Technologies, Department of Health Technologies
Curriculum: School of Science
This dissertation was accepted for the defence of the degree of Doctor of Philosophy in Biomedical Engineering and Medical Physics on 16/06/2025

Supervisor: Prof. Ivo Fridolin
School of Information Technologies
Tallinn University of Technology
Tallinn, Estonia

Co-supervisor: MD, PhD Merike Luman
School of Information Technologies
Tallinn University of Technology
Tallinn, Estonia

Opponents: Associate Prof. Fokko Wieringa
Artificial Kidney Lab
Universitair Medisch Centrum Utrecht
Utrecht, Netherlands

Prof. MD Aivars Pētersons
Department of Internal Diseases
Riga Stradiņš University
Riga, Latvia

Defence of the thesis: 15/07/2025, Tallinn

Declaration:
Hereby I declare that this doctoral thesis, my original investigation and achievement, submitted for the doctoral degree at Tallinn University of Technology has not been submitted for doctoral or equivalent academic degree.

Joosep Paats

---
signature

European Union
European Regional
Development Fund

Investing
in your future

ISSN 2585-6898 (publication)
ISBN 978-9916-80-328-8 (publication)
ISSN 2585-6901 (PDF)
ISBN 978-9916-80-329-5 (PDF)
DOI https://doi.org/10.23658/taltech.49/2025
Printed by EVG Print

Paats, J. (2025). *Novel Spent Dialysate Based Optical Methods: Towards More Universal Dose Quantification of Haemodialysis* [TalTech Press]. https://doi.org/10.23658/taltech.49/2025

TALLINNA TEHNIKAÜLIKOOL
DOKTORITÖÖ
49/2025

Uudsed dialüsaadipõhised optilised meetodid universaalsema hemodialüüsravi doosi määramiseks

JOOSEP PAATS

TAL TECH
KIRJASTUS

Contents

List of publications

The list of author's publications, on the basis of which the thesis has been prepared:

I **Paats, J.**, Adoberg, A., Arund, J., Fridolin, I., Lauri, K., Leis, L., Luman, M., Tanner, R. (2021). Optical Method and Biochemical Source for the Assessment of the Middle-Molecule Uremic Toxin β2-Microglobulin in Spent Dialysate. *Toxins*, *13*, 255. https://doi.org/10.3390/toxins13040255

II **Paats, J.**, Adoberg, A., Arund, J., Dhondt, A., Fernström, A., Fridolin, I., Glorieux, G., Gonzalez Parra, E., Holmar, J., Leis, L., Luman, M., Perez-Gomez, V. M., Sanchez-Ospina, D., Segelmark, M., Uhlin, F., Ortiz, A. (2023). Time-averaged concentration estimation of uraemic toxins with different removal kinetics: a novel approach based on intradialytic spent dialysate measurements. *Clinical Kidney Journal*, *16*(4), 735–744. https://doi.org/10.1093/ckj/sfac273

III **Paats, J.**, Adoberg, A., Leis, L., Arund, J., Lauri, K., Luman, M., Tanner, R., Holmar, J., Pilt, K., Fridolin, I. (2025). Intradialytic optical assessment of C-mannosyl tryptophan removal using spent dialysate. Scientific Reports, 15(1), 20052. https://doi.org/10.1038/s41598-025-01844-z

Author's contribution to the publications

Contribution to the papers in this thesis are:

I Major role in manuscript writing, sample preparation, spectrophotometric and spectrofluorometric data processing, data analysis and development of predictive model.

II Major role in manuscript writing, sample preparation, chromatographic analysis, data processing and data analysis.

III Major role in manuscript writing, sample preparation, chromatographic analysis, spectrophotometric and spectrofluorometric data processing, data analysis and development of predictive model.

Other related publications

1. **Paats, J.,** Adoberg, A., Arund, J., Dhondt, A., Fernström, A., Fridolin, I., Glorieux, G., Leis, L., Luman, M., Gonzalez-Parra, E., Perez-Gomez, V. M., Pilt, K., Sanchez-Ospina, D., Segelmark, M., Uhlin, F., & Arduan Ortiz, A. (2020). Serum Levels and Removal by Haemodialysis and Haemodiafiltration of Tryptophan-Derived Uremic Toxins in ESKD Patients. *International Journal of Molecular Sciences*, *21*(4), 1522. https://doi.org/10.3390/ijms21041522

2. Adoberg, A., **Paats, J.,** Arund, J., Dhondt, A., Fridolin, I., Glorieux, G., Holmar, J., Lauri, K., Leis, L., Luman, M., Pilt, K., Uhlin, F., & Tanner, R. (2022). Treatment with Paracetamol Can Interfere with the Intradialytic Optical Estimation in Spent Dialysate of Uric Acid but Not of Indoxyl Sulfate. *Toxins*, *14*(9), 610. https://doi.org/10.3390/toxins14090610

3. Holmar, J., Arund, J., Adoberg, A., Leis, L., Luman, M., **Paats, J.,** Pilt, K., Tanner, R., & Fridolin, I. (2023). Optical Real-Time Cardiorenal Toxin Uric Acid Measurement During Hemodialysis Using a Miniaturized Optical Sensor. *2023 45th Annual International Conference of the IEEE Engineering in Medicine & Biology Society (EMBC)*, 1–4. https://doi.org/10.1109/EMBC40787.2023.10340379

4. Leis, L., Adoberg, A., **Paats, J.,** Holmar, J., Arund, J., Karai, D., Luman, M., Pilt, K., Taklaja, P., Tanner, R., & Fridolin, I. (2023). *Hemodialysis Optical Monitoring Toward Greener Technology: A Potential for Water Saving Dialysis Treatment.* In Nordic-Baltic Conference on Biomedical Engineering and Medical Physics (pp. 162–171). https://doi.org/10.1007/978-3-031-37132-5_21

5. Arund, J., Tanner, R., Fridolin, I., & **Paats, J.** (2024). *Multiparametric optical method and device for determining uremic solutes, including uremix toxins, in biological fluids* (US20240102930A1). U.S. Patent and Trademark Office. https://worldwide.espacenet.com/publicationDetails/biblio?CC=US&NR=20241029 30A1&KC=A1&FT=D

6. **Paats, J.,** Arund, J., Pilt, K., Adoberg, A., Leis, L., Luman, M., Holmar, J., Tanner, R., & Fridolin, I. (2024). Online Uric Acid Concentration Estimation in Blood from Spent Dialysate Measurements Using an Optical Sensor. In T. Jarm, R. Šmerc, & S. Mahnič-Kalamiza (Eds.), *IFMBE Proceedings* (pp. 178–187). Springer. https://doi.org/10.1007/978-3-031-61628-0_20

Introduction

Chronic kidney disease (CKD) is a non-communicable disease that affects over 8% of the global population (Jager et al., 2019; Guo et al., 2025) and is a major driver of premature mortality (Kovesdy, 2022; A. Francis et al., 2024). In the end stage of CKD (ESKD), life-sustaining kidney replacement therapy (KRT) is required to remove uraemic solutes and excessive fluid, normally excreted by the kidneys, and thereby prevent death from uraemic syndrome (Vanholder et al., 2018, 2025). Globally, around 4 million patients are receiving KRT of which haemodialysis (HD) accounts for approximately 70% (Bello et al., 2022), with this figure reaching up to 98% in Japan (Hasegawa et al., 2025).

However, ESKD patients on chronic HD have amongst the highest mortality (Boenink et al., 2024; Flythe & Watnick, 2024) and the lowest health-related quality of life reported in patients with chronic diseases (Ranchin & Shroff, 2024; van Oevelen et al., 2024), despite advancements in HD treatment technologies and patient outcomes (Canaud et al., 2020; Bello et al., 2022). Therefore, improvements in HD treatment quality and adequacy are essential to enhance the long-term prognosis of ESKD patients.

Although it has been acknowledged and advocated that HD treatment adequacy should be more personalised and multidimensional (Chan et al., 2019; Rosner et al., 2021; Torreggiani et al., 2021), Kt/V urea remains the basic recommended measure in clinical guidelines for dialysis dose quantification regardless of insufficiently representing removal of other clinically significant uraemic solutes (Meyer et al., 2011; Vanholder, Glorieux, et al., 2015; Rosner et al., 2021). Indeed, it has been proposed to prescribe HD dose using multiple measures, including clearance of additional biomarkers such as prototypical middle molecule β-2-microglobulin (B2M), and residual kidney function as measures among other biological and clinical markers (Chan et al., 2019; Vanholder et al., 2019; Rosner et al., 2021; Torreggiani et al., 2021).

On the other hand, it has been suggested that the impact of HD treatment, independent of dialysis strategies, on different solutes removal could be best described by the actual blood concentrations of uraemic solutes over a period, i.e., time-averaged concentration (TAC) (Eloot et al., 2009, 2012), or using pre-dialysis concentrations (Rosner et al., 2021). Still, implementation of these suggestions in practice requires methods and measurement tools for evaluating and monitoring biomarker-related measures, which can be challenging due to the lack of availability of cheap, easily performed, and accurate technologies (Canaud et al., 2020; Rosner et al., 2021; Torreggiani et al., 2021).

Non-invasive spent dialysate based traditional Kt/V urea monitoring technologies are proven to be reliable, cost-effective alternatives for conventional blood sample-based analysis, using enzymatic-, conductivity- and optical sensors for spent dialysate analysis (Lindsay & Sternby, 2001; Rački et al., 2005; Uhlin et al., 2006; Kanagasundaram et al., 2008; Castellarnau et al., 2010). Furthermore, fluorescence and ultraviolet (UV) absorption measurements of spent dialysate have shown broader applicability for real-time and on-line monitoring of prototypical marker molecules of protein-bound and small water-soluble uraemic solutes, such as indoxyl sulfate (IS) and uric acid (UA) with reasonable accuracy for clinical practice (Holmar et al., 2012; Arund et al., 2024; Paats et al., 2024). Yet, a reliable optical method for middle molecules marker removal monitoring has not been developed despite attempts (Holmar et al., 2011; Lauri et al., 2020; Uhlin et al., 2015).

In addition, the preservation of residual kidney function remains of great importance for ESKD patients as it contributes to the removal of uraemic solutes and maintaining homeostasis (Davenport, 2017; Torreggiani et al., 2021). Nevertheless, monitoring of residual kidney function of ESKD patients remains challenging with the current techniques for which endogenous kidney function marker-based (such as creatinine, cystatin C, B2M, β-trace protein) equations are potential alternatives (Shafi et al., 2016; Davenport, 2017; Shafi & Levey, 2018).

C-mannosyl tryptophan (CMW) is a novel endogenous kidney function marker (Yonemura et al., 2004; Sekula et al., 2016), which levels are strongly related to glomerular filtration rate (GFR), and one of the strongest and independent markers of GFR decline and health outcomes such as death in the cohort of non-dialysis CKD patients (Steinbrenner et al., 2021, 2024; van der Burgh et al., 2024). Therefore, knowledge of CMW levels of ESKD patients could be useful for monitoring residual kidney function and evaluating the overall effectiveness of HD treatment in lowering uraemic solutes. While CMW is an intrinsic fluorophore (Horiuchi et al., 1994; Gutsche et al., 1999), no attempt has been made so far to evaluate CMW concentration in spent dialysate using optical methods and removal characteristics of CMW during HD remain unknown.

The purpose of this thesis was to explore novel spent dialysate based optical methods, which could be applied for more universal dose quantification of HD with the potential of ensuring more adequate HD treatment. In specific, the thesis focused on development of predictive models based on optical measurements of spent dialysate using a spectrophotometer and a spectrofluorometer to monitor removal of B2M as a marker of middle molecules and evaluate intradialytic levels and removal of endogenous kidney function marker CMW. Furthermore, the feasibility of estimating intradialytic serum TAC values from spent dialysate concentrations was studied.

The thesis is prepared based on three publications. **Publication I** explores the contribution of middle molecules to the optical properties of spent dialysate and provides a novel advanced optical method based on the UV absorbance and fluorescence of the spent dialysate for the evaluation of B2M haemodialytic removal and concentration in spent dialysate as a marker of middle-sized uremic retention molecules. **Publication II** studies the feasibility of estimating intradialytic TAC of clinically relevant prototypical uraemic solutes of urea, UA, IS, and B2M in blood from spent dialysate measurements using high-performance liquid chromatography (HPLC). **Publication III** evaluates levels of an endogenous novel biomarker CMW in ESKD patients' blood and spent dialysate during the dialysis for the first time and investigates the possibility of optics-based estimation of haemodialytic removal and TAC of CMW.

Abbreviations

AGEs	advanced glycation end-products
B2M	β-2-microglobulin
CKD	chronic kidney disease
CMW	C-mannosyl tryptophan
eGFR	estimated glomerular filtration rate
ESI	electrospray ionisation
ESKD	end stage kidney disease
EUTox	European Uremic Toxin Work Group
GFB	glomerular filtration barrier
GFR	glomerular filtration rate
HD	haemodialysis
HDF	haemodiafiltration
HPLC	high-performance liquid chromatography
IS	indoxyl sulfate
KDIGO	Kidney Disease: Improving Global Outcomes
KRT	kidney replacement therapy
Kt/V	dialysis dose efficacy parameter
K_{uf}	ultrafiltration coefficient
$M_{ln}D$	logarithmic mean concentration of a solute in spent dialysate
Qb	blood flow rate
Qd	dialysate flow rate
RR	reduction ratio
SC	sieving coefficient
spKt/V	single-pool Kt/V
TAC	time-averaged concentration
TDC	total dialysate collection
TRS	total removed solute
UA	uric acid
URR	urea reduction ratio
UV	ultraviolet
Vs	substitution volume

1 Kidneys and kidney replacement therapy

1.1 Kidneys

The kidneys (Latin: *renes*) are paired, bean-shaped organs located in the retroperitoneal space of the abdominal cavity. They form a functional part of the urinary system and are essential for maintaining homeostasis in the human body by controlling the volume, ionic constituent, osmolarity, and pH of plasma, as well as removing metabolic waste products and exogenous substances from plasma to urine. These functions are accomplished through regulation of the excretion rates of water, specific ions (Na^+, K^+, Ca^{2+}, Mg^{2+}, Cl^-, HCO_3^-, H^+, HPO_4^{2-} and $H_2PO_4^-$), solutes (e.g., urea and creatinine), and their relative excretion rates into urine. Additionally, kidneys are involved in the production or metabolism of hormones, such as adrenaline, angiotensin II, and vitamin D. (Stanfield, 2013).

The functional units of the kidney are the nephrons (Figure 1), where blood is purified and urine is formed based on processes of filtration, reabsorption, secretion and excretion.

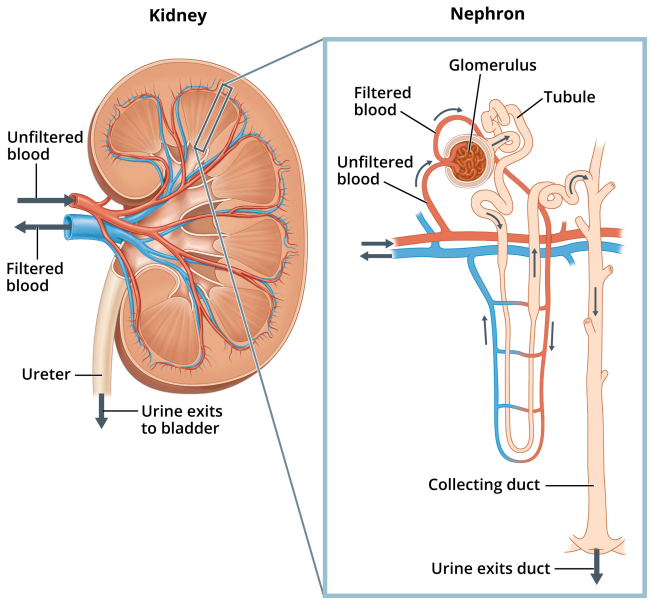

Figure 1. Kidney and nephron (National Institute of Diabetes and Digestive and Kidney Diseases, 2024).

At rest state, 20–25% of the cardiac output is directed to the kidneys. The first step of blood purification in nephrons involves glomerular filtration, which is the ultrafiltration of plasma through the glomerular capillaries to Bowman's capsule, producing glomerular filtrate, also termed primary urine. In healthy young adults, about 180 L of primary urine is produced per day, corresponding to a GFR of 125 mL/min (Julian et al., 2009; Stanfield, 2013).

The composition of glomerular filtrate resembles that of plasma, except it lacks cells and most of the plasma proteins, which is determined by the properties of the glomerular filtration barrier (GFB) between the glomerular capillaries and Bowman's capsule (Haraldsson et al., 2008; Julian et al., 2009). The GFB is structurally complex, being composed primarily of glomerular endothelial cells, glomerular basement

membrane, and podocytes, which together achieve highly size- and charge-dependent permeability-selectivity of solutes (Haraldsson et al., 2008; Menon et al., 2012). Often, the permeability of the GFB for a solute with ultrafiltration is characterised by the sieving coefficient (SC), which is the ratio of a solute concentration in the filtrate to the solute concentration in plasma water in the absence of a diffusion gradient, with values ranging from 0 (no passage) to 1 (free passage) (Ronco, 1998). Specifically, macromolecules with molecular weight of 60–70 kDa, such as albumin, are largely retained in the capillary lumen and have negligible SC close to 0, whereas molecules with molecular weight < 20 kDa, such as urea, water, electrolytes, proteins, and glycose permeate the GFB freely (Haraldsson et al., 2008; Julian et al., 2009).

Next, glomerular filtrate flows through the renal tubules, from where water and solutes are actively and passively transported to the interstitial fluid surrounding tubules and are thereafter reabsorbed into the peritubular capillaries by diffusion. This includes glucose, amino acids, proteins, and electrolytes. Additionally, some solutes diffuse or are actively and selectively secreted from the peritubular capillaries to the interstitial fluid and then through the renal tubular cells into the ultrafiltrate, in a process reverse to reabsorption (Stanfield, 2013).

The resulting fluid is directed to collecting ducts from individual nephrons where the fluid's composition is further modified similarly before being excreted as a urine, approximately 1–2 L per day (Stanfield, 2013).

1.2 Chronic kidney disease and kidney failure

With aging, GFR declines gradually over time, even in the absence of comorbidities or CKD, with a decline rate between 0.37 and 1.07 mL/min/year for healthy adults (Guppy et al., 2024). In the presence of disease, GFR decline or impairment of other kidney functions can occur at an increased rate and lead to CKD, for which diabetes mellitus, hypertension, and heart disease are the leading underlying causes (A. Francis et al., 2024).

According to the Kidney Disease: Improving Global Outcomes (KDIGO) 2024 guidelines (P. E. Stevens et al., 2024), CKD is defined as usually irreversible abnormalities of kidney structure or function, present over 3 months, with health implications. Various markers of kidney damage are used to characterise specific functions of kidneys (Tesch, 2010; Zhang & Parikh, 2019), with the most used markers for CKD determination being GFR < 60 mL/min per 1.73 m^2 of body surface area, or urine albumin-to-creatinine ratio > 30 mg/g (> 3 mg/mmol). In clinical decision-making, CKD categorisation and progression monitoring, estimated GFR (eGFR) values are mainly used (P. E. Stevens et al., 2024), calculated using equations based on endogenously produced creatinine levels in serum, rather than measuring plasma clearance of exogenous filtration markers (L. A. Stevens & Levey, 2009).

CKD is a progressive disease, and if uncontrolled, it can lead to ESKD, i.e., chronic kidney failure or stage 5 of CKD, when GFR has dropped below 15 mL/min per 1.73 m^2 of body surface area (P. E. Stevens et al., 2024). Independent of CKD, kidney failure can also occur acutely, often as a complication of another serious illness, trauma, or intoxication, which can be reversible. In either case, KRT is required for patient survival, chronically or temporarily, to remove excessive fluid and waste products.

KRT can be applied to patients in the form of kidney transplantation or blood purification via dialysis. Dialysis options include peritoneal dialysis or HD, which use the

peritoneum (a serous membrane inside the abdomen) or an artificial kidney for blood purification, respectively.

Although transplantation is the preferred modality of KRT for cost-effectiveness and patient survival, it is not available for all ESKD patients due to a shortage of organ donors or contraindications for transplantation (Abecassis et al., 2008). Therefore, HD is the most common option at the initiation of KRT (Boenink et al., 2024) and accounts for approximately 70% of all KRT and about 90% of all dialysis treatment (Bello et al., 2022). Despite being a life-sustaining therapy and an interim solution for patients awaiting a kidney transplant, HD does not replace all the kidney functions, such as metabolic, endocrine, and immune functions, or selective secretion of substances. Moreover, the simultaneous removal of all uraemic solutes remains challenging (Rosner et al., 2021). Consequently, ESKD patients, who are mainly on intermittent HD treatment, suffer from symptoms related to uraemia due to the accumulation of uraemic solutes (Vanholder et al., 2018), and the five-year survival rate after initiation of HD treatment is roughly around 40% (Boenink et al., 2024; Flythe & Watnick, 2024).

1.3 Haemodialysis

During HD treatment, the patient's blood is transported extracorporeally through an artificial dialyser, which is composed of semipermeable hollow fibres, surrounded by dialysis solution flowing counter current to the blood in the fibres (Figure 2).

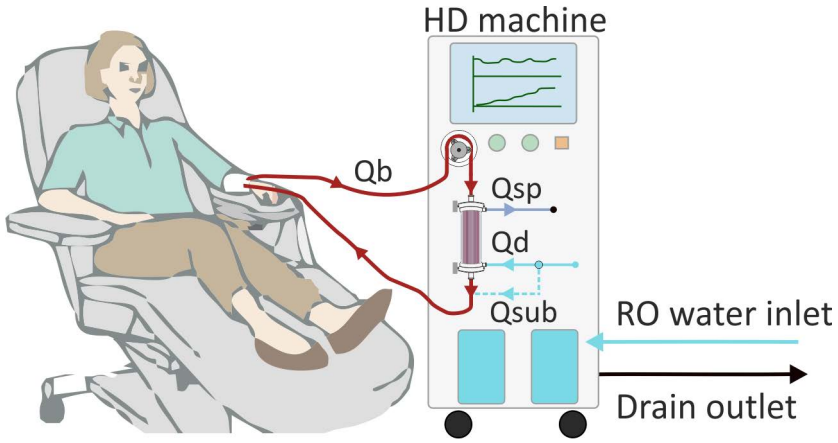

Figure 2. Haemodialyser and haemodialysis machine in post-dilution haemodiafiltration regime. In case of zero net ultrafiltration, ultrafiltration rate is equal to substitution fluid's flow rate (Qsub) and spent dialysate flow rate (Qsp) is the sum of Qsub and dialysate flow rate (Qd); with Qb marking the blood flow rate.

In maintenance HD, the movement of solutes across the semipermeable membrane of fibres is bidirectional, and the removal of substances from the bloodstream is mainly driven by mechanisms of diffusion and convection. These processes are influenced by the properties of the specific dialyser and treatment settings, such as the flow rates of blood and dialysis solution, and the transmembrane pressure of a dialyser, which are regulated with HD's machine (Azar & Canaud, 2013).

1.3.1 Dialyser membranes and haemodialysis modalities

To achieve biocompatibility and size-selective removal of substances during HD, various types of polymers are used to manufacture dialyser membranes (Tangvoraphonkchai & Davenport, 2017), with polysulfone-based membranes being the most used membranes in HD treatment (Ronco & Clark, 2018; Bowry & Chazot, 2021). Regardless of the composition, hollow fibres of modern dialysers have a relatively standard inner diameter of 180–220 µm, wall thickness of 20–50 µm and length of 20–24 cm; with thousands of fibres together resulting in a total membrane surface area in range of 1.4 to 2.2 m^2 (Clark et al., 2017; Ronco & Clark, 2018).

Apart from fibre dimensions and physiochemical properties of the membrane, the main properties of the membrane that influence the efficacy of solutes removal are morphological: mean pore size, size distribution, and porosity of the membrane. In terms of size-dependent membrane permeability, the solute is able to permeate the membrane if the mean pore size of membrane is higher than that of the specific solute (Ronco & Clark, 2018; Bowry & Chazot, 2021).

In addition to the abovementioned, other parameters can be used to characterise properties of dialyser membranes, such as the ultrafiltration coefficient (K_{uf}), the diffusive mass transfer coefficient, hydrophilicity, and sieving curves (Ronco & Clark, 2018).

Along with the development of dialyser membranes, contemporary classification of membranes has been proposed based on the water permeability, characterised by K_{uf}, and the permeability of membranes for different solutes (Ronco & Clark, 2018; García-Prieto et al., 2023). Accordingly, dialysers are categorised as low-flux (K_{uf} < 20 mL/min/mmHg) and high-flux (K_{uf} > 20 mL/min/mmHg) (Bowry et al., 2021), medium cut-off or high cut-off (Ronco & Clark, 2018), with each dialyser having different SC for solutes in terms of molecular weight (Figure 3) (Storr & Ward, 2018; García-Prieto et al., 2023). Meanwhile, medium cut-off membranes are considered to have sieving curves closest to native GFB (Storr & Ward, 2018).

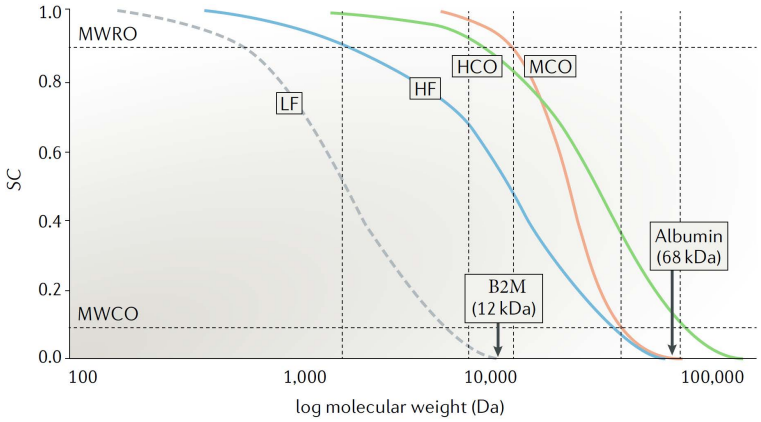

Figure 3. Classification of dialyser membranes according to the water permeability and sieving coefficients (SC) to low-flux (LF), high-flux (HF), medium cut-off (MCO) and high cut-off (HCO) membranes. The horizontal lines of molecular weight cut-off (MWCO) and molecular weight retention onset (MWRO) correspond to SC values of 0.1 and 0.9, respectively, adapted with permission from SNCSC (Ronco & Clark, 2018).

Moreover, HD modalities are distinguished based on the dominant mechanism of solutes removal as conventional HD (diffusion), hemofiltration (convection), or haemodiafiltration (HDF), which combines both diffusion and convection (Azar & Canaud, 2013). To compensate for the loss of blood volume during HDF therapy due to ultrafiltration, sterile substitution fluid, with a composition similar to the dialysis solution, is directed to the bloodstream either up- or downstream (in pre- or post-dilution HDF, respectively) of the dialyser (Canaud et al., 2024). In clinical practice, the type of modality, dialyser, and treatment settings are chosen based on the patient-specific clinical needs (Azar & Canaud, 2013).

1.3.2 Solutes removal during haemodialysis

In the case of using HDF modality and dialysers with the negligible effect of adsorption on solutes removal, such as polysulfone-based dialysers (Ficheux et al., 2011), the clearance of blood from uraemic solutes by a dialyser can be described using blood-side measurements as:

$$K_{\mathrm{Tot}} = K_{\mathrm{Diff}} + K_{\mathrm{Conv}} = \frac{Q_{\mathrm{b}} \cdot (C_{\mathrm{Bi}} - C_{\mathrm{Bo}})}{C_{\mathrm{Bi}}} + Q_{\mathrm{F}} \cdot \frac{C_{\mathrm{Bo}}}{C_{\mathrm{Bi}}}, \quad (1)$$

where K_{Tot} is the total volume of blood completely cleared of a given solute per unit time [L·min^{-1}] through a combination of diffusive K_{Diff} and convective K_{Conv} clearances; Q_{b} is the blood flow rate into the dialyser [L·min^{-1}], Q_{F} is the ultrafiltration rate [L·min^{-1}] and C_{Bi} and C_{Bo} are blood inlet and outlet concentrations of a given solute [mmol·L^{-1}], respectively (Sargent & Gotch, 1979). In other words, whole blood clearance (K_{Tot}) is the ratio of mass removal rate to the blood concentration of a solute (C_{Bi}) (Clark, 2001).

Therefore, in addition to the blood-side measurements, the clearance of a substance from blood can be quantified from spent dialysate measurements with the knowledge of C_{Bi} due to mass balance across the dialyser:

$$K_{\mathrm{D}} = \frac{Q_{\mathrm{d}} \cdot C_{\mathrm{Do}}}{C_{\mathrm{Bi}}}, \quad (2)$$

where K_{D} is dialysate-side solute clearance, Q_{d} is the flow rate of dialysate [L·min^{-1}], and C_{Do} is outlet concentrations of a given solute in spent dialysate [mmol·L^{-1}] (Clark, 2001).

As the primary mechanism of solute removal for smaller solutes is diffusion and clinically applied convection rates have a smaller effect (Ficheux et al., 2000) on the total clearance, Equation 1 can be simplified as follows (Sargent & Gotch, 1979):

$$K_{\mathrm{Tot}} = K_{\mathrm{Diff}} = \frac{Q_{\mathrm{b}} \cdot (C_{\mathrm{Bi}} - C_{\mathrm{Bo}})}{C_{\mathrm{Bi}}} = \frac{Q_{\mathrm{d}} \cdot C_{\mathrm{Do}}}{C_{\mathrm{Bi}}}. \quad (3)$$

If the dialyser remains functional during HD and treatment settings, such as K_{tot} and Q_{d} are known, the blood concentration of smaller solutes can be estimated from solutes' spent dialysate concentrations (Fridolin et al., 2002; Ficheux et al., 2010):

$$C_{\mathrm{Bi}} = \frac{Q_{\mathrm{d}}}{K_{\mathrm{Tot}}} \cdot C_{\mathrm{Do}}. \quad (4)$$

However, according to the Fick's law of diffusion (Ronco, 1998), the solute's diffusive removal depends on its diffusion coefficient, which is inversely related to the particle radius as per the Stokes–Einstein relation (Pstras et al., 2022). Consequently, diffusive clearance decreases with increasing solute molecular weight, while the contribution of convective removal to total clearance increases for larger molecules when using the HDF modality (Clark et al., 2017). Therefore, when predicting blood concentrations of larger

solutes, convective clearance should be accounted for, which depends on the ultrafiltration rate and SC of a specific dialyser for a solute (Ronco, 1998).

Although in vivo measured SC of marker molecules could be available for dialysers, these are not directly applicable in clinical settings due to membrane and blood interactions, which can cause secondary membrane formation and concentration polarisation that affects the efficacy of convective solute clearance and results in discrepancies between blood-side and dialysate-side measurements (Röckel et al., 1986; Clark, 2001; Hulko et al., 2018; Ronco & Clark, 2018; Melchior et al., 2021; Zawada et al., 2022). This increases the complexity of predicting blood concentrations of larger solutes.

Nonetheless, for smaller solutes, diffusive clearance is primarily affected by the blood flow rate, described by a parabolic function (Ronco, 1998; Ouseph & Ward, 2001; Bhimani et al., 2010; Azar & Canaud, 2013), and the clearance values for individual solutes can be precisely predicted with the knowledge of treatment settings (Ficheux et al., 2000).

Although HD treatment is conventionally prescribed for ESKD patients thrice weekly with 3-4 hours per session (Htay et al., 2021), these patients still suffer from symptoms of uraemia, caused by uraemic solutes with diverse physicochemical characteristics and dialytic removal patterns that complicates their removal with HD as efficiently as with kidneys (Vanholder et al., 2018; Rosner et al., 2021).

2 Uraemic solutes

Uraemia, uraemic syndrome in other words, can be described as a malfunctioning of different organ systems, which results from the accumulation of organic waste products that would be excreted or metabolised by the kidneys under normal conditions, leading to increased morbidity and mortality (Meyer & Hostetter, 2007; Glassock, 2008; Vanholder et al., 2018).

Several hundred different uraemic retention solutes have been identified that have elevated levels in uraemia (Duranton et al., 2012; Tanaka et al., 2015; Vanholder et al., 2018; Hu et al., 2022; European Uremic Toxins Work Group, 2025). Specifically, uraemic solutes that contribute to the uraemic syndrome and may directly exert pathophysiological effects are termed uraemic toxins based on experimental research, observational studies, and randomised controlled trials (Vanholder et al., 2018, 2025).

2.1 Classification of uraemic solutes

Historically, uraemic solutes have been subdivided into three main groups by the European Uremic Toxin Work Group (EUTox), considering their physicochemical characteristics that affect dialytic removal: small, middle, and protein-bound uraemic solutes (Vanholder et al., 2003). However, a more recent classification (Rosner et al., 2021) proposes further distinguishing subgroups of middle molecules (Table 1), as the effect of convective therapies and different HD membranes on their clearance significantly varies among these subgroups. To describe the removal of a myriad of uraemic solutes from different classes, the usage of representative biomarkers with correlation to clinical symptoms and outcomes has been proposed (Rosner et al., 2021), also considered as known markers in Publication I, II, and III of this thesis.

Table 1. Classification of uraemic solutes and selected prototype biomarkers with known toxicity.

Class of molecules	**Molecular weight**	**Prototype biomarkers**	**Molecular weight of the prototype**
Small water-soluble molecules	< 500 Da	Urea, uric acid	60 Da; 168 Da
Protein-bound molecules	Mostly < 500 Da	Indoxyl sulfate	213 Da
Middle molecules - small-middle molecules - medium-middle molecules - large-middle molecules	 (0.5–15 kDa) (> 15–25 kDa) (> 25–58 kDa).	β-2-microglobulin κ- light chain λ- light chain	11.8 kDa 22.5 kDa 45 kDa

Within the group of small water-soluble molecules, solutes' clearance in the dialyser is high and similar among solutes, primarily determined by diffusion (Eloot et al., 2005; Ponda et al., 2010). Yet, the removal kinetics of these molecules from the body can vary due to different distribution volumes, compartmentalisation patterns, and intercompartmental transport mechanisms of solutes (Eloot et al., 2005; Schneditz et al., 2009; Meyer et al., 2011). For compartmentalised solutes with slow intercompartmental

transport, the effective clearance from the patient's body may be remarkably reduced, as the mass transfer rate between compartments can limit the inflow of solute to the blood that is presented to the dialyser, even if the clearance of the solute in the dialyser is high (Schneditz & Daugirdas, 2001; Ponda et al., 2010).

For protein-bound molecules, only the unbound fraction of a solute in the blood is removable by diffusion through the dialyser, as solely the unbound, free solute, contributes to the diffusion-driving concentration gradient across the dialyser membrane (Meyer et al., 2004, 2011). Consequently, dialyser clearance of a solute is inversely related to its percentage of protein binding (Meyer et al., 2004; Eloot et al., 2016). Since the free fraction of a protein-bound solute can constitute less than 1% of the total solute in blood (Duranton et al., 2012; Daneshamouz et al., 2021), removal of protein-bound uraemic solutes is significantly hampered in comparison to small water-soluble molecules with similar size due to protein binding (Meert et al., 2008; Sirich et al., 2012; Eloot et al., 2016), posing a challenge for current KRT strategies (Sánchez-Ospina et al., 2024).

Regarding the removal of middle molecules, conventional diffusion-based HD with a low-flux dialyser is incapable of removing middle molecules as low-flux membranes are nearly impermeable for this group of uraemic solutes, unlike small water-soluble molecules (Leypoldt et al., 1999; Eknoyan et al., 2002; Meyer & Hostetter, 2007). To overcome the limitations of conventional diffusive removal of middle molecules, HD therapy with a medium cut-off membrane or convective HDF with high-flux membranes could be used, offering higher clearances of larger solutes (Armenta-Alvarez et al., 2023; García-Prieto et al., 2023; Biedunkiewicz et al., 2024). Although HDF therapy increases dialyser clearance of middle molecules, which is linearly related to ultrafiltration rate (Lornoy et al., 2000), the lowering of middle molecules' levels remains limited by intercompartmental transfer rates within the body, independent of modality (Ward et al., 2006). Therefore, it has been proposed to increase the time and frequency of KRT rather than focusing on increasing the extracorporeal clearance to lower the levels of middle molecules (Ward et al., 2006).

2.1.1 Endogenous kidney function markers

While it is important to reduce uraemic toxins levels with KRT to alleviate symptoms of uraemia (Hu et al., 2022), levels of endogenously produced uraemic retention solutes also provide valuable information for diagnosis and prognosis, as they can serves as biomarkers of kidney function, disease progression, and health outcomes (Tesch, 2010; Schanstra et al., 2015; Steinbrenner et al., 2021, 2024).

Ideally, reliable biomarkers of kidney function should be accurately measurable, indicate and identify specific types of kidney disease or kidney injury, and provide easily interpretable information applicable across various populations (Tesch, 2010). In particular, endogenous solutes should have a constant production rate, and the solutes' levels should not be influenced by non-kidney function determinants, such as diet, muscle mass, inflammation, medication, and extrarenal elimination prior to dialysis treatment (Levey et al., 2014; Khader et al., 2025). Moreover, endogenous solutes should be metabolically and chemically stable in biofluids over time to accurately determine their levels (Gao et al., 2021; Karger et al., 2021), and correlate the biomarkers levels with residual kidney function in CKD patients prior to ESKD (Levey et al., 2014; Wasung et al., 2015). In addition, endogenous solute levels can be correlated with total kidney function for dialysis patients, which also accounts for the function provided by KRT, with the knowledge of solute's dialysis clearance and the solute's generation rate (Daugirdas et al., 2015; Shafi & Levey, 2018; Tattersall, 2018).

In routine clinical practice, the most established endogenous kidney function biomarker is creatinine, which is used to estimate GFR employing serum creatinine-based equations, additionally including demographic and clinical variables as surrogates for non-GFR determinants (Levey et al., 2014; Wasung et al., 2015; P. E. Stevens et al., 2024). To overcome limitations of creatinine-based equations and improve accuracy of estimations, use of alternative kidney function biomarkers has been explored, such as urea, cystatin C, B2M, β-trace protein – either in combination with creatinine or independently (Levey et al., 2014; Lopez-Giacoman & Madero, 2015; Wasung et al., 2015; Breit & Weinberger, 2016; Coresh et al., 2019; Thompson & Joy, 2022).

Still, the search continues to identify novel, reliable endogenous biomarkers that are less influenced by non-kidney function determinants to accurately evaluate kidney function and predict health outcomes (Sekula et al., 2016; Shafi et al., 2016; van der Burgh et al., 2024).

In recent large population metabolomic studies, CMW, also known as C-gylcosyltryptophan, has emerged as a metabolite, which concentration in serum and urine is the most strongly and independently correlated with CKD risk, progression and patients' death (Steinbrenner et al., 2021, 2024; van der Burgh et al., 2024) among thousands of other studied metabolites. Moreover, serum concentration of CMW is strongly correlated with eGFR in different stages of CKD patients (Niewczas et al., 2014; Sekula et al., 2016; Denburg et al., 2021; Steinbrenner et al., 2021; van der Burgh et al., 2024); with CMW being even more strongly correlated to measured GFR compared to the established serum creatinine-based eGFR (Sekula et al., 2016; Takahira et al., 2001; Yonemura et al., 2004).

In detail, monomeric CMW, with a molecular weight of 366 Da, is a degradation of C-mannosylatated proteins, a metabolite arising from the only known form of protein C-linked glycosylation in humans (Furmanek & Hofsteenge, 2000; Schjoldager et al., 2020; Minakata et al., 2021). CMW is thought to be not further catabolised in the body (Minakata et al., 2020, 2021) and be metabolically stable and resistant to hydrolysis due to the C-C bond between single α-mannose and a tryptophan residue (Hossain et al., 2018). As the clearance of CMW from the blood is similar to that of freely filtered inulin (Takahira et al., 2001), a decline in GFR leads to reduced CMW excretion from the body via urine (Horiuchi et al., 1994; Gutsche et al., 1999), resulting in exponentially rising serum concentration of CMW (Takahira et al., 2001; Morita et al., 2021). Although CMW possesses many properties of an ideal kidney function marker, chromatographical methods and mass spectrometry remain the only known methods of quantification of CMW in biofluids, which, while accurate, are costly and time-consuming.

2.2 Analysis methods of uraemic solutes

In routine clinical practice, fast, cost-effective, and standardised methods should be employed to ensure reliable and reproducible quantification of uraemic solutes' concentration in biofluids.

A variety of analytical techniques are available and used to identify and quantify uraemic solutes, such as enzymatic, colorimetric, immunological methods, chemiluminescence, nephelometry, and gel electrophoresis or chromatography coupled with ultraviolet or fluorescence spectroscopy, electrochemical detectors, mass spectrometry or nuclear magnetic resonance (Duranton et al., 2012; Vanholder, Boelaert, et al., 2015; Karger et al., 2021; Narimani et al., 2021).

In clinical chemistry, rapid standardised colorimetric or enzymatic methods are primarily used to determine small water-soluble solutes, such as biomarkers of creatinine, urea and UA (Elin et al., 1982; P. S. Francis et al., 2002; Karger et al., 2021; Narimani et al., 2021). As colorimetric methods can be influenced by other endogenous substances, such as the Jaffe reaction, and enzymatic methods require specific reagents to quantify each substance, HPLC has been proven to be a more versatile technique in research for simultaneous and accurate quantification of different uraemic solutes (Arund et al., 2012; Salazar, 2014; J. Zhao, 2015).

For protein-bound solutes, HPLC remains the most used technique, as it has the highest selectivity and sensitivity for quantifying the protein-bound solutes' levels. (Duranton et al., 2012; Fernandes et al., 2023; Shafiee et al., 2024). Besides, less time-consuming and inexpensive enzymatic- and immunoassays have been developed for routine analysis of the total concentration of some protein-bound uraemic toxins, such as prototype biomarker IS, yet with inferior analytical performance (Duranton et al., 2012; Fushimi et al., 2019; Abe et al., 2021; Duan et al., 2022; Shafiee et al., 2024). Still, before HPLC analysis of blood samples, additional sample preparation is required to determine the concentration of unbound or total fraction of protein-bound solutes (Vanholder et al., 1992).

For total concentration determination, solutes can be displaced from blood proteins in the sample by heat denaturation of proteins or by protein precipitation by applying an organic solvent, acid, or salt to the sample (Poesen et al., 2015; van Gelder et al., 2020; Shafiee et al., 2024). While equilibrium dialysis is the gold standard method for the separation of the unbound fraction of the solute, ultrafiltration of the sample through a protein-impermeable filter can provide results with similar accuracy for most solutes, including IS (Fabresse et al., 2020). Therefore, ultrafiltration remains the most used method in the analysis of the free concentration of protein-bound uraemic toxins due to the simpler and faster sample preparation procedure (Lee et al., 2010; Eloot et al., 2016; Fabresse et al., 2020; Fernandes et al., 2023).

Considering HPLC's accuracy and capacity for simultaneous determination of uraemic solutes (Arund et al., 2012, 2016; Boelaert et al., 2013; J. Zhao, 2015; Poesen et al., 2015; van Gelder et al., 2020; Fernandes et al., 2023), reversed-phase HPLC was chosen as a method of choice for determining the uraemic solutes concentration of UA, IS, and CMW in Publications I, II, and III of this thesis. Moreover, for total concentration determination of protein-bound IS, serum samples were heated to denature proteins (Fagugli et al., 2002; Boelaert et al., 2013) as the most efficient deproteinisation method (Vanholder et al., 1992); and ultrafiltration was used to remove proteins from the samples prior to the analysis of small water-soluble uraemic solutes, such as UA and CMW as described earlier (Eloot et al., 2016).

Middle molecules related to CKD, such as B2M, parathyroid hormone and cystatin-C, are routinely measured with immunoassays, turbidimetry, and nephelometry that allow accurate detection of individual molecules (Duranton et al., 2012; Karger et al., 2021; Sivanathan et al., 2022). Whereas, HPLC analysis or capillary electrophoresis coupled with mass spectrometry are more versatile tools for simultaneous and accurate analysis of proteins based on the mass-to-charge ratio of specific ions of proteins or their fragments; though this can require additional sample preparation prior to analysis, such as derivatisation or digestion of proteins with proteases (Kolch et al., 2005; Merchant, 2010; Mischak et al., 2015; Yang et al., 2022; Birhanu, 2023).

Despite their accuracy, time-consuming analyses and expensive laboratory equipment limit the widespread application of mass spectrometry- and HPLC-based analyses for routine measurement of uraemic solutes in clinical practice.

3 Haemodialysis treatment adequacy

Historically, the adequacy of HD treatment has been estimated based on blood urea concentrations employing different measures such as, TAC, urea reduction ratio (URR), and Kt/V, with the Kt/V urea being currently the most precise, tested, and applied measure to quantify the delivered dialysis dose (Lowrie et al., 1981; Gotch & Sargent, 1985; Owen et al., 1993; Lopot et al., 2004; Daugirdas et al., 2015; Steyaert et al., 2019).

Mathematically, URR is expressed as the reduction ratio (RR) of blood urea concentration during HD treatment:

$$RR = \frac{C_0 - C_t}{C_0} \times 100\ \%, \tag{5}$$

where C_0 and C_t are pre- and post-dialysis urea blood concentrations [mmol/L], respectively (Owen et al., 1993). Although URR is related to the patients' mortality and serves as a straightforward dialysis adequacy measure (Owen et al., 1993), its use to quantify dialysis dose has been discouraged because the corresponding Kt/V values observed at given URR can vary broadly in individual patients, leading to inaccuracies (Daugirdas, 1995; Sherman et al., 1995), especially when URR exceeds 65% (Sherman et al., 1995).

In the case of using the simplified form of Kt/V formula, which assumes no urea generation during dialysis and a fixed urea distribution volume in the body, Kt/V can be calculated as:

$$\frac{Kt}{V} = -\ln\frac{C_t}{C_0}, \tag{6}$$

where K is dialyser clearance of urea [mL/min], t is duration of dialysis [min], V is urea distribution volume in patient [mL], and C_0 and C_t are pre- and post-dialysis urea blood concentrations [mmol/L], respectively (Gotch & Sargent, 1985).

Whereas most commonly, single-pool Kt/V (spKt/V), which takes urea generation and urea distribution volume changes into account, is used as a standard tool to evaluate the delivered dose of HD treatment by solving the second-generation Daugirdas formula, assuming urea is distributed in a single compartment (Daugirdas, 1993):

$$\frac{spKt}{V} = -\ln\left(\frac{C_t}{C_0} - 0.008\left(\frac{t}{60}\right)\right) + \left(4 - 3.5\frac{C_t}{C_0}\right)\frac{UF}{W}, \tag{7}$$

where UF stands for net ultrafiltration [kg], and W is dry body weight of the patient [kg] (Daugirdas, 1993). Using the measure of sp/KtV, current clinical guidelines recommend achieving a minimum delivered dialysis dose of 1.2 per session for the conventional intermittent thrice weekly HD to be considered adequate (Tattersall et al., 2007; Daugirdas et al., 2015; Watanabe et al., 2015; Ashby et al., 2019). Moreover, other forms of Kt/V, such as equilibrated Kt/V and standardised Kt/V have been developed to account for treatment frequency and multicompartmental removal kinetics (Vanholder et al., 2019).

Although Kt/V urea is clinically recognised measure that is used for evaluating efficacy of dialysis treatment, it has several limitations (Meyer et al., 2011; Daugirdas et al., 2015; Vanholder et al., 2019).

Indeed, urea is the most abundantly accumulating uraemic solute in ESKD and serves a marker of small water-soluble uraemic solutes, yet urea itself is relatively nontoxic (Depner, 2001; Vanholder, Glorieux, et al., 2015; Weiner et al., 2015). As the transport

of urea across the erythrocyte membranes is facilitated by transporters (D. Zhao et al., 2007), haemodialytic removal of urea is not dependent on haematocrit, and the general compartmentalisation effects are modest for urea, even in comparison with other small water-soluble solutes, which clearance is limited to plasma flow and intercompartmental transfer rates (Eloot et al., 2005; Schneditz et al., 2009; Ponda et al., 2010; Meyer et al., 2011).

As Kt/V urea does not represent removal kinetics of other solutes (Meert et al., 2008; Sirich et al., 2012; Eloot et al., 2016; Biedunkiewicz et al., 2024), it is acknowledged that efficacy and adequacy of HD cannot be evaluated using urea as a single biomarker, and alternative indices have been proposed to be included to optimise dialysis treatment, based on biomarkers, which are related to uraemic toxicity and clinical outcomes (Meyer et al., 2011; Daugirdas et al., 2015; Chan et al., 2019; Vanholder et al., 2019; Rosner et al., 2021; Torreggiani et al., 2021).

The time-averaged concentration (TAC) concept of individual solutes has been suggested by Eloot et al. to be the most useful marker to evaluate the effect of HD treatment on solute levels over time, independent of the size and removal characteristics of solutes, dialysis strategies, and schedules (Lopot & Válek, 1988; Lopot et al., 2004; Kanagasundaram et al., 2008; Eloot et al., 2009, 2012). Historically TAC of urea was used as a dialysis adequacy measure, being related to patients' hospitalisation rates and symptoms, prior to the concept of Kt/V, which was proved to be more strongly related to patients' mortality based on epidemiological data (Gotch & Sargent, 1985; Vanholder et al., 2019). However, as there were no other molecules, which levels were strongly correlated to clinical symptoms and outcomes, and the TAC calculations were cumbersome, the TAC concept was abandoned at that time (Lopot et al., 2004; Vanholder et al., 2019). TAC enables the evaluation of the combined effect of HD treatment, residual kidney function, and solutes generation rate on solutes levels, as TAC depends on the net removal and generation of solutes (Lopot & Válek, 1988).

Mathematically, TAC of a solute is expressed as:

$$TAC = \frac{1}{T_{\mathrm{TOT}}} \int_0^{T_{\mathrm{TOT}}} \mathrm{c(t)}\,\mathrm{dt}, \tag{8}$$

where c(t) is the concentration of a solute in patient's blood at specific time point and T_{TOT} is the total time over the period, which can be intradialytic or interdialytic period; ergo, TAC describes average concentration of a solute over a specific period (Lopot & Válek, 1988).

Considering that blood concentration of a solute is proportional to the solute's spent dialysate concentration (Equation 4), intradialytic TAC can be evaluated from the average concentration of a solute in the spent dialysate during the dialysis session, assuming negligible effect of solute's generation and residual kidney function on the change of blood levels during dialysis.

With the knowledge of the total volume of spent dialysate or spent dialysate flow rate and treatment time, the average spent dialysate concentration can be used to calculate total removed solute (TRS) as in case of total dialysate collection (TDC):

$$TRS = D_{\mathrm{T}} \cdot W_{\mathrm{T}}, \tag{9}$$

where D_{T} marks the concentration of uraemic solute in the TDC tank and W_{T} is the weight of the spent dialysate in the TDC tank, considering the density of spent dialysate is close to 1.008 kg/L (Eloot et al., 2007).

In other words, intradialytic TAC, dialyser clearance *K* and treatment time *t* are the main determinants of the TRS, i.e., net removal of solute, during HD treatment (Kanagasundaram et al., 2008; Ficheux et al., 2010; Lim et al., 2018):

$$TRS = K \cdot TAC \cdot t. \quad (10)$$

Therefore, intradialytic TAC can also be estimated from non-invasive spent dialysate measurements without the need for blood sampling (Kanagasundaram et al., 2008; Ficheux et al., 2010; Lim et al., 2018), similar to parameters of RR and Kt/V, which reflect fractional removal of urea from the body (Lindsay & Sternby, 2001; Rački et al., 2005; Uhlin et al., 2006; Castellarnau et al., 2010). In specific, TAC could be used to objectively evaluate the efficacy of newer convective treatment strategies or medium- and high-cut of membranes on lowering the levels of prototypical uraemic solutes that are related to clinical outcomes and mortality, including B2M (Watanabe et al., 2015) and IS (Vanholder et al., 2014; Fan et al., 2019).

4 Optical monitoring of dialysis adequacy

Spent dialysate based HD adequacy monitoring has proven to be a reliable, non-invasive alternative to traditional blood sample-based measure Kt/V urea evaluation, using enzymatic-, conductivity- and optical sensors for spent dialysate analysis (Lindsay & Sternby, 2001; Rački et al., 2005; Uhlin et al., 2006; Kanagasundaram et al., 2008; Castellarnau et al., 2010), and offers a direct method for dialysis quantification (Canaud et al., 1999). Optical sensors have been integrated into commercially available HD machines manufactured by B-Braun (Melsungen, Germany), Nikkisio (Tokyo, Japan), and conductivity-sensors to the machines of Fresenius Medical Care (Bad Homburg vor der Höhe), which provide real-time feedback of urea removal online (Petitclerc & Ridel, 2021).

4.1 Optical properties of spent dialysate

In regards to optical properties, spent dialysate has been considered to be transparent and weakly light-scattering medium, similarly to biofluids of vitreous humour and aqueous humour of the front chamber of the eye, containing chromophoric and fluorophoric uraemic solutes (Tuchin, 2007; Uhlin & Fridolin, 2023). In such a medium, the light that has been transmitted to the medium is either reflected, absorbed, or propagated through the medium without further interactions, rendering the effect of scattering insignificant on the attenuation of light intensity. If the molecules in the medium absorb the light, the absorbed optical energy may lead to chemical reactions, intramolecular energy transfer, be reemitted as light, or dissipate as heat when the excited molecule transitions back to the ground state. (Welch & van Gemert, 2011)

4.2 Bouguer-Beer-Lambert law and fluorescence intensity of spent dialysate

Considering that the attenuation of light in spent dialysate mainly arises from light absorption due to chromophores, the solutes are stable, and the chromophores concentration and light intensity are not extremely high, the Bouguer-Lambert-Beer law can be used to describe the loss of intensity of monochromatic and collimated light that has been transmitted through a spent dialysate (Uhlin & Fridolin, 2023).

According to the Bouguer-Beer-Lambert law, the loss of the intensity of light transmitted through a solution containing a single chromophore, quantified as absorbance A(λ), is the product of the concentration of a solute c [M], optical path length d [cm] and molar extinction coefficient of a solute ε [cm^{-1} M^{-1}] at a wavelength of λ:

$$A(\lambda) = log\frac{I_0}{I} = \varepsilon(\lambda) \cdot c \cdot d, \tag{11}$$

where I_0 is the initial intensity of incident light transmitted to the solution [W], and I denotes the light intensity after passing through the solution [W]. Thus, the Bouguer-Beer-Lambert law correlates a chromophore's concentration with the solution's absorbance at a certain wavelength. Whereas the molar extinction coefficient and solution's absorbance depend on the wavelength of light. (Tissue, 2012; Mayerhöfer et al., 2020; Uhlin & Fridolin, 2023)

When multiple chromophores are present in the solution, the total absorbance at a given wavelength is the sum effect of all chromophores in the solution, and Equation 11 can be written as:

$$A(\lambda) = log\frac{I_0}{I} = (\varepsilon_1(\lambda) \cdot c_1 + \varepsilon_2(\lambda) \cdot c_2 + \cdots + \varepsilon_n(\lambda) \cdot c_n)d\,, \tag{12}$$

where the subscripts refer to the molar absorption coefficient and concentration of individual chromophores (Tissue, 2012; Uhlin & Fridolin, 2023).

If part of the photon's energy, absorbed by a chromophore, is subsequently reemitted as a photon while the excited chromophore relaxes to a lower energy state after being excited with light, the molecule is termed fluorophore. Generally, the emitted photon has lower energy than the absorbed photon, i.e., emitted light has a longer wavelength than excitation light (Lakowicz, 2006; Welch & van Gemert, 2011).

For a dilute solution containing a single fluorophore, fluorescence intensity I_F [W] at the excitation and emission wavelengths pairs (λ_{ex} and λ_{em}) is a function of the quantum yield of a fluorophore φ at λ_{em}, concentration of a fluorophore c [M], molar extinction coefficient of a fluorophore ε [cm^{-1} M^{-1}], optical path length d [cm] and intensity of the excitation light I_0 [W] at λ_{ex}, expressed mathematically as (Welch & van Gemert, 2011):

$$I_F(\lambda_{\mathrm{ex}}, \lambda_{\mathrm{em}}) = \varphi(\lambda_{\mathrm{em}}) \cdot c \cdot \varepsilon(\lambda_{\mathrm{ex}}) \cdot d \cdot I_0(\lambda_{\mathrm{ex}}) \quad (13).$$

Since fluorescence commonly occurs from molecules with abundant delocalised electrons, such as aromatic compounds, and given that the shape of the emission spectrum is dependent on the fluorophore's chemical structure and independent of excitation wavelength, fluorescence spectroscopy is considered to be more specific and sensitive in comparison to the light absorption spectroscopy for quantification of solutes (Lakowicz, 2006; Welch & van Gemert, 2011). Still, the fluorophore's local environment and properties of the solution, such as temperature, polarity, pH, and interactions with other molecules, can influence the quantum yield and emission maxima of the fluorophores (Lakowicz, 2006; Albani, 2007; Welch & van Gemert, 2011; McKay et al., 2018). Though, the composition and quality of dialysis solution are strictly controlled, and in spent dialysate the aforementioned parameters vary in a small physiological range (Azar & Canaud, 2013; Locatelli et al., 2015).

Moreover, light attenuation in spent dialysate due to other chromophores (Arund et al., 2012) must be accounted for to ensure a linear response between the fluorescence intensity and fluorophore's concentration, as both excitation and emission light are attenuated in solutions with absorbance values > 0.05 at corresponding wavelengths due to inner filter effect, which distorts apparent quantum yield (Lakowicz, 2006). The inner filter effect can be compensated mathematically by considering the solution's absorbance or measurement results with different cuvette cell configurations (Lakowicz, 2006; Welch & van Gemert, 2011; Fonin et al., 2014; Wang et al., 2017; Kumar Panigrahi & Kumar Mishra, 2019).

However, spent dialysate contains various endogenous fluorophores, often with overlapping emission or excitation spectra, and the measurable fluorescence intensity at specific excitation and emission wavelengths results from the combined effect of these fluorophores and reflects their concentrations (Arund et al., 2016; Kalle et al., 2016, 2019; Meibaum et al., 2020). For example, fluorescence at excitation wavelength of 280 nm and emission at 360 nm is predominantly attributable to protein-bound metabolites of tryptophan such as IS (Swan et al., 1983; Barnett & Veening, 1985; Arund et al., 2016; Meibaum et al., 2020), and at excitation of 320 nm fluorescence intensity is related to metabolites of B6 vitamin such as 4-pyridoxic acid (Kalle et al., 2016) or the glycation end product pentosidine (Kalle et al., 2019). At the same time, light attenuation in spent dialysate mainly arises from light-absorbing small water-soluble chromophores, such as UA, creatinine, and hippuric acid (Lauri et al., 2010; Arund et al., 2012; Donadio et al., 2013).

To overcome the limitations of measuring the fluorescence of multi-fluorophoric samples, measurements at multiple excitation and emission wavelengths can be performed (Welch & van Gemert, 2011). This approach enables identification of the intrinsic fluorescence of individual fluorophores and quantify fluorophore's concentration in spent dialysate using predictive models (Kalle et al., 2019; Lauri et al., 2020; Arund et al., 2024). Similarly, light absorption could be measured at multiple wavelengths to improve the accuracy of chromophores quantification in spent dialysate (Holmar et al., 2012; Donadio et al., 2013; Uhlin & Fridolin, 2023; Paats et al., 2024).

By performing multi-wavelength measurements and using predictive models, it has been possible to achieve clinically acceptable accuracy for quantifying absolute concentration of prototypical marker molecules, such as IS or UA (Holmar et al., 2012; Arund et al., 2024; Paats et al., 2024), despite possible interferences of other chromophores and fluorophores, including metabolites and medications (Arund et al., 2012; Adoberg et al., 2022). As a result, clinical parameters, such as TRS, RR, and Kt/V, could be evaluated from optical signals of spent dialysate. Furthermore, it is possible to assess the relative removal of substances during HD even when the substance itself does not substantially contribute to the optical properties of spent dialysate but has similar removal characteristics in comparison to the chromophores or fluorophores that form the optical signal, as is the case for urea, electrolytes etc. (Uhlin & Fridolin, 2023).

Aim of the study

The purpose of this thesis was to explore novel spent dialysate based optical methods, which could be applied for more universal dose quantification of HD with the potential of ensuring more adequate HD treatment.

The specific aims of the studies were:

- to evaluate the contribution of middle molecules to the optical signals of spent dialysate;
- to develop a novel advanced method based on the optical signals of spent dialysate for monitoring the intradialytic removal of B2M as the prototypical marker of middle molecules;
- to evaluate the feasibility of estimating intradialytic serum TAC for prototypical marker molecules of urea, UA, IS, and B2M from their spent dialysate concentrations using HPLC;
- to characterise the levels of endogenous kidney function marker CMW in ESKD patients' blood and spent dialysate and its intradialytic removal;
- to develop an optical method for estimating intradialytic levels and removal of CMW.

By concentrating on these specific objectives, this thesis seeks to validate the potential of spent dialysate based optical methods for more universal dose quantification of HD, which could be used to personalise HD treatment and improve adequacy.

5 Experimental methods

5.1 Clinical studies

All clinical studies on which this dissertation is based were conducted in accordance with the principles of the Declaration of Helsinki. Prior to performing studies, the study protocols were approved by local ethical committees: Tallinn Medical Research Ethics Committee at the National Institute for Health Development, Estonia, decision no. 2205 (27.12.2017), Linköping Regional Medical Research Ethics Committee, Linköping, Sweden, decision no. 2017/593-31 (17.01.2018); Commissie voor Medische Ethiek at Ghent University Hospital, Ghent, Belgium, decision no. B670201938627 (15.02.2019); Fundación Jiménez Díaz Clinical Research Ethics Committee, Madrid, Spain, decisions (no. 9/18, 8.05.2018) and (no. 13/18, 10.7.2018).

Clinically stable patients on chronic thrice-weekly HD treatment with vascular access capable of blood flow over 300 mL/min were enrolled in the studies from North Estonia Medical Centre (Publication I; II; III) in Tallinn, Estonia (22 patients); Linköping University Hospital (Publication II) in Linköping, Sweden, (21 patients); Ghent University Hospital (Publication II) in Ghent, Belgium (15 patients) and from Fundación Jiménez Díaz University Hospital Health Research Institute (Publication II) in Madrid, Spain (20 patients). A detailed overview of patients' clinical characteristics has been presented in Supplementary Table 1 of Publication II.

Each patient was monitored during four different midweek HD sessions with predefined treatment settings, which varied the haemodialytic removal efficacy of uraemic solutes. Modifiable treatment settings included blood flow rate, dialysis solution flow rate, substitution volume, and effective membrane area of dialyser. For HD procedures, Fresenius Medical Care HD machines were used (Fresenius Medical Care, Bad Homburg v. d. Höfe, Germany). All patients, excluding one patient, were dialyzed with polysulfone membrane dialysers as specified in Supplementary Table 2 of Publication II, containing low-flux and high-flux dialysers.

To evaluate the efficacy of different HD treatments, blood and spent dialysate samples were collected for analyses from arterial blood lines or from the drain tube outlet of HD machine, respectively (Figure 8 in Appendix 1). Concentration of uraemic solutes was determined in the collected samples with HPLC or clinical chemistry laboratory analyses, based on which HD efficacy parameters were calculated.

Table 2 provides an overview of the patients' characteristics, applied treatment settings, analysed samples, and uraemic solutes in the conducted studies.

Table 2. Overview of the main patients' characteristics, applied treatment settings, analysed samples, and uraemic solutes in the conducted studies.

	Publication I	**Publication II**	**Publication III**
Patient cohort size	22	78	22
Gender, male/female	17/5	61/17	17/5
Age, mean ± SD	55 ± 17	63 ± 16	55 ± 17
Number of treatment sessions (modality)	88 (66 HDF, 22 HD)	312 (234 HDF; 78 HD)	88 (66 HDF, 22 HD)
Dialysis's machine model	Fresenius 5008	Fresenius 4008 Fresenius 5008 Fresenius 6008	Fresenius 5008
Treatment time, min	240	240	240
Qb*, mL/min	300.8 ± 12.7; 200 ± 0; 299.7 ± 1.0; 364.2 ± 27.1	316 (297-347); 199 (199-200); 297 (296-300); 375(356-395)	296 (295–297) 199 (198–199) 297 (296–298) 368 (356–377)
Qd*, mL/min	470.8 ± 105.4; 300 ± 0; 799.8 ± 0.9; 800.0 ± 0.0	496 (411-500); 300 (298-300); 800 (796-800); 800 (795-800)	359 (355–493); 297 (297–298); 789 (788–795); 791 (788–796)
Vs*, L	21.1 ± 3.1; 0; 15.3 ± 1.4; 25.3 ± 2.8	22.5 (19.6-24.6) 0; 14.9 (14.8-15.2); 25.2 (22.5-27.3)	22.0 (20.0–23.0); 0; 14.9 (14.9–15); 25.2 (23–27.9);
Blood sampling times	NIL	pre- and post-dialysis	pre- and post-dialysis; 30 min post-dialysis
Dialysate sampling times	7; 60; 120; 180; 240 min after the start of session; TDC	7; 240 min after the start of session; TDC	7; 60; 120; 180; 240 min after the start of session; TDC
Analysed uraemic solutes	B2M	Urea, UA, IS, B2M	Urea, CMW
HD efficacy parameters	RR, TRS	TAC, TRS	RR, TRS, TAC

*Given as mean (±SD) or median (interquartile range).

5.2 HPLC analysis (Publication II, III)

All the collected blood and spent dialysate samples were subjected to reversed-phase HPLC analyses to determine concentration of UA and IS (Publication II), and CMW (Publication III) in the samples.

5.2.1 Sample preparation

Prior to HPLC analysis, serum fraction was separated from blood samples after sample drawing. The blood samples were allowed to clot for 30 min in Becton Dickinson Vacutainer SST II Advance tubes (Franklin Lakes, NJ, USA) and thereafter centrifuged for 20 min at 3000 g immediately. The resulting supernatant (serum) was separated from the blood cells and subjected to further preparation and analysis.

To determine the total IS concentration in serum (Publication II), serum samples were first deproteinised by heat denaturation (Vanholder et al., 1992; Boelaert et al., 2013). For this purpose, serum samples were diluted 1:3 with normal saline solution in Eppendorf Protein LoBind 1.5 mL tubes (Hamburg, Germany), homogenised by vortexing at 1500 rpm for 1 min, and heated at 95 °C for 30 min to denature proteins and thereby displace the protein-bound fraction of IS from proteins. Next, the samples were rapidly cooled to 4°C and centrifuged afterwards at 21.900 g for 10 min to precipitate denaturised proteins. The resulting supernatant in the volume of 400 µL was purified of remaining denaturised proteins by centrifugal ultrafiltration at 14.000 g for 3 h at 37 °C using Sartorius Vivacon 30 kDa cut-off filters (Göttingen, Germany).

To determine the concentration of protein non-bound UA (Publication II) and CMW Publication III) in serum samples, 400 µL of untreated serum was similarly filtrated through Sartorius Vivacon 30 kDa cut-off filters as described above to remove proteins from the samples prior to HPLC analysis for preventing HPLC column clogging.

The resulting ultrafiltrates of serum samples were acidified with 1 µL of formic acid (Sigma-Adrich, St. Louis, MO, USA) to stabilise UA to an undissociated form and improve the separation of compounds. In order to determine the concentration of analytes in spent dialysate samples (Publication II, III), 10 µL of formic acid was added to each spent dialysate sample of 5 mL for the same purpose without additional sample pretreatment prior to HPLC analysis.

5.2.2 HPLC system and analysis conditions

HPLC analysis was conducted with the Ultimate 3000 Series HPLC system from Dionex, a division of Thermo Scientific (Sunnyvale, CA, USA), consisting of a quaternary gradient pump unit, a thermostated autosampler, a column oven, a diode array spectrophotometric detector, and a fluorescence detector. Mass spectra (Publication III) were analysed with quadrupole time-of-flight mass spectrometer micrOTOF-Q II with an electrospray ionisation (ESI) source (Bruker, Billerica, USA) coupled to the HPLC system.

The stationary phase comprised two continuous columns of Poroshell 120 C18 2.7 µm 4.6 x 150 mm with a security guard Poroshell 120 C18 2.7 µm 4.6 x 5 mm from Agilent Instruments (Santa Clara, CA, United States) maintained at 40 °C. Chromatographic separation was achieved by applying a three-step gradient elution program (Table 3) developed earlier (Arund et al., 2016) at a flow rate of 0.6 mL/min. The mobile phase was made of a mixture of 0.05 M formic acid adjusted to pH 4.25 with ammonium hydroxide (A), and a mixture of HPLC grade methanol and HPLC-S grade acetonitrile in the volume ratio of 9:1, both from Honeywell (Charlotte, NC, USA), with 0.05 M ammonium formate salt (B).

Table 3. HPLC gradient program (Arund et al., 2016).

Step	Time, min	Solvent A, %	Solvent B, %	Curve type
0	0	99	1	
1	6	99	1	linear
2	39	10	90	concave upward
3	15	10	90	linear

The compounds were detected based on recorded signals of fluorescence at excitation 280 nm and emission at 360 nm (IS and CMW) and UV light absorption at 280 nm (UA). Chromatographic data were processed with Chromeleon 7.1 software by Thermo Scientific (Waltham, MA, USA). For HPLC system calibration, aqueous calibration standard solutions were analysed, made of reference solutions with purity > 98%: CMW from Toronto Research Chemicals Inc (Toronto, Ontario, Canada), IS and UA from Sigma-Aldrich (St. Louis, MO, USA). Compounds' concentrations in samples were subsequently quantified based on the peak areas using calibration curves.

To validate the chromatographic peak of CMW of serum and the spent dialysate samples (Publication III), part of the post-column eluate flow was directed to the mass spectrometer using a flow splitter. Mass spectra were registered in negative ion mode with the following operating conditions: mass range of m/z 50–700; ion source temperature of 200 °C, ESI voltage of 4.5 kV, ESI nebulisation gas flow of 8.0 L/min, drying gas flow of 1.2 bar, detector voltage of 2.03 kV, acquisition rate of 1 Hz. For validation of the CMW peak, retention time and fluorescence spectra of samples were compared with those of the standard solution of CMW and confirmed by the MS/MS fragment ion mass of the precursor ion of m/z^{-1} 365.14 ± 0.03, specific to CMW (Gutsche et al., 1999; Yamamoto et al., 2019). Data were acquired with Compass HyStar (version 3.2) and analysed with Compass DataAnalysis (version 4.0 SP1) software, both from Bruker (Billerica, USA).

5.3 Clinical laboratory analysis (Publication I, II, III)

In Publication I, concentration of B2M in spent dialysate samples was determined in clinical chemistry laboratory (SYNLAB Eesti OÜ, Tallinn, Estonia) with IMMULITE 2000 immunoassay autoanalyzer using sandwich type immunochemical assay (Siemens Healthineers AG, Erlangen, Germany) with imprecision (coefficient of variation) of 10%.

In Publication II, concentrations of B2M, UA, and urea in spent dialysate and serum samples in the multicentre study were determined in local clinical chemistry laboratories (Synlab Eesti OÜ in Estonia, Clinical Chemistry Laboratory at Linköping University Hospital in Sweden, Clinical Biochemistry Laboratory at Fundación Jiménez Díaz University Hospital Health Research Institute, in Madrid, Spain, and Laboratory of Clinical Chemistry and Clinical Analysis at Ghent University Hospital, in Ghent, Belgium) using standardised laboratory methods.

In Publication III, concentration of urea in spent dialysate samples was determined in clinical chemistry laboratory (SYNLAB Eesti OÜ, Tallinn, Estonia) using standardised laboratory methods. For this purpose, ADVIA 1800 autoanalyzer (Siemens Healthcare Diagnostics Inc., Erlangen, Germany) with imprecision (coefficient of variation) of 4% was used.

5.4 Optical measurements (Publications I, III)

UV light absorption spectra and fluorescence spectra of spent dialysate samples (Publication I, III) were measured at room temperature using UV-3600 spectrophotometer or RF-6000 spectrofluorometer, respectively, both from Shimadzu (Kyoto, Japan). To distinguish the optical spectra of middle molecules' fraction from spectra of small water-soluble molecules in Publication I, spent dialysate samples in volume of 12 mL were centrifuged using filter tubes with a cut-off limit of 1 kDa (Pall Laboratory Macrosep® type MAP001C37, Pal Corp., Ann Arbor, MI, USA) at 37 C for 40 min at 2375.75 g. The optical spectra of ultrafiltrates were measured in addition to spent dialysate samples, and the corresponding differences were considered to be specific to the middle molecules' fraction.

UV light absorption spectra of dialysate samples were recorded over a wavelength range of 190–400 nm ($\Delta\lambda$ = 1 nm) with a bandwidth of 2 nm using a quartz cuvette with an optical path length of 5 mm and pure dialysis solution as a reference, or additionally with the corresponding filtrate as a reference in Publication I.

Fluorescence spectra of dialysate samples and filtrates were recorded over the excitation wavelength range of 200–400 nm ($\Delta\lambda$ =10 nm) and the emission wavelength range of 210–600 nm ($\Delta\lambda$ = 1 nm) using a quartz cuvette with a path length of 4 mm, and bandwidths of both monochromators of 5 nm.

Additionally, an optical sensor prototype (Optofluid Technologies OÜ, Tallinn, Estonia) was connected to the outflow of HD machine for on-line measurements of light absorption and fluorescence during each session to evaluate sampling quality.

5.5 Data analysis

To ensure data quality, all measurement results were evaluated for potential errors and data conformity during data preprocessing. Specifically, the results of the sensor prototype and spectrophotometry were compared to find sampling errors, i.e., sampling during self-tests of HD machine (Supplementary Figure 1 of Publication II). Additionally, HPLC and clinical laboratory determined UA concentrations were compared to detect possible errors related to sample handling and analyses. Erroneous data, including HD sessions with unstable treatment settings (Uhlin et al., 2006), and concentrations of uraemic solutes below the quantification limit of clinical laboratory analyses, were omitted from the dataset prior to data analysis.

5.5.1 Development of predictive models

Predictive models were developed to estimate concentrations of B2M (Publication I) and CMW (Publication III) in spent dialysate based on laboratory measured light absorbance and fluorescence of spent dialysate. Prior to model development, fluorescence spectra were mathematically corrected for the primary inner filter effect based on the recorded light absorbance values at excitation wavelengths (Fonin et al., 2014; Wang et al., 2017) to compensate for the attenuation of excitation light intensity in samples containing chromophores in high concentrations. In Publication III, the fluorescence spectra were additionally smoothed using the moving average filter with the window size of 10.

A preselection of the predictor variables was done based on regression analysis, evaluating the relationship between concentration of uraemic solutes and of UV absorbance and fluorescence. Forward stepwise regression was thereafter used to create models with up to three variables based on calibration datasets (50% of data).

A variable was included in the model if its p-value was < 0.05 for an F-test, indicating a significant reduction in the sum of squared errors of the model.

In addition to the calibration dataset, the general performance of the models was tested on a separate validation dataset (50% of the data).

The accuracy of the models was evaluated using regression and Bland-Altman analysis (Giavarina, 2015). Systematic error (BIAS) was calculated for the models as follows:

$$BIAS = \frac{\sum_{i=1}^{N} e_i}{N} \quad (14),$$

where N is the total number of observations and e_i is the i-th residual (difference between HPLC or laboratory determined, and model predicted values).

Similarly, the standard error of performance corrected for BIAS was calculated for the models based on the residuals:

$$SE = \sqrt{\frac{\sum_{i=1}^{N}(e_i - BIAS)^2}{N-1}} \quad (15).$$

5.5.2 Haemodialysis efficacy parameters

Removal efficacy of uraemic toxins during HD was evaluated based on reduction ratio as RR (Publication I, III), and total removed solute as TRS (Publication I, III, III).

RR was calculated from uraemic solutes' concentrations in blood or spent dialysate samples at the start and at the end of the dialysis procedure using Equation 5. TRS of uraemic solutes was calculated based on the TDC tank weight and concentrations of uraemic solutes in the spent dialysate TDC tank using Equation 9.

In publications (II, III), intradialytic TAC of uraemic toxins in blood was determined as logarithmic mean concentration as proposed earlier (Garred, 1995; Lim et al., 2018):

$$TAC = \frac{(C_0 - C_\mathrm{t})}{\ln(\frac{C_0}{C_\mathrm{t}})} \quad (16),$$

where C_0 and C_t are HPLC or laboratory determined pre- and post-dialysis blood concentrations of uraemic toxins.

Linear regression analysis was used to evaluate intradialytic TAC of uraemic solutes from spent dialysate based TRS (Publication II) and logarithmic mean concentration ($M_{\ln}D$) (Publication II, III).

$M_{\ln}D$ was calculated from spent dialysate concentrations as:

$$M_{\ln}D = \frac{(D_7 - D_{240})}{\ln(\frac{D_7}{D_{240}})} \quad (17),$$

where D_7 and D_{240} are uraemic solutes concentrations in spent dialysate samples taken 7 and 240 min after the start of dialysis, respectively.

Prior to regression analysis in Publication II, TAC was normalised by effective blood flow rate to compensate for dialyser clearance, and $M_{\ln}D$ was normalised by spent dialysate flow rate to compensate for spent dialysate flow rate dependent sample dilution. To compare blood and spent dialysate based concentrations at time moment (t) directly in Publication III, spent dialysate concentrations (D_t) were normalised ($D_{t\,\mathrm{norm}}$) by blood flow and spent dialysate flow rates prior to calculation of $M_{\ln}D$ and regression analysis according to Equation 18:

$$D_{t\,\mathrm{norm}} = D_t \cdot \frac{Q_\mathrm{d} + Q_\mathrm{subs} + UF}{Q_\mathrm{b}} \quad (18),$$

where Q_b marks effective blood flow and the numerator "dialysate flow rate (Q_d) + substitution rate (Qsubs) + net ultrafiltration rate (UF), which is not compensated for patient" is the flow rate of spent dialysate.

5.5.3 Statistical tests

To evaluate the agreement between serum and dialysate based HD efficacy parameters, Bland-Altman analysis was used as described above (Equations 14 & 15). The Anderson-Darling test was used to evaluate whether datasets are normally distributed. In the case of normal distribution of data, Student's two-tailed paired t-test was used to compare mean values of related variables from the same subject, whereas the unpaired two-tailed t-test was used for comparison of the differences between treatment modalities. For non-normally distributed data, the Wilcoxon test was applied. A p-value of < 0.05 was considered significant in all statistical tests.

6 Results and discussion

6.1 Intradialytic removal monitoring of B2M using spent dialysate (Publication I)

B2M is a prototypic marker molecule for middle molecules removal, which has been proposed for routine monitoring to enhance treatment efficacy and optimise patient outcomes (Watanabe et al., 2015; Canaud et al., 2020; Rosner et al., 2021). Although high-volume HDF and expanded HD therapy with medium cut-off membranes outperform conventional HD in removing middle molecules (García-Prieto et al., 2023; Biedunkiewicz et al., 2024; Battaglia et al., 2025), the reduction of middle molecules blood levels still remains challenging with dialysis therapies (Ward & Daugirdas, 2024; Battaglia et al., 2025; Sirich, 2025). While high-dose hemodiafiltration appears to improve ESKD patients' survival and outcomes over high-flux HD, the role of middle molecule clearance in these benefits is unclear, as concentrations or clearances of middle molecules have not been reported in the related studies (Vernooij et al., 2022; Blankestijn et al., 2023; Shroff et al., 2023; Battaglia et al., 2025). Still, B2M has strong evidence of toxicity (Vanholder et al., 2018), and elevated B2M pre-dialysis levels have been strongly and independently associated with higher mortality of ESKD patients and several pathologies (Cheung et al., 2006; Okuno et al., 2008; Liabeuf et al., 2012; Watanabe et al., 2015; Argyropoulos et al., 2017).

Yet, no reliable dialysate-based optical method exists for intradialytic monitoring of middle molecules removal to objectively evaluate their dialytic removal, although previous studies have found strong correlations between middle molecules and optical signals of spent dialysate (Holmar et al., 2011; Uhlin et al., 2015; Lauri et al., 2020). The aim of Publication I was to develop a novel advanced optical method based on the UV absorbance and fluorescence of the spent dialysate for evaluating B2M removal and concentration in spent dialysate as a marker of middle molecules, and investigate the contribution of middle molecules to the optical properties of spent dialysate.

The results of Publication I showed a strong correlation between UV absorbance and the concentration of B2M in spent dialysate samples (N = 375) when using high-flux HDF, with $R^2 > 0.8$ in the range of 220-320 nm and local maxima at 222 nm ($R^2 = 0.881$), * 274 nm ($R^2 = 0.862$), and 311 nm ($R^2 = 0.865$). The latest being similar to the earlier observations (Uhlin et al., 2015), which found a maximum correlation at 314 ($R^2 = 0.861$).

An evident difference in UV absorbance spectra of spent dialysate samples and corresponding filtrates, containing solutes < 1kDa, was found. However, the regression analysis between the UV absorbance of spent dialysate samples and corresponding filtrates indicated that the variation caused by middle molecules is negligible in the UV region > 230 nm, but the resulting difference in UV absorbance of filtrates and dialysate samples is proportional to the absorbance of spent dialysate samples. This is consistent with the literature that light absorption in spent dialysate is mainly caused by small water-soluble solutes (Lauri et al., 2010; Arund et al., 2012; Donadio et al., 2013) with UV-absorbing peptide bonds (Rosenheck & Doty, 1961) and aromatic side chains of amino acids (Prasad et al., 2017) of middle molecules contributing minimally.

The strongest correlation between the fluorescence of spent dialysate and the concentration of B2M in spent dialysate was found in the region with wavelengths of excitation at 350–370 nm and emission wavelengths at 500–555 nm with R^2 up to 0.859. Similarly, in close proximity to these results, a previous smaller-scale study (Holmar et al.,

2011) found the strongest correlation between the concentration of B2M in spent dialysate and its fluorescence using excitation/emission at 370/456 nm (R^2 = 0.90, N = 69).

Whereas the apparent fluorescence of middle molecules was identified to have maximum emission at 325–335 nm if excited at 280 nm, and approximately 10 times weaker emission intensity at advanced glycation end-product (AGEs) specific region of 430–550 nm with excitation at 350 nm; in both regions low-flux HD and high-flux HDF modalities had the largest differences for middle molecules fluorescence. Specifically, middle molecules contributed on average 26,09 ± 6,68% to the overall fluorescence of the spent dialysate at excitation/emission wavelengths of 280/325 nm at the beginning of high-flux HDF therapy, in contrast to low-flux HD having negligible contribution. This was further confirmed by the regression analysis (Figure 4).

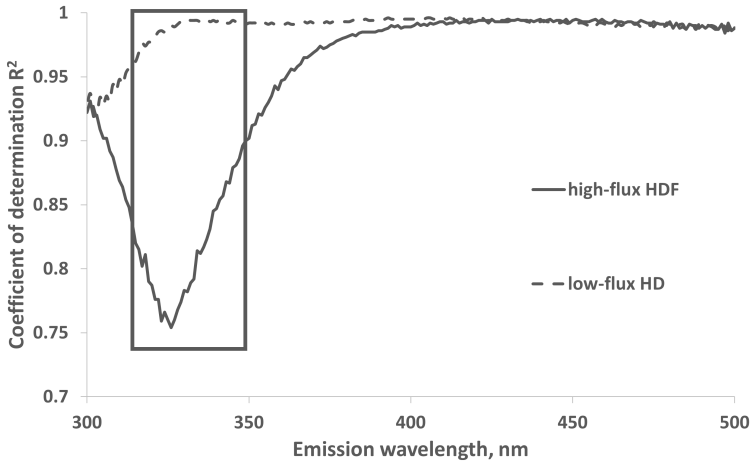

Figure 4. Correlation between fluorescence emission intensity of spent dialysate samples (excitation at 280 nm) and corresponding filtrates, containing uraemic solutes < 1 kDa, from low-flux HD and high-flux HDF modalities (N=17) sampled 7 min after the start of the dialysis. The emission region with the highest correlation between B2M in the spent dialysate at excitation 280 nm, used in the final regression model, is marked with a rectangle (modified from Publication I).

The primary source of middle molecules' fluorescence, with maximum emission at 332 nm and excitation at 280 nm, was attributed to the intrinsic fluorescence of tryptophan residues in the hydrophobic environments of proteins and peptides, based on the literature (Vivian & Callis, 2001; Lakowicz, 2006). This is similar to the intrinsic fluorescence of tryptophan residues in B2M under native conditions, which occurs approximately at 337 nm (Narang et al., 2013). While AGEs (Perrone et al., 2020) seem to be the main contributor to the fluorescence of middle molecules at the longer emission wavelengths of 430-550 nm if excited at 350 nm, being close to the emission maximum (460 nm) of AGE-modified B2M if excited at 350-360 nm (Miyata et al., 1993; Kalle et al., 2015). This corresponds to a fluorescence region with the strongest correlation between the fluorescence of spent dialysate and the concentration of B2M in spent dialysate of Publication I and an earlier study (Holmar et al., 2011).

Including the fluorescence regions with highest contribution of middle molecules to the optical signals of spent dialysate and UV absorbance as parameters, a predictive model for estimating B2M concentration was developed and validated on independent data.

The model incorporated UV absorbance at 280 nm and fluorescence at excitation/emission pairs of 280/325 nm and 350/555 nm as parameters, achieving an accuracy (BIAS±SE) of 0.000 ± 0,272 mg/L with a correlation coefficient of 0.966 for the calibration group, and an accuracy of 0.061 ± 0,340 mg/L with a correlation coefficient 0.953 for the validation group between the laboratory estimated and model predicted B2M concentrations in spent dialysate, respectively (Figure 5). For the entire cohort, the model demonstrated a correlation coefficient of 0.958 and an accuracy of 0.000 ± 0.304 mg/L, surpassing the performance of previously reported predictive models (Holmar et al., 2011; Lauri et al., 2020).

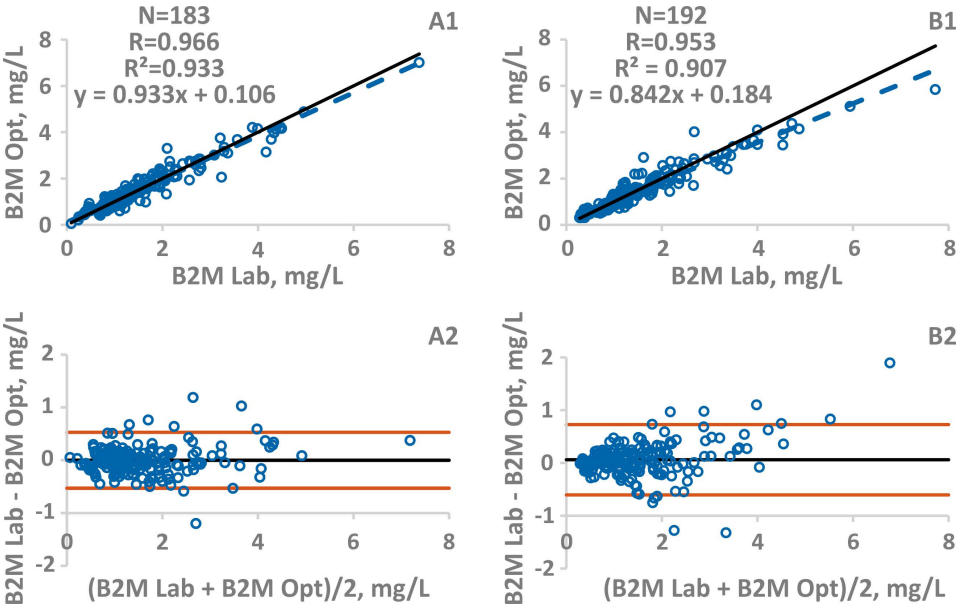

Figure 5. Scatter plots and Bland-Altman plots of the calibration (A1 & A2) and the validation (B1 & B2) groups comparing laboratory (Lab) determined and model predicted (Opt) B2M concentrations, respectively (modified from Publication I).

In addition, the laboratory estimated and model predicted values for HD performance parameters of RR (73.37 ± 10.39% and 72.06 ± 7.77%, respectively) and TRS (234.5 ± 72.8 mg and 228.6 ± 83.9 mg, respectively) were not statistically different ($p > 0.35$).

In summary, the findings from Publication I indicate that UV absorption and fluorescence measurements could be used to estimate the concentration of B2M in spent dialysate and monitor intradialytic removal of middle molecules, which have a considerable contribution to the overall optical properties of spent dialysate. Although tryptophan of proteins and peptides and advanced glycation end-products were provisionally identified as main contributors to the optical signal of middle molecules, further research is suggested to identify specific middle molecular uraemic toxins behind the optical properties of spent dialysate.

6.2 Estimation of intradialytic blood time-averaged concentration of uraemic toxins using spent dialysate (Publication II)

Traditional, Kt/V urea-based HD adequacy assessment insufficiently represents the removal of other clinically significant uraemic solutes (Meyer et al., 2011; Vanholder, Glorieux, et al., 2015). This necessitates more universal dialysis dose quantification, which is appropriate for evaluating the efficacy of modern dialysis strategies in removing prototypical markers and solutes related to ESKD patients' outcomes, such as B2M or IS (Meyer et al., 2011; Vanholder, Glorieux, et al., 2015; Vanholder et al., 2019; Rosner et al., 2021).

Among the measures of dialysis adequacy, TAC is considered the most useful marker for comparing different dialysis strategies in terms of their effectiveness in reducing uraemic solute levels over time, being universally applicable to uraemic solutes with different removal kinetics (Eloot et al., 2009, 2012). Conventionally, repeated blood sampling is required to calculate TAC from the area under the concentration curve of the solute over the inter- or intradialytic period (Lopot et al., 2004; Kanagasundaram et al., 2008; Eloot et al., 2009). However, multiple intra-dialytic blood samples are necessary for accurate TAC calculation during dialysis as relying solely on pre- and post-dialysis samples can cause errors, especially for solutes with higher intercompartmental resistance (Garred, 1995; Kanagasundaram et al., 2008; Eloot et al., 2009).

The aim of Publication II was to estimate intradialytic serum TAC for prototypical marker molecules of urea, UA, IS and B2M from their spent dialysate concentrations non-invasively.

A strong correlation was observed between intradialytic serum TAC and $M_{In}D$ values for all solutes (Figure 6), regardless of HD treatment modality and dialyser.

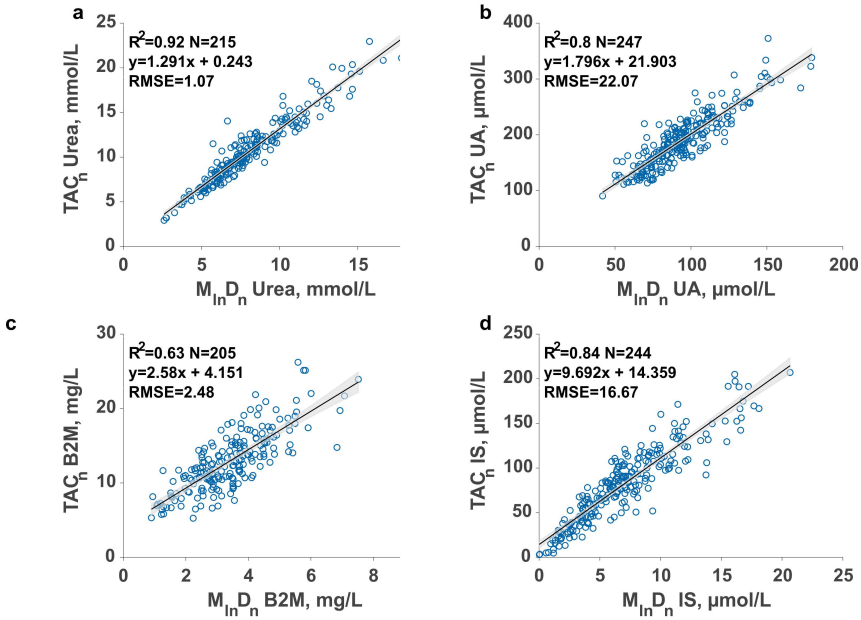

Figure 6. Correlation between serum intradialytic TACs of (a) urea, (b) UA, (c) B2M, and (d) IS in and MlnD values in spent dialysate, normalised by effective blood or spent dialysate flow rates, respectively; grey area indicates the 95% CI of the slope (modified from Publication II).

For HDF and HD modalities separately, the strongest correlation was seen for urea (R^2 = 0.91 (N = 152), R^2 = 0.96 (N = 63)) and the weakest correlation for B2M (R^2 = 0.62 (N = 168), R^2 = 0.83 (N = 37)), respectively. Also, TRS was generally strongly correlated to intradialytic TAC values (R^2 > 0.59) and $M_{ln}D$ values (R^2 > 0.89) for the studied uraemic solutes in case TAC and $M_{ln}D$ values were normalised by effective blood or spent dialysate flow rates, respectively.

Moreover, using linear regression equations describing the abovementioned relationships (Figures 2 & 3, in Publication II), the estimated TAC values closely matched the calculated values, and the random error between the calculated and the estimated TAC values remained consistent across the entire concentration range.

The variation in correlation coefficients among the uraemic solutes indicated that solute-dependent kinetic behaviour affects intradialytic TAC estimation, i.e., pre- and post-dialysis blood samples-based TAC may overestimate the actual intradialytic TAC. This is valid particularly for solutes with slow intercompartment clearance such as B2M, which serum levels decrease rapidly at the start of dialysis (Ward et al., 2006; Kanagasundaram et al., 2008; Eloot et al., 2012; Ward & Daugirdas, 2024). Consequently, the strongest correlation was found for urea, which has minimal resistance to inter-compartmental shifts, and the weakest correlation for B2M, which exhibits the highest intercompartmental resistance among the studied solutes (Meyer et al., 2011; Eloot et al., 2012). In this regard, employing double pool-kinetics or multiple intra-dialytic blood sampling is necessary for more accurate intradialytic serum TAC calculations (Kanagasundaram et al., 2008) as a reference, instead of using approach, which assumes single-pool removal kinetics (Garred, 1995; Lim et al., 2018).

Based on these results, it is feasible to evaluate intradialytic serum TAC of urea, UA, IS and, B2M from their concentrations in spent dialysate non-invasively. The findings created conditions for online optical monitoring of serum TAC from spent dialysate concentrations and pave the way for optimising predictive models for each uraemic toxin, considering real-time values of dialysis machine treatment settings, dialyser specifications and patient-related parameters, including blood access recirculation and haematocrit.

6.3 Intradialytic monitoring of kidney function marker C-mannosyl tryptophan using spent dialysate (Publication III)

CMW is an endogenous metabolite with a molecular weight of 366 Da arising from the degradation of C-mannosylated proteins, the only known form of protein C-linked glycosylation in humans (Furmanek & Hofsteenge, 2000; Schjoldager et al., 2020; Minakata et al., 2021). Recent large-scale metabolomic studies have independently identified CMW as independent and one of the strongest markers of eGFR decline and health outcomes such as death in the cohort of non-dialysis CKD patients among thousands of other studied metabolites (Steinbrenner et al., 2021, 2024; van der Burgh et al., 2024). In addition, there is a strong correlation between CMW levels and GFR; thus, CMW is considered to be a residual kidney function marker (Takahira et al., 2001; Yonemura et al., 2004; Niewczas et al., 2014; Sekula et al., 2016; Denburg et al., 2021; Steinbrenner et al., 2021; van der Burgh et al., 2024).

Despite CMW is a promising biomarker and an endogenous uraemic solute with potential toxicity, the levels of CMW and its dialytic removal characteristics have not

been assessed so far for ESKD patients undergoing dialysis therapy, and their relationship to clinical outcomes of ESKD patients remains unexplored.

Publication III aimed to determine the levels of CMW in ESKD patients' blood and spent dialysate during the dialysis employing HPLC, and investigate the possibility of optics-based estimation of haemodialytic removal and TAC of CMW.

The results of Publication III showed that the median (interquartile range) concentration of CMW in serum samples was 2.78 (2.20–3.22) µmol/L at the start and 0.52 (0.38–0.73) µmol/L at the end of treatment, and in spent dialysate samples 0.64 (0.52–0.79) µmol/L and 0.13 (0.08–0.22) µmol/L, respectively. In comparison to the previous studies reporting CMW levels in healthy subjects (Yonemura et al., 2004; Sekula et al., 2017), CMW levels of ESKD patients are, presumably more than 10 times higher than the average normal concentration in healthy controls. This is similar to the 13–16-fold increase reported by Tanaka et al., who did relative comparison of mass spectrometric peak areas of CMW (Tanaka et al., 2015) in healthy controls and ESKD patients.

The treatment settings similarly affect the removal efficacy of CMW and urea, with the RR of CMW being higher than the RR of urea (Figure 7).

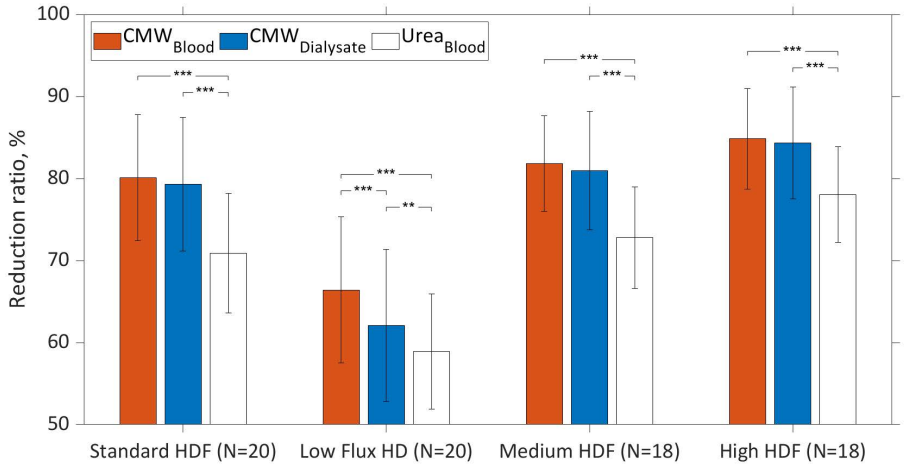

*Figure 7. RR (mean ± SD) of CMW and urea for HD and different HDF modalities (Table 2) evaluated based on serum and spent dialysate samples collected from the start and end of the dialysis sessions; intra-modality differences, evaluated using paired two-tailed t-tests, are denoted as follows: *** ($p < 0.001$), ** ($p < 0.01$), * ($p < 0.05$). Modified from Publication III.*

In detail, RRs of both solutes were significantly higher ($p < 0.001$) for the most efficient HDF modality in comparison with low-flux HD with RRs (± SD) of 84.8 ± 6.1% vs 66.4 ± 8.9% for CMW and RRs (± SD) of 78.1 ± 5.8% vs 58.9 ± 7.0% for urea. For both solutes, the rebound effect significantly affected effective RR ($p < 0.01$), whereas the extent of the rebound effect was not statistically different between the solutes ($p = 0.530$). These results show that the removal of CMW is characteristic of the removal of small water-soluble compounds, in contrast to the removal characteristics of unmodified tryptophan, which is a protein-bound solute (Paats et al., 2020).

The serum and spent dialysate concentrations of CMW were strongly correlated after normalisation of spent dialysate concentration by treatment settings ($r = 0.981$),

which shows it is possible to evaluate CMW concentrations in blood and HD performance parameters from spent dialysate concentrations.

The multiparametric linear regression model, which was developed to estimate spent dialysate CMW concentrations, had relatively high accuracy (BIAS ± SE) on both calibration and validation sets: 0.00 ± 0.07 µmol/L with r = 0.960, and -0.02 ± 0.07 µmol/L with r = 0.939 — comparing HPLC determined CMW concentrations to model estimated values, respectively. The developed model allows to estimate CMW concentrations in spent dialysate from optical measurements and to evaluate HD performance parameters using optical measurements (Table 4).

Table 4. Haemodialysis performance parameters based on RR, TRS, and TAC of CMW. Results based on HPLC analysis of serum or spent dialysate samples were compared with the results calculated from the output of the optics-based (Opt) model using the Wilcoxson test. Numerical values are given as median and interquartile range (Q1–Q3).

Clinical parameter	**CMW HPLC median (Q1-Q3)**	**CMW Opt median (Q1-Q3)**	***p-value***	**Accuracy (BIAS ± SE)**	**Pearson correlation coefficient**
$RR_{dialysate}$ (%, N=74)	78.7 (68.6–85.7)	78.5 (67.0–84.6)	0.811	0.7 ± 3.7	0.958
RR_{serum} (%, N=72)	80.3 (72.3–85.9)	77.8 (66.1–84.5)	0.347	2.4 ± 4.9	0.939
TRS (µmol, N=86)	40.25 (34.29–47.89)	43.84 (36.75–52.12)	0.213	−1.72 ± 7.95	0.792
TAC (µmol/L, N=72)	1.34 (1.13–1.54)	1.39 (1.17–1.59)	0.442	0.00± 0.25	0.717

Overall, the results of Publication III described the levels of CMW in ESKD patients and the intradialytic removal of CMW for the first time. Additionally, the feasibility of non-invasive optical monitoring of intradialytic CMW concentrations in spent dialysate and CMW-based HD adequacy parameters was demonstrated, which enables to elaborate the role of CMW in ESKD patients' outcomes in future studies.

Conclusions

In conclusion, this thesis demonstrated that novel spent dialysate based optical methods could be applied for more universal dose quantification of HD, which may provide more adequate HD treatment.

The main findings of the thesis are:

- This thesis identified that middle molecules form a considerable fraction of optical signals of spent dialysate, presumably originating from intrinsic fluorescence of tryptophan in peptides and proteins, and AGEs.
- Multiwavelength optical measurements of spent dialysate allow to estimate concentration of B2M in spent dialysate and to monitor intradialytic removal of middle molecules with high accuracy.
- For the first time, endogenous kidney function biomarker CMW levels were determined in ESKD patients, which are evidently over 10 times higher than in healthy subjects of previous studies.
- Intradialytic removal of CMW was compared to that of urea and was found to be similar to that of small water-soluble uraemic solutes. Using optical measurements of UV absorption and fluorescence of spent dialysate, intradialytic levels and removal of CMW can be accurately monitored. In future studies, this could help to elaborate the role of CMW in ESKD patients' health outcomes and evaluate residual kidney function.
- Spent dialysate concentrations and TRS of uraemic solutes are proportional to the intradialytic TAC of uraemic solutes in patients' blood. This thesis demonstrates for the first time that blood concentration of urea, UA, IS, and B2M can be similarly predicted from their spent dialysate concentrations using treatment settings. This approach may prove useful in evaluating the effect of HD treatment on the actual solute levels over time.
- Spent dialysate based optical monitoring can be used to evaluate clinically relevant parameters such as TAC, TRS, and RR, which make it possible to assess HD adequacy more universally. Therefore, optical monitoring of HD can be used as a non-invasive tool to potentially improve patients' health outcomes.

References

Abe, T., Onoda, M., Matsuura, T., Sugimura, J., Obara, W., Sasaki, N., Kato, T., Tatsumi, K., & Maruyama, T. (2021). Evaluation of a new measurement method of indoxyl sulfate in hemodialysis patients. *Therapeutic Apheresis and Dialysis*, *25*(1), 44–49. https://doi.org/10.1111/1744-9987.13500

Abecassis, M., Bartlett, S. T., Collins, A. J., Davis, C. L., Delmonico, F. L., Friedewald, J. J., Hays, R., Howard, A., Jones, E., Leichtman, A. B., Merion, R. M., Metzger, R. A., Pradel, F., Schweitzer, E. J., Velez, R. L., & Gaston, R. S. (2008). Kidney Transplantation as Primary Therapy for End-Stage Renal Disease: A National Kidney Foundation/Kidney Disease Outcomes Quality Initiative (NKF/KDOQI™) Conference. *Clinical Journal of the American Society of Nephrology*, *3*(2), 471–480. https://doi.org/10.2215/CJN.05021107

Adoberg, A., Paats, J., Arund, J., Dhondt, A., Fridolin, I., Glorieux, G., Holmar, J., Lauri, K., Leis, L., Luman, M., Pilt, K., Uhlin, F., & Tanner, R. (2022). Treatment with Paracetamol Can Interfere with the Intradialytic Optical Estimation in Spent Dialysate of Uric Acid but Not of Indoxyl Sulfate. *Toxins*, *14*(9), 610. https://doi.org/10.3390/toxins14090610

Albani, J. R. (2007). New Insights in the Interpretation of Tryptophan Fluorescence. *Journal of Fluorescence*, *17*(4), 406–417. https://doi.org/10.1007/s10895-007-0183-3

Argyropoulos, C. P., Chen, S. S., Ng, Y.-H., Roumelioti, M.-E., Shaffi, K., Singh, P. P., & Tzamaloukas, A. H. (2017). Rediscovering Beta-2 Microglobulin As a Biomarker across the Spectrum of Kidney Diseases. *Frontiers in Medicine*, *4*. https://doi.org/10.3389/fmed.2017.00073

Armenta-Alvarez, A., Lopez-Gil, S., Osuna, I., Grobe, N., Tao, X., Ferreira Dias, G., Wang, X., Chao, J., Raimann, J. G., Thijssen, S., Perez-Grovas, H., Canaud, B., Kotanko, P., & Madero, M. (2023). Removal of Middle Molecules and Dialytic Albumin Loss: A Cross-over Study of Medium Cutoff and High-Flux Membranes with Hemodialysis and Hemodiafiltration. *Kidney360*, *4*(8), 1095–1102. https://doi.org/10.34067/KID.0000000000000185

Arund, J., Luman, M., Uhlin, F., Tanner, R., & Fridolin, I. (2016). Is Fluorescence Valid to Monitor Removal of Protein Bound Uremic Solutes in Dialysis? *PLOS ONE*, *11*(5), e0156541. https://doi.org/10.1371/journal.pone.0156541

Arund, J., Tanner, R., Fridolin, I., & Paats, J. (2024). *Multiparametric optical method and device for determining uremic solutes, including uremix toxins, in biological fluids* (US20240102930A1). U.S. Patent and Trademark Office. https://worldwide.espacenet.com/publicationDetails/biblio?CC=US&NR=2024102930A1&KC=A1&FT=D

Arund, J., Tanner, R., Uhlin, F., & Fridolin, I. (2012). Do Only Small Uremic Toxins, Chromophores, Contribute to the Online Dialysis Dose Monitoring by UV Absorbance? *Toxins*, *4*(10), 849–861. https://doi.org/10.3390/toxins4100849

Ashby, D., Borman, N., Burton, J., Corbett, R., Davenport, A., Farrington, K., Flowers, K., Fotheringham, J., Andrea Fox, R. N., Franklin, G., Gardiner, C., Martin Gerrish, R. N., Greenwood, S., Hothi, D., Khares, A., Koufaki, P., Levy, J., Lindley, E., Macdonald, J., … Wilkie, M. (2019). Renal Association Clinical Practice Guideline on Haemodialysis. *BMC Nephrology*, *20*(1), 379. https://doi.org/10.1186/s12882-019-1527-3

Azar, A. T., & Canaud, B. (2013). *Hemodialysis System* (pp. 99–166). https://doi.org/10.1007/978-3-642-27458-9_3

Barnett, A. L., & Veening, H. (1985). Liquid-chromatographic study of fluorescent compounds in hemodialysate solutions. *Clinical Chemistry*, *31*(1), 127–130. http://www.ncbi.nlm.nih.gov/pubmed/3917379

Battaglia, Y., Shroff, R., Meijers, B., Nistor, I., Alfano, G., Franssen, C., Luyckx, V., Liakopoulos, V., Mantovani, A., Baciga, F., Caccia, F., Momentè, C., Davenport, A., Blankestijn, P. J., Covic, A., Combe, C., & Basile, C. (2025). Haemodiafiltration versus high-flux haemodialysis—a Consensus Statement from the EuDial Working Group of the ERA. *Nephrology Dialysis Transplantation*. https://doi.org/10.1093/ndt/gfaf024

Bello, A. K., Okpechi, I. G., Osman, M. A., Cho, Y., Htay, H., Jha, V., Wainstein, M., & Johnson, D. W. (2022). Epidemiology of haemodialysis outcomes. *Nature Reviews Nephrology*, *18*(6), 378–395. https://doi.org/10.1038/s41581-022-00542-7

Bhimani, J. P., Ouseph, R., & Ward, R. A. (2010). Effect of increasing dialysate flow rate on diffusive mass transfer of urea, phosphate and 2-microglobulin during clinical haemodialysis. *Nephrology Dialysis Transplantation*, *25*(12), 3990–3995. https://doi.org/10.1093/ndt/gfq326

Biedunkiewicz, J., Zakrzewska, A., Małgorzewicz, S., Komorniczak, M., Jasiulewicz, K., Płonka, N., Tarasewicz, A., Jankowska, M., Biedunkiewicz, B., Dębska-Ślizień, A., & Tylicki, L. (2024). Comparison of uremic toxin removal between expanded hemodialysis and high volume online hemodiafiltrations in different modes. *Acta Biochimica Polonica*, *71*. https://doi.org/10.3389/abp.2024.13715

Birhanu, A. G. (2023). Mass spectrometry-based proteomics as an emerging tool in clinical laboratories. *Clinical Proteomics*, *20*(1), 32. https://doi.org/10.1186/s12014-023-09424-x

Blankestijn, P. J., Vernooij, R. W. M., Hockham, C., Strippoli, G. F. M., Canaud, B., Hegbrant, J., Barth, C., Covic, A., Cromm, K., Cucui, A., Davenport, A., Rose, M., Török, M., Woodward, M., & Bots, M. L. (2023). Effect of Hemodiafiltration or Hemodialysis on Mortality in Kidney Failure. *New England Journal of Medicine*, *389*(8), 700–709. https://doi.org/10.1056/NEJMoa2304820

Boelaert, J., Lynen, F., Glorieux, G., Eloot, S., Van Landschoot, M., Waterloos, M.-A., Sandra, P., & Vanholder, R. (2013). A novel UPLC–MS–MS method for simultaneous determination of seven uremic retention toxins with cardiovascular relevance in chronic kidney disease patients. *Analytical and Bioanalytical Chemistry*, *405*(6), 1937–1947. https://doi.org/10.1007/s00216-012-6636-9

Boenink, R., Bonthuis, M., Boerstra, B. A., Astley, M. E., de Sousa, I. R. M., Helve, J., Komissarov, K. S., Comas, J., Radunovic, D., Buchwinkler, L., Hommel, K., Gjorgjievski, N., Galvão, A. A., Mitsides, N., Vidas, M. M., Dębska-Ślizień, A. M., Ambrus, C., Slon-Roblero, M. F., ten Dam, M. A. G. J., … Stel, V. S. (2024). The ERA Registry Annual Report 2022: Epidemiology of Kidney Replacement Therapy in Europe, with a focus on sex comparisons. *Clinical Kidney Journal*. https://doi.org/10.1093/ckj/sfae405

Bowry, S. K., & Chazot, C. (2021). The scientific principles and technological determinants of haemodialysis membranes. *Clinical Kidney Journal*, *14*(Suppl 4), i5–i16. https://doi.org/10.1093/ckj/sfab184

Bowry, S. K., Kircelli, F., & Misra, M. (2021). Flummoxed by flux: the indeterminate principles of haemodialysis. *Clinical Kidney Journal*, *14*(Supplement_4), i32–i44. https://doi.org/10.1093/ckj/sfab182

Breit, M., & Weinberger, K. M. (2016). Metabolic biomarkers for chronic kidney disease. *Archives of Biochemistry and Biophysics*, *589*, 62–80. https://doi.org/10.1016/j.abb.2015.07.018

Canaud, B., Bosc, J. yves, Vaussenat, F., Leray-Moragues, H., Leblanc, M., Garred, L. J., & Mion, C. (1999). Quantitation in Hemodialysis: Adequacy Measurement Revisited. *Seminars in Dialysis*, *12*(5), 370–375. https://doi.org/10.1046/j.1525-139X.1999.99061.x

Canaud, B., Collins, A., & Maddux, F. (2020). The renal replacement therapy landscape in 2030: reducing the global cardiovascular burden in dialysis patients. *Nephrology Dialysis Transplantation*, *35*(Supplement_2), ii51–ii57. https://doi.org/10.1093/ndt/gfaa005

Canaud, B., Gagel, A., Peters, A., Maierhofer, A., & Stuard, S. (2024). Does online high-volume hemodiafiltration offer greater efficiency and sustainability compared with high-flux hemodialysis? A detailed simulation analysis anchored in real-world data. *Clinical Kidney Journal*, *17*(6). https://doi.org/10.1093/ckj/sfae147

Castellarnau, A., Werner, M., Günthner, R., & Jakob, M. (2010). Real-time Kt/V determination by ultraviolet absorbance in spent dialysate: technique validation. *Kidney International*, *78*(9), 920–925. https://doi.org/10.1038/ki.2010.216

Chan, C. T., Blankestijn, P. J., Dember, L. M., Gallieni, M., Harris, D. C. H., Lok, C. E., Mehrotra, R., Stevens, P. E., Wang, A. Y.-M., Cheung, M., Wheeler, D. C., Winkelmayer, W. C., Pollock, C. A., Abu-Alfa, A. K., Bargman, J. M., Bleyer, A. J., Brown, E. A., Davenport, A., Davies, S. J., … Zakharova, E. (2019). Dialysis initiation, modality choice, access, and prescription: conclusions from a Kidney Disease: Improving Global Outcomes (KDIGO) Controversies Conference. *Kidney International*, *96*(1), 37–47. https://doi.org/10.1016/j.kint.2019.01.017

Cheung, A. K., Rocco, M. V., Yan, G., Leypoldt, J. K., Levin, N. W., Greene, T., Agodoa, L., Bailey, J., Beck, G. J., Clark, W., Levey, A. S., Ornt, D. B., Schulman, G., Schwab, S., Teehan, B., & Eknoyan, G. (2006). Serum β-2 Microglobulin Levels Predict Mortality in Dialysis Patients: Results of the HEMO Study. *Journal of the American Society of Nephrology*, *17*(2), 546–555. https://doi.org/10.1681/ASN.2005020132

Clark, W. R. (2001). Quantitative Characterization of Hemodialyzer Solute and Water Transport. *Seminars in Dialysis*, *14*(1), 32–36. https://doi.org/10.1046/j.1525-139x.2001.00011.x

Clark, W. R., Gao, D., Neri, M., & Ronco, C. (2017). *Solute Transport in Hemodialysis: Advances and Limitations of Current Membrane Technology* (pp. 84–99). https://doi.org/10.1159/000479258

Coresh, J., Inker, L. A., Sang, Y., Chen, J., Shafi, T., Post, W. S., Shlipak, M. G., Ford, L., Goodman, K., Perichon, R., Greene, T., & Levey, A. S. (2019). Metabolomic profiling to improve glomerular filtration rate estimation: a proof-of-concept study. *Nephrology, Dialysis, Transplantation : Official Publication of the European Dialysis and Transplant Association - European Renal Association*, *34*(5), 825–833. https://doi.org/10.1093/ndt/gfy094

Daneshamouz, S., Eduok, U., Abdelrasoul, A., & Shoker, A. (2021). Protein-bound uremic toxins (PBUTs) in chronic kidney disease (CKD) patients: Production pathway, challenges and recent advances in renal PBUTs clearance. *NanoImpact*, *21*, 100299. https://doi.org/10.1016/j.impact.2021.100299

Daugirdas, J. T. (1993). Second generation logarithmic estimates of single-pool variable volume Kt/V. *Journal of the American Society of Nephrology*, *4*(5), 1205–1213. https://doi.org/10.1681/ASN.V451205

Daugirdas, J. T. (1995). Simplified Equations for Monitoring Kt/V, PCRn, eKt/V, and ePCRn. *Advances in Renal Replacement Therapy*, *2*(4), 295–304. https://doi.org/10.1016/S1073-4449(12)80028-8

Daugirdas, J. T., Depner, T. A., Inrig, J., Mehrotra, R., Rocco, M. V., Suri, R. S., Weiner, D. E., Greer, N., Ishani, A., MacDonald, R., Olson, C., Rutks, I., Slinin, Y., Wilt, T. J., Rocco, M., Kramer, H., Choi, M. J., Samaniego-Picota, M., Scheel, P. J., … Brereton, L. (2015). KDOQI Clinical Practice Guideline for Hemodialysis Adequacy: 2015 Update. *American Journal of Kidney Diseases*, *66*(5), 884–930. https://doi.org/10.1053/j.ajkd.2015.07.015

Davenport, A. (2017). Measuring residual renal function for hemodialysis adequacy: Is there an easier option? *Hemodialysis International*, *21*, S41–S46. https://doi.org/10.1111/hdi.12592

Denburg, M. R., Xu, Y., Abraham, A. G., Coresh, J., Chen, J., Grams, M. E., Feldman, H. I., Kimmel, P. L., Rebholz, C. M., Rhee, E. P., Vasan, R. S., Warady, B. A., & Furth, S. L. (2021). Metabolite Biomarkers of CKD Progression in Children. *Clinical Journal of the American Society of Nephrology*, *16*(8), 1178–1189. https://doi.org/10.2215/CJN.00220121

Depner, T. A. (2001). Uremic Toxicity: Urea and Beyond. *Seminars in Dialysis*, *14*(4), 246–251. https://doi.org/10.1046/j.1525-139X.2001.00072.x

Donadio, C., Calia, D., Ghimenti, S., Onor, M., Colombini, E., Fuoco, R., & Di Francesco, F. (2013). Uric acid is the major determinant of absorbance in spent dialysate allowing spectrophotometric evaluation of dialysis dose. *Journal of Nephrology*. https://doi.org/10.1007/s40620-013-0003-6

Duan, S., Pi, J., Wang, C.-H., Hou, Y.-C., Andy Lee, C.-Y., Lin, C.-J., Shi, L., Young, K.-C., & Sun, H.-Y. (2022). Assessment of ELISA-based method for the routine examination of serum indoxyl sulfate in patients with chronic kidney disease. *Heliyon*, *8*(12), e12220. https://doi.org/10.1016/j.heliyon.2022.e12220

Duranton, F., Cohen, G., De Smet, R., Rodriguez, M., Jankowski, J., Vanholder, R., & Argiles, A. (2012). Normal and Pathologic Concentrations of Uremic Toxins. *Journal of the American Society of Nephrology*, *23*(7), 1258–1270. https://doi.org/10.1681/ASN.2011121175

Eknoyan, G., Beck, G. J., Cheung, A. K., Daugirdas, J. T., Greene, T., Kusek, J. W., Allon, M., Bailey, J., Delmez, J. A., Depner, T. A., Dwyer, J. T., Levey, A. S., Levin, N. W., Milford, E., Ornt, D. B., Rocco, M. V., Schulman, G., Schwab, S. J., Teehan, B. P., & Toto, R. (2002). Effect of Dialysis Dose and Membrane Flux in Maintenance Hemodialysis. *New England Journal of Medicine*, *347*(25), 2010–2019. https://doi.org/10.1056/NEJMoa021583

Elin, R. J., Johnson, E., & Chesler, R. (1982). Four methods for determining uric acid compared with a candidate reference method. *Clinical Chemistry*, *28*(10), 2098–2100. https://doi.org/10.1093/clinchem/28.10.2098

Eloot, S., Dhondt, A., Vierendeels, J., De Wachter, D., Verdonck, P., & Vanholder, R. (2007). Temperature and concentration distribution within the Genius® dialysate container. *Nephrology Dialysis Transplantation*, *22*(10), 2962–2969. https://doi.org/10.1093/ndt/gfm356

Eloot, S., Schneditz, D., Cornelis, T., Van Biesen, W., Glorieux, G., Dhondt, A., Kooman, J., & Vanholder, R. (2016). Protein-Bound Uremic Toxin Profiling as a Tool to Optimize Hemodialysis. *PLOS ONE*, *11*(1), e0147159. https://doi.org/10.1371/journal.pone.0147159

Eloot, S., Schneditz, D., & Vanholder, R. (2012). What can the dialysis physician learn from kinetic modelling beyond Kt/Vurea? *Nephrology Dialysis Transplantation*, *27*(11), 4021–4029. https://doi.org/10.1093/ndt/gfs367

Eloot, S., Torremans, A. N., De Smet, R., Marescau, B., De Wachter, D., De Deyn, P. P., Lameire, N., Verdonck, P., & Vanholder, R. (2005). Kinetic behavior of urea is different from that of other water-soluble compounds: The case of the guanidino compounds. *Kidney International*, *67*(4), 1566–1575. https://doi.org/10.1111/j.1523-1755.2005.00238.x

Eloot, S., van Biesen, W., Dhondt, A., de Smet, R., Marescau, B., De Deyn, P. P., Verdonck, P., & Vanholder, R. (2009). Impact of increasing haemodialysis frequency versus haemodialysis duration on removal of urea and guanidino compounds: a kinetic analysis. *Nephrology Dialysis Transplantation*, *24*(7), 2225–2232. https://doi.org/10.1093/ndt/gfp059

European Uremic Toxins Work Group. (2025). *The European Uremic Toxins (EUTox) Database*. https://database.uremic-toxins.org/home.php

Fabresse, N., Uteem, I., Lamy, E., Massy, Z., Larabi, I. A., & Alvarez, J.-C. (2020). Quantification of free and protein bound uremic toxins in human serum by LC-MS/MS: Comparison of rapid equilibrium dialysis and ultrafiltration. *Clinica Chimica Acta*, *507*, 228–235. https://doi.org/10.1016/j.cca.2020.04.032

Fagugli, R. M., De Smet, R., Buoncristiani, U., Lameire, N., & Vanholder, R. (2002). Behavior of non-protein-bound and protein-bound uremic solutes during daily hemodialysis. *American Journal of Kidney Diseases*, *40*(2), 339–347. https://doi.org/10.1053/ajkd.2002.34518

Fan, P.-C., Chang, J. C.-H., Lin, C.-N., Lee, C.-C., Chen, Y.-T., Chu, P.-H., Kou, G., Lu, Y.-A., Yang, C.-W., & Chen, Y.-C. (2019). Serum indoxyl sulfate predicts adverse cardiovascular events in patients with chronic kidney disease. *Journal of the Formosan Medical Association*, *118*(7), 1099–1106. https://doi.org/10.1016/j.jfma.2019.03.005

Fernandes, S. R., Meireles, A. N., Marques, S. S., Silva, L., Barreiros, L., Sampaio-Maia, B., Miró, M., & Segundo, M. A. (2023). Sample preparation and chromatographic methods for the determination of protein-bound uremic retention solutes in human biological samples: An overview. *Journal of Chromatography B*, *1215*, 123578. https://doi.org/10.1016/j.jchromb.2022.123578

Ficheux, A., Argilés, A., Mion, H., & Mion, C. M. (2000). Influence of convection on small molecule clearances in online hemodiafiltration. *Kidney International*, *57*(4), 1755–1763. https://doi.org/10.1038/sj.ki.4495463

Ficheux, A., Gayrard, N., Szwarc, I., Andress, D., Soullier, S., Duny, Y., Goubert, G., Thomas, M., Bismuth-Mondolfo, J., Daurès, J.-P., Brunet, P., Servel, M.-F., & Argilés, A. (2011). The use of SDS-PAGE scanning of spent dialysate to assess uraemic toxin removal by dialysis. *Nephrology, Dialysis, Transplantation : Official Publication of the European Dialysis and Transplant Association - European Renal Association*, *26*(7), 2281–2289. https://doi.org/10.1093/ndt/gfq709

Ficheux, A., Gayrard, N., Szwarc, I., Soullier, S., Bismuth-Mondolfo, J., Brunet, P., Servel, M.-F., & Argiles, A. (2010). Use of spent dialysate analysis to estimate blood levels of uraemic solutes without blood sampling: urea. *Nephrology Dialysis Transplantation*, *25*(3), 873–879. https://doi.org/10.1093/ndt/gfp539

Flythe, J. E., & Watnick, S. (2024). Dialysis for Chronic Kidney Failure. *JAMA*, *332*(18), 1559. https://doi.org/10.1001/jama.2024.16338

Fonin, A. V, Sulatskaya, A. I., Kuznetsova, I. M., & Turoverov, K. K. (2014). Fluorescence of dyes in solutions with high absorbance. Inner filter effect correction. *PloS One*, *9*(7), e103878. https://doi.org/10.1371/journal.pone.0103878

Francis, A., Harhay, M. N., Ong, A. C. M., Tummalapalli, S. L., Ortiz, A., Fogo, A. B., Fliser, D., Roy-Chaudhury, P., Fontana, M., Nangaku, M., Wanner, C., Malik, C., Hradsky, A., Adu, D., Bavanandan, S., Cusumano, A., Sola, L., Ulasi, I., & Jha, V. (2024). Chronic kidney disease and the global public health agenda: an international consensus. *Nature Reviews Nephrology*, *20*(7), 473–485. https://doi.org/10.1038/s41581-024-00820-6

Francis, P. S., Lewis, S. W., & Lim, K. F. (2002). Analytical methodology for the determination of urea: current practice and future trends. *TrAC Trends in Analytical Chemistry*, *21*(5), 389–400. https://doi.org/10.1016/S0165-9936(02)00507-1

Fridolin, I., Magnusson, M., & Lindberg, L.-G. (2002). On-Line Monitoring of Solutes in Dialysate Using Absorption of Ultraviolet Radiation: Technique Description. *The International Journal of Artificial Organs*, *25*(8), 748–761. https://doi.org/10.1177/039139880202500802

Furmanek, A., & Hofsteenge, J. (2000). Protein C-mannosylation: facts and questions. *Acta Biochimica Polonica*, *47*(3), 781–789. http://www.ncbi.nlm.nih.gov/pubmed/11310977

Fushimi, Y., Tatebe, J., Okuda, Y., Ishii, T., Ujiie, S., & Morita, T. (2019). Performance evaluation of an Indoxyl Sulfate Assay Kit "NIPRO." *Clinical Chemistry and Laboratory Medicine (CCLM)*, *57*(11), 1770–1776. https://doi.org/10.1515/cclm-2019-0218

Gao, J., Ulvik, A., McCann, A., Ueland, P. M., & Meyer, K. (2021). Microheterogeneity and preanalytical stability of protein biomarkers of inflammation and renal function. *Talanta*, *223*, 121774. https://doi.org/10.1016/j.talanta.2020.121774

García-Prieto, A., de la Flor, J. C., Coll, E., Iglesias, E., Reque, J., & Valga, F. (2023). Expanded hemodialysis: what's up, Doc? *Clinical Kidney Journal*, *16*(7), 1071–1080. https://doi.org/10.1093/ckj/sfad033

Garred, L. J. (1995). Dialysate-Based Kinetic Modeling. *Advances in Renal Replacement Therapy*, *2*(4), 305–318. https://doi.org/10.1016/S1073-4449(12)80029-X

Giavarina, D. (2015). Understanding Bland Altman analysis. *Biochemia Medica*, *25*(2), 141–151. https://doi.org/10.11613/BM.2015.015

Glassock, R. J. (2008). Uremic Toxins: What Are They? An Integrated Overview of Pathobiology and Classification. *Journal of Renal Nutrition*, *18*(1), 2–6. https://doi.org/10.1053/j.jrn.2007.10.003

Gotch, F. A., & Sargent, J. A. (1985). A mechanistic analysis of the National Cooperative Dialysis Study (NCDS). *Kidney International*, *28*(3), 526–534. https://doi.org/10.1038/ki.1985.160

Guo, J., Jiao, W., Xia, S., Xiang, X., Zhang, Y., Ge, X., & Sun, Q. (2025). The global, regional, and national patterns of change in the burden of chronic kidney disease from 1990 to 2021. *BMC Nephrology*, *26*(1), 136. https://doi.org/10.1186/s12882-025-04028-z

Guppy, M., Thomas, E. T., Glasziou, P., Clark, J., Jones, M., O'Hara, D. V., & Doust, J. (2024). Rate of decline in kidney function with age: a systematic review. *BMJ Open*, *14*(11), e089783. https://doi.org/10.1136/bmjopen-2024-089783

Gutsche, B., Grun, C., Scheutzow, D., & Herderich, M. (1999). Tryptophan glycoconjugates in food and human urine. *The Biochemical Journal*, *343 Pt 1*(Pt 1), 11–19. http://www.ncbi.nlm.nih.gov/pubmed/10493906

Haraldsson, B., Nyström, J., & Deen, W. M. (2008). Properties of the Glomerular Barrier and Mechanisms of Proteinuria. *Physiological Reviews*, *88*(2), 451–487. https://doi.org/10.1152/physrev.00055.2006

Hasegawa, M., Kato, H., Yoshioka, T., & Goto, R. (2025). The estimation of healthcare cost of kidney transplantation in Japan using large-scale administrative databases. *Clinical and Experimental Nephrology*, *29*(3), 350–358. https://doi.org/10.1007/s10157-024-02551-1

Holmar, J., Arund, J., Uhlin, F., Tanner, R., & Fridolin, I. (2011). *Beta2-microglobulin Measurements in the Spent Dialysate Using Fluorescence Spectra* (pp. 1035–1038). https://doi.org/10.1007/978-3-642-23508-5_269

Holmar, J., Fridolin, I., Uhlin, F., Lauri, K., & Luman, M. (2012). Optical Method for Cardiovascular Risk Marker Uric Acid Removal Assessment during Dialysis. *The Scientific World Journal*, *2012*, 1–8. https://doi.org/10.1100/2012/506486

Horiuchi, K., Yonekawa, O., Iwahara, K., Kanno, T., Kurihara, T., & Fujise, Y. (1994). A Hydrophilic Tetrahydro-β-Carboline in Human Urine. *The Journal of Biochemistry*, *115*(2), 362–366. https://doi.org/10.1093/oxfordjournals.jbchem.a124343

Hossain, T. J., Manabe, S., Ito, Y., Iida, T., Kosono, S., Ueda, K., Hosomi, A., Inoue, D., & Suzuki, T. (2018). Enrichment and characterization of a bacterial mixture capable of utilizing C-mannosyl tryptophan as a carbon source. *Glycoconjugate Journal*, *35*(2), 165–176. https://doi.org/10.1007/s10719-017-9807-2

Htay, H., Bello, A. K., Levin, A., Lunney, M., Osman, M. A., Ye, F., Ashuntantang, G. E., Bellorin-Font, E., Gharbi, M. B., Davison, S. N., Ghnaimat, M., Harden, P., Jha, V., Kalantar-Zadeh, K., Kerr, P. G., Klarenbach, S., Kovesdy, C. P., Luyckx, V. A., Neuen, B., … Johnson, D. W. (2021). Hemodialysis Use and Practice Patterns: An International Survey Study. *American Journal of Kidney Diseases*, *77*(3), 326-335.e1. https://doi.org/10.1053/j.ajkd.2020.05.030

Hu, J.-R., Myint, L., Levey, A. S., Coresh, J., Inker, L. A., Grams, M. E., Guallar, E., Hansen, K. D., Rhee, E. P., & Shafi, T. (2022). A metabolomics approach identified toxins associated with uremic symptoms in advanced chronic kidney disease. *Kidney International*, *101*(2), 369–378. https://doi.org/10.1016/j.kint.2021.10.035

Hulko, M., Haug, U., Gauss, J., Boschetti-de-Fierro, A., Beck, W., & Krause, B. (2018). Requirements and Pitfalls of Dialyzer Sieving Coefficients Comparisons. *Artificial Organs*, *42*(12), 1164–1173. https://doi.org/10.1111/aor.13278

Jager, K. J., Kovesdy, C., Langham, R., Rosenberg, M., Jha, V., & Zoccali, C. (2019). A single number for advocacy and communication—worldwide more than 850 million individuals have kidney diseases. *Nephrology Dialysis Transplantation*, *34*(11), 1803–1805. https://doi.org/10.1093/ndt/gfz174

Julian, B. A., Suzuki, H., Suzuki, Y., Tomino, Y., Spasovski, G., & Novak, J. (2009). Sources of urinary proteins and their analysis by urinary proteomics for the detection of biomarkers of disease. *PROTEOMICS – Clinical Applications*, *3*(9), 1029–1043. https://doi.org/10.1002/prca.200800243

Kalle, S., Kressa, H., Tanner, R., Holmar, J., & Fridolin, I. (2015). *Fluorescence of Beta-2-microglobulin in the Spent Dialysate* (pp. 59–62). https://doi.org/10.1007/978-3-319-12967-9_16

Kalle, S., Tanner, R., Arund, J., Tomson, R., Luman, M., & Fridolin, I. (2016). 4-Pyridoxic Acid in the Spent Dialysate: Contribution to Fluorescence and Optical Monitoring. *PLOS ONE*, *11*(9), e0162346. https://doi.org/10.1371/journal.pone.0162346

Kalle, S., Tanner, R., Luman, M., & Fridolin, I. (2019). Free Pentosidine Assessment Based on Fluorescence Measurements in Spent Dialysate. *Blood Purification*, *47*(1–3), 85–93. https://doi.org/10.1159/000493522

Kanagasundaram, N. S., Greene, T., Larive, A. B., Daugirdas, J. T., Depner, T. A., & Paganini, E. P. (2008). Dosing intermittent haemodialysis in the intensive care unit patient with acute renal failure--estimation of urea removal and evidence for the regional blood flow model. *Nephrology Dialysis Transplantation*, *23*(7), 2286–2298. https://doi.org/10.1093/ndt/gfm938

Karger, A. B., Eckfeldt, J. H., Rynders, G. P., Chaudhari, J., Miao, S., Van Lente, F., Coresh, J., Levey, A. S., & Inker, L. A. (2021). Long-Term Longitudinal Stability of Kidney Filtration Marker Measurements: Implications for Epidemiological Studies and Clinical Care. *Clinical Chemistry*, *67*(2), 425–433. https://doi.org/10.1093/clinchem/hvaa237

Khader, N. A., Kamath, V. G., Kamath, S. U., Rao, I. R., & Prabhu, A. R. (2025). Kidney function estimation equations: a narrative review. *Irish Journal of Medical Science (1971 -)*. https://doi.org/10.1007/s11845-025-03874-y

Kolch, W., Neusüß, C., Pelzing, M., & Mischak, H. (2005). Capillary electrophoresis–mass spectrometry as a powerful tool in clinical diagnosis and biomarker discovery. *Mass Spectrometry Reviews*, *24*(6), 959–977. https://doi.org/10.1002/mas.20051

Kovesdy, C. P. (2022). Epidemiology of chronic kidney disease: an update 2022. *Kidney International Supplements*, *12*(1), 7–11. https://doi.org/10.1016/J.KISU.2021.11.003

Kumar Panigrahi, S., & Kumar Mishra, A. (2019). Inner filter effect in fluorescence spectroscopy: As a problem and as a solution. *Journal of Photochemistry and Photobiology C: Photochemistry Reviews*, *41*, 100318. https://doi.org/10.1016/j.jphotochemrev.2019.100318

Lakowicz, J. R. (Ed.). (2006). *Principles of Fluorescence Spectroscopy*. Springer US. https://doi.org/10.1007/978-0-387-46312-4

Lauri, K., Arund, J., Holmar, J., Tanner, R., Kalle, S., Luman, M., & Fridolin, I. (2020). Removal of Urea, β2-Microglobulin, and Indoxyl Sulfate Assessed by Absorbance and Fluorescence in the Spent Dialysate During Hemodialysis. *ASAIO Journal*, *66*(6), 698–705. https://doi.org/10.1097/MAT.0000000000001058

Lauri, K., Arund, J., Tanner, R., Jerotskaja, J., Luman, M., & Fridolin, I. (2010). Behaviour of uremic toxins and UV absorbance in respect to low and high flux dialyzers. *Estonian Journal of Engineering*, *16*(1), 95. https://doi.org/10.3176/eng.2010.1.09

Lee, C.-T., Kuo, C.-C., Chen, Y.-M., Hsu, C.-Y., Lee, W.-C., Tsai, Y.-C., Ng, H.-Y., Kuo, L.-C., Chiou, T. T.-Y., Yang, Y.-K., Cheng, B.-C., & Chen, J.-B. (2010). Factors Associated with Blood Concentrations of Indoxyl Sulfate and p -Cresol in Patients Undergoing Peritoneal Dialysis. *Peritoneal Dialysis International: Journal of the International Society for Peritoneal Dialysis*, *30*(4), 456–463. https://doi.org/10.3747/pdi.2009.00092

Levey, A. S., Inker, L. A., & Coresh, J. (2014). GFR Estimation: From Physiology to Public Health. *American Journal of Kidney Diseases*, *63*(5), 820–834. https://doi.org/10.1053/j.ajkd.2013.12.006

Leypoldt, J. K., Cheung, A. K., & Deeter, R. B. (1999). Rebound kinetics of β2-microglobulin after hemodialysis. *Kidney International*, *56*(4), 1571–1577. https://doi.org/10.1046/j.1523-1755.1999.00669.x

Liabeuf, S., Lenglet, A., Desjardins, L., Neirynck, N., Glorieux, G., Lemke, H. D., Vanholder, R., Diouf, M., Choukroun, G., & Massy, Z. A. (2012). Plasma beta-2 microglobulin is associated with cardiovascular disease in uremic patients. *Kidney International*, *82*(12), 1297–1303. https://doi.org/10.1038/KI.2012.301

Lim, P.-S., Lin, Y., Chen, M., Xu, X., Shi, Y., Bowry, S., & Canaud, B. (2018). Precise Quantitative Assessment of the Clinical Performances of Two High-Flux Polysulfone Hemodialyzers in Hemodialysis: Validation of a Blood-Based Simple Kinetic Model Versus Direct Dialysis Quantification. *Artificial Organs*, *42*(5), E55–E66. https://doi.org/10.1111/aor.13011

Lindsay, R. M., & Sternby, J. (2001). Future Directions in Dialysis Quantification. *Seminars in Dialysis*, *14*(4), 300–307. https://doi.org/10.1046/j.1525-139X.2001.00067.x

Locatelli, F., La Milia, V., Violo, L., Del Vecchio, L., & Di Filippo, S. (2015). Optimizing haemodialysate composition. *Clinical Kidney Journal*, *8*(5), 580–589. https://doi.org/10.1093/ckj/sfv057

Lopez-Giacoman, S., & Madero, M. (2015). Biomarkers in chronic kidney disease, from kidney function to kidney damage. *World Journal of Nephrology*, *4*(1), 57–73. https://doi.org/10.5527/wjn.v4.i1.57

Lopot, F., Nejedlý, B., & Sulková, S. (2004). Physiology in daily hemodialysis in terms of the time average concentration/time average deviation concept. *Hemodialysis International*, *8*(1), 39–44. https://doi.org/10.1111/j.1492-7535.2004.00073.x

Lopot, F., & Válek, A. (1988). Time-averaged Concentration—Time-averaged Deviation: A New Concept in Mathematical Assessment of Dialysis Adequacy. *Nephrology Dialysis Transplantation*, *3*(6), 846–848. https://doi.org/10.1093/oxfordjournals.ndt.a091768

Lornoy, W., Becaus, I., Billiouw, J. M., Sierens, L., Van Malderen, P., & D'Haenens, P. (2000). On-line haemodiafiltration. Remarkable removal of β2-microglobulin. Long-term clinical observations. *Nephrology Dialysis Transplantation*, *15*(suppl_1), 49–54. https://doi.org/10.1093/oxfordjournals.ndt.a027964

Lowrie, E. G., Laird, N. M., Parker, T. F., & Sargent, J. A. (1981). Effect of the Hemodialysis Prescription on Patient Morbidity. *New England Journal of Medicine*, *305*(20), 1176–1181. https://doi.org/10.1056/NEJM198111123052003

Mayerhöfer, T. G., Pahlow, S., & Popp, J. (2020). The Bouguer-Beer-Lambert Law: Shining Light on the Obscure. *ChemPhysChem*, *21*(18), 2029–2046. https://doi.org/10.1002/cphc.202000464

McKay, G., Korak, J. A., & Rosario-Ortiz, F. L. (2018). Temperature Dependence of Dissolved Organic Matter Fluorescence. *Environmental Science & Technology*, *52*(16), 9022–9032. https://doi.org/10.1021/acs.est.8b00643

Meert, N., Eloot, S., Waterloos, M.-A., Van Landschoot, M., Dhondt, A., Glorieux, G., Ledebo, I., & Vanholder, R. (2008). Effective removal of protein-bound uraemic solutes by different convective strategies: a prospective trial. *Nephrology Dialysis Transplantation*, *24*(2), 562–570. https://doi.org/10.1093/ndt/gfn522

Meibaum, J., Krause, S., Hillmer, H., Marcelli, D., & Strohhöfer, C. (2020). Identification and characterisation of fluorescent substances in spent dialysis fluid. *The International Journal of Artificial Organs*, *43*(9), 579–586. https://doi.org/10.1177/0391398820901826

Melchior, P., Erlenkötter, A., Zawada, A. M., Delinski, D., Schall, C., Stauss-Grabo, M., & Kennedy, J. P. (2021). Complement activation by dialysis membranes and its association with secondary membrane formation and surface charge. *Artificial Organs*, *45*(7), 770–778. https://doi.org/10.1111/aor.13887

Menon, M. C., Chuang, P. Y., & He, C. J. (2012). The Glomerular Filtration Barrier: Components and Crosstalk. *International Journal of Nephrology*, *2012*, 1–9. https://doi.org/10.1155/2012/749010

Merchant, M. L. (2010). Mass Spectrometry in Chronic Kidney Disease Research. *Advances in Chronic Kidney Disease*, *17*(6), 455–468. https://doi.org/10.1053/j.ackd.2010.09.003

Meyer, T. W., & Hostetter, T. H. (2007). Uremia. *New England Journal of Medicine*, *357*(13), 1316–1325. https://doi.org/10.1056/NEJMra071313

Meyer, T. W., Leeper, E. C., Bartlett, D. W., Depner, T. A., Lit, Y. Z., Robertson, C. R., & Hostetter, T. H. (2004). Increasing Dialysate Flow and Dialyzer Mass Transfer Area Coefficient to Increase the Clearance of Protein-bound Solutes. *Journal of the American Society of Nephrology*, *15*(7), 1927–1935. https://doi.org/10.1097/01.ASN.0000131521.62256.F0

Meyer, T. W., Sirich, T. L., & Hostetter, T. H. (2011). Dialysis Cannot be Dosed. *Seminars in Dialysis*, *24*(5), 471–479. https://doi.org/10.1111/j.1525-139X.2011.00979.x

Minakata, S., Inai, Y., Manabe, S., Nishitsuji, K., Ito, Y., & Ihara, Y. (2020). Monomeric C-mannosyl tryptophan is a degradation product of autophagy in cultured cells. *Glycoconjugate Journal*, *37*(5), 635–645. https://doi.org/10.1007/s10719-020-09938-8

Minakata, S., Manabe, S., Inai, Y., Ikezaki, M., Nishitsuji, K., Ito, Y., & Ihara, Y. (2021). Protein C-Mannosylation and C-Mannosyl Tryptophan in Chemical Biology and Medicine. *Molecules*, *26*(17), 5258. https://doi.org/10.3390/molecules26175258

Mischak, H., Delles, C., Vlahou, A., & Vanholder, R. (2015). Proteomic biomarkers in kidney disease: issues in development and implementation. *Nature Reviews Nephrology*, *11*(4), 221–232. https://doi.org/10.1038/nrneph.2014.247

Miyata, T., Oda, O., Inagi, R., Iida, Y., Araki, N., Yamada, N., Horiuchi, S., Taniguchi, N., Maeda, K., & Kinoshita, T. (1993). beta 2-Microglobulin modified with advanced glycation end products is a major component of hemodialysis-associated amyloidosis. *The Journal of Clinical Investigation*, *92*(3), 1243–1252. https://doi.org/10.1172/JCI116696

Morita, S., Inai, Y., Minakata, S., Kishimoto, S., Manabe, S., Iwahashi, N., Ino, K., Ito, Y., Akamizu, T., & Ihara, Y. (2021). Quantification of serum C-mannosyl tryptophan by novel assay to evaluate renal function and vascular complications in patients with type 2 diabetes. *Scientific Reports*, *11*(1), 1946. https://doi.org/10.1038/s41598-021-81479-y

Narang, D., Sharma, P. K., & Mukhopadhyay, S. (2013). Dynamics and dimension of an amyloidogenic disordered state of human β2-microglobulin. *European Biophysics Journal*, *42*(10), 767–776. https://doi.org/10.1007/s00249-013-0923-z

Narimani, R., Esmaeili, M., Rasta, S. H., Khosroshahi, H. T., & Mobed, A. (2021). Trend in creatinine determining methods: Conventional methods to molecular-based methods. *Analytical Science Advances*, *2*(5–6), 308–325. https://doi.org/10.1002/ansa.202000074

National Institute of Diabetes and Digestive and Kidney Diseases, N. I. of H. (2024). *Kidney and nephron - Labeled*. https://www.niddk.nih.gov/news/media-library/11236

Niewczas, M. A., Sirich, T. L., Mathew, A. V., Skupien, J., Mohney, R. P., Warram, J. H., Smiles, A., Huang, X., Walker, W., Byun, J., Karoly, E. D., Kensicki, E. M., Berry, G. T., Bonventre, J. V., Pennathur, S., Meyer, T. W., & Krolewski, A. S. (2014). Uremic solutes and risk of end-stage renal disease in type 2 diabetes: metabolomic study. *Kidney International*, *85*(5), 1214–1224. https://doi.org/10.1038/ki.2013.497

Okuno, S., Ishimura, E., Kohno, K., Fujino-Katoh, Y., Maeno, Y., Yamakawa, T., Inaba, M., & Nishizawa, Y. (2008). Serum 2-microglobulin level is a significant predictor of mortality in maintenance haemodialysis patients. *Nephrology Dialysis Transplantation*, *24*(2), 571–577. https://doi.org/10.1093/ndt/gfn521

Ouseph, R., & Ward, R. A. (2001). Increasing Dialysate Flow Rate Increases Dialyzer Urea Mass Transfer-Area Coefficients During Clinical Use. *American Journal of Kidney Diseases*, *37*(2), 316–320. https://doi.org/10.1053/ajkd.2001.21296

Owen, W. F., Lew, N. L., Liu, Y., Lowrie, E. G., & Lazarus, J. M. (1993). The Urea Reduction Ratio and Serum Albumin Concentration as Predictors of Mortality in Patients Undergoing Hemodialysis. *New England Journal of Medicine*, *329*(14), 1001–1006. https://doi.org/10.1056/NEJM199309303291404

Paats, J., Adoberg, A., Arund, J., Dhondt, A., Fernström, A., Fridolin, I., Glorieux, G., Leis, L., Luman, M., Gonzalez-Parra, E., Perez-Gomez, V. M., Pilt, K., Sanchez-Ospina, D., Segelmark, M., Uhlin, F., & Arduan Ortiz, A. (2020). Serum Levels and Removal by Haemodialysis and Haemodiafiltration of Tryptophan-Derived Uremic Toxins in ESKD Patients. *International Journal of Molecular Sciences*, *21*(4), 1522. https://doi.org/10.3390/ijms21041522

Paats, J., Arund, J., Pilt, K., Adoberg, A., Leis, L., Luman, M., Holmar, J., Tanner, R., & Fridolin, I. (2024). Online Uric Acid Concentration Estimation in Blood from Spent Dialysate Measurements Using an Optical Sensor. In T. Jarm, R. Šmerc, & S. Mahnič-Kalamiza (Eds.), *IFMBE Proceedings* (pp. 178–187). Springer. https://doi.org/10.1007/978-3-031-61628-0_20

Perrone, A., Giovino, A., Benny, J., & Martinelli, F. (2020). Advanced Glycation End Products (AGEs): Biochemistry, Signaling, Analytical Methods, and Epigenetic Effects. *Oxidative Medicine and Cellular Longevity*, *2020*, 3818196. https://doi.org/10.1155/2020/3818196

Petitclerc, T., & Ridel, C. (2021). Routine online assessment of dialysis dose: Ionic dialysance or UV-absorbance monitoring? *Seminars in Dialysis*, *34*(2), 116–122. https://doi.org/10.1111/sdi.12949

Poesen, R., Mutsaers, H. A. M., Windey, K., van den Broek, P. H., Verweij, V., Augustijns, P., Kuypers, D., Jansen, J., Evenepoel, P., Verbeke, K., Meijers, B., & Masereeuw, R. (2015). The Influence of Dietary Protein Intake on Mammalian Tryptophan and Phenolic Metabolites. *PLOS ONE*, *10*(10), e0140820. https://doi.org/10.1371/journal.pone.0140820

Ponda, M. P., Quan, Z., Melamed, M. L., Raff, A., Meyer, T. W., & Hostetter, T. H. (2010). Methylamine clearance by haemodialysis is low. *Nephrology Dialysis Transplantation*, *25*(5), 1608–1613. https://doi.org/10.1093/ndt/gfp629

Prasad, S., Mandal, I., Singh, S., Paul, A., Mandal, B., Venkatramani, R., & Swaminathan, R. (2017). Near UV-Visible electronic absorption originating from charged amino acids in a monomeric protein. *Chemical Science*, *8*(8), 5416–5433. https://doi.org/10.1039/C7SC00880E

Pstras, L., Ronco, C., & Tattersall, J. (2022). Basic physics of hemodiafiltration. *Seminars in Dialysis*, *35*(5), 390–404. https://doi.org/10.1111/sdi.13111

Rački, S., Zaputović, L., Maleta, I., Gržetić, M., Mavrić, Ž., Devčić, B., & Vujičić, B. (2005). Assessment of Hemodialysis Adequacy by Ionic Dialysance: Comparison to Standard Method of Urea Removal. *Renal Failure*, *27*(5), 601–604. https://doi.org/10.1080/08860220500200262

Ranchin, B., & Shroff, R. (2024). Haemodiafiltration improves survival in patients receiving dialysis. *The Lancet*, *404*(10464), 1703–1705. https://doi.org/10.1016/S0140-6736(24)01938-X

Röckel, A., Hertel, J., Fiegel, P., Abdelhamid, S., Panitz, N., & Walb, D. (1986). Permeability and secondary membrane formation of a high flux polysulfone hemofilter. *Kidney International*, *30*(3), 429–432. https://doi.org/10.1038/ki.1986.202

Ronco, C. (1998). The haemodialysis system: basic mechanisms of water and solute transport in extracorporeal renal replacement therapies. *Nephrology Dialysis Transplantation*, *13*(90006), 3–9. https://doi.org/10.1093/ndt/13.suppl_6.3

Ronco, C., & Clark, W. R. (2018). Haemodialysis membranes. *Nature Reviews Nephrology*, *14*(6), 394–410. https://doi.org/10.1038/s41581-018-0002-x

Rosenheck, K., & Doty, P. (1961). The far ultraviolet absorption spectra of polypeptide and protein solutions and their dependence on conformation. *Proceedings of the National Academy of Sciences*, *47*(11), 1775–1785. https://doi.org/10.1073/pnas.47.11.1775

Rosner, M. H., Reis, T., Husain-Syed, F., Vanholder, R., Hutchison, C., Stenvinkel, P., Blankestijn, P. J., Cozzolino, M., Juillard, L., Kashani, K., Kaushik, M., Kawanishi, H., Massy, Z., Sirich, T. L., Zuo, L., & Ronco, C. (2021). Classification of Uremic Toxins and Their Role in Kidney Failure. *Clinical Journal of the American Society of Nephrology*, *16*(12), 1918–1928. https://doi.org/10.2215/CJN.02660221

Salazar, J. H. (2014). Overview of Urea and Creatinine. *Laboratory Medicine*, *45*(1), e19–e20. https://doi.org/10.1309/LM920SBNZPJRJGUT

Sánchez-Ospina, D., Mas-Fontao, S., Gracia-Iguacel, C., Avello, A., González de Rivera, M., Mujika-Marticorena, M., & Gonzalez-Parra, E. (2024). Displacing the Burden: A Review of Protein-Bound Uremic Toxin Clearance Strategies in Chronic Kidney Disease. *Journal of Clinical Medicine*, *13*(5). https://doi.org/10.3390/jcm13051428

Sargent, J. A., & Gotch, F. A. (1979). Principles and Biophysics of Dialysis. In *Replacement of Renal Function by Dialysis* (pp. 38–68). Springer Netherlands. https://doi.org/10.1007/978-94-009-9327-3_3

Schanstra, J. P., Zürbig, P., Alkhalaf, A., Argiles, A., Bakker, S. J. L., Beige, J., Bilo, H. J. G., Chatzikyrkou, C., Dakna, M., Dawson, J., Delles, C., Haller, H., Haubitz, M., Husi, H., Jankowski, J., Jerums, G., Kleefstra, N., Kuznetsova, T., Maahs, D. M., … Vanholder, R. (2015). Diagnosis and Prediction of CKD Progression by Assessment of Urinary Peptides. *Journal of the American Society of Nephrology*, *26*(8), 1999–2010. https://doi.org/10.1681/ASN.2014050423

Schjoldager, K. T., Narimatsu, Y., Joshi, H. J., & Clausen, H. (2020). Global view of human protein glycosylation pathways and functions. *Nature Reviews Molecular Cell Biology*, *21*(12), 729–749. https://doi.org/10.1038/s41580-020-00294-x

Schneditz, D., & Daugirdas, J. T. (2001). Compartment Effects in Hemodialysis. *Seminars in Dialysis*, *14*(4), 271–277. https://doi.org/10.1046/j.1525-139X.2001.00066.x

Schneditz, D., Yang, Y., Christopoulos, G., & Kellner, J. (2009). Rate of creatinine equilibration in whole blood. *Hemodialysis International*, *13*(2), 215–221. https://doi.org/10.1111/j.1542-4758.2009.00351.x

Sekula, P., Dettmer, K., Vogl, F. C., Gronwald, W., Ellmann, L., Mohney, R. P., Eckardt, K.-U., Suhre, K., Kastenmüller, G., Oefner, P. J., & Köttgen, A. (2017). From Discovery to Translation: Characterization of C-Mannosyltryptophan and Pseudouridine as Markers of Kidney Function. *Scientific Reports*, *7*(1), 17400. https://doi.org/10.1038/s41598-017-17107-5

Sekula, P., Goek, O.-N., Quaye, L., Barrios, C., Levey, A. S., Römisch-Margl, W., Menni, C., Yet, I., Gieger, C., Inker, L. A., Adamski, J., Gronwald, W., Illig, T., Dettmer, K., Krumsiek, J., Oefner, P. J., Valdes, A. M., Meisinger, C., Coresh, J., … Köttgen, A. (2016). A Metabolome-Wide Association Study of Kidney Function and Disease in the General Population. *Journal of the American Society of Nephrology*, *27*(4), 1175–1188. https://doi.org/10.1681/ASN.2014111099

Shafi, T., & Levey, A. S. (2018). Measurement and Estimation of Residual Kidney Function in Patients on Dialysis. *Advances in Chronic Kidney Disease*, *25*(1), 93–104. https://doi.org/10.1053/j.ackd.2017.09.001

Shafi, T., Michels, W. M., Levey, A. S., Inker, L. A., Dekker, F. W., Krediet, R. T., Hoekstra, T., Schwartz, G. J., Eckfeldt, J. H., & Coresh, J. (2016). Estimating residual kidney function in dialysis patients without urine collection. *Kidney International*, *89*(5), 1099–1110. https://doi.org/10.1016/j.kint.2015.10.011

Shafiee, S., Dastmalchi, S., Gharekhani, A., & Shayanfar, A. (2024). Analysis of indoxyl sulfate in biological fluids with emphasis on sample preparation techniques: A comprehensive analytical review. *Heliyon*, *10*(15), e35032. https://doi.org/10.1016/j.heliyon.2024.e35032

Sherman, R. A., Cody, R. P., Rogers, M. E., & Solanchick, J. C. (1995). Accuracy of the urea reduction ratio in predicting dialysis delivery. *Kidney International*, *47*(1), 319–321. https://doi.org/10.1038/ki.1995.41

Shroff, R., Basile, C., van der Sande, F., Mitra, S., Combe, C., Alfano, G., Covic, A., Franssen, C., Liakopoulos, V., Luyckx, V. A., & Meijers, B. (2023). Haemodiafiltration for all: are we CONVINCEd? *Nephrology Dialysis Transplantation*, *38*(12), 2663–2665. https://doi.org/10.1093/ndt/gfad136

Sirich, T. L. (2025). Can Intermittent Hemodialysis Normalize Plasma Solute Levels? *Kidney360*, *6*(3), 340–342. https://doi.org/10.34067/KID.0000000699

Sirich, T. L., Luo, F. J.-G., Plummer, N. S., Hostetter, T. H., & Meyer, T. W. (2012). Selectively increasing the clearance of protein-bound uremic solutes. *Nephrology Dialysis Transplantation*, *27*(4), 1574–1579. https://doi.org/10.1093/ndt/gfr691

Sivanathan, P. C., Ooi, K. S., Mohammad Haniff, M. A. S., Ahmadipour, M., Dee, C. F., Mokhtar, N. M., Hamzah, A. A., & Chang, E. Y. (2022). Lifting the Veil: Characteristics, Clinical Significance, and Application of β-2-Microglobulin as Biomarkers and Its Detection with Biosensors. *ACS Biomaterials Science & Engineering*, *8*(8), 3142–3161. https://doi.org/10.1021/acsbiomaterials.2c00036

Stanfield, C. L. (2013). *Principles of Human Physiology* (5th ed.). Pearson Education.

Steinbrenner, I., Schultheiss, U. T., Bächle, H., Cheng, Y., Behning, C., Schmid, M., Yeo, W.-J., Yu, B., Grams, M. E., Schlosser, P., Stockmann, H., Gronwald, W., Oefner, P. J., Schaeffner, E., Eckardt, K.-U., Köttgen, A., & Sekula, P. (2024). Associations of Urine and Plasma Metabolites With Kidney Failure and Death in a Chronic Kidney Disease Cohort. *American Journal of Kidney Diseases*, *84*(4), 469–481. https://doi.org/10.1053/j.ajkd.2024.03.028

Steinbrenner, I., Schultheiss, U. T., Kotsis, F., Schlosser, P., Stockmann, H., Mohney, R. P., Schmid, M., Oefner, P. J., Eckardt, K.-U., Köttgen, A., Sekula, P., Eckardt, K.-U., Meiselbach, H., Schneider, M. P., Schiffer, M., Prokosch, H.-U., Bärthlein, B., Beck, A., Reis, A., … Nadal, J. (2021). Urine Metabolite Levels, Adverse Kidney Outcomes, and Mortality in CKD Patients: A Metabolome-wide Association Study. *American Journal of Kidney Diseases*, *78*(5), 669–677. https://doi.org/10.1053/j.ajkd.2021.01.018

Stevens, L. A., & Levey, A. S. (2009). Measured GFR as a Confirmatory Test for Estimated GFR. *Journal of the American Society of Nephrology*, *20*(11), 2305–2313. https://doi.org/10.1681/ASN.2009020171

Stevens, P. E., Ahmed, S. B., Carrero, J. J., Foster, B., Francis, A., Hall, R. K., Herrington, W. G., Hill, G., Inker, L. A., Kazancıoğlu, R., Lamb, E., Lin, P., Madero, M., McIntyre, N., Morrow, K., Roberts, G., Sabanayagam, D., Schaeffner, E., Shlipak, M., … Levin, A. (2024). KDIGO 2024 Clinical Practice Guideline for the Evaluation and Management of Chronic Kidney Disease. *Kidney International*, *105*(4), S117–S314. https://doi.org/10.1016/j.kint.2023.10.018

Steyaert, S., Holvoet, E., Nagler, E., Malfait, S., & Van Biesen, W. (2019). Reporting of "dialysis adequacy" as an outcome in randomised trials conducted in adults on haemodialysis. *PLOS ONE*, *14*(2), e0207045. https://doi.org/10.1371/journal.pone.0207045

Storr, M., & Ward, R. A. (2018). Membrane innovation: closer to native kidneys. *Nephrology Dialysis Transplantation*, *33*(suppl_3), iii22–iii27. https://doi.org/10.1093/ndt/gfy228

Swan, J. S., Kragten, E. Y., & Veening, H. (1983). Liquid-chromatographic study of fluorescent materials in uremic fluids. *Clinical Chemistry*, *29*(6), 1082–1084. http://www.ncbi.nlm.nih.gov/pubmed/6851098

Takahira, R., Yonemura, K., Yonekawa, O., Iwahara, K., Kanno, T., Fujise, Y., & Hishida, A. (2001). Tryptophan glycoconjugate as a novel marker of renal function. *The American Journal of Medicine*, *110*(3), 192–197. https://doi.org/10.1016/S0002-9343(00)00693-8

Tanaka, H., Sirich, T. L., Plummer, N. S., Weaver, D. S., & Meyer, T. W. (2015). An Enlarged Profile of Uremic Solutes. *PLOS ONE*, *10*(8), e0135657. https://doi.org/10.1371/journal.pone.0135657

Tangvoraphonkchai, K., & Davenport, A. (2017). Enhancing dialyser clearance—from target to development. *Pediatric Nephrology*, *32*(12), 2225–2233. https://doi.org/10.1007/s00467-017-3647-y

Tattersall, J. (2018). Residual renal function in incremental dialysis. *Clinical Kidney Journal*, *11*(6), 853–856. https://doi.org/10.1093/ckj/sfy082

Tattersall, J., Martin-Malo, A., Pedrini, L., Basci, A., Canaud, B., Fouque, D., Haage, P., Konner, K., Kooman, J., Pizzarelli, F., Tordoir, J., Vennegoor, M., Wanner, C., ter Wee, P., & Vanholder, R. (2007). EBPG guideline on dialysis strategies. *Nephrology Dialysis Transplantation*, *22*(Supplement 2), ii5–ii21. https://doi.org/10.1093/ndt/gfm022

Tesch, G. H. (2010). Review: Serum and urine biomarkers of kidney disease: A pathophysiological perspective. *Nephrology*, *15*(6), 609–616. https://doi.org/10.1111/j.1440-1797.2010.01361.x

Thompson, L. E., & Joy, M. S. (2022). Endogenous markers of kidney function and renal drug clearance processes of filtration, secretion, and reabsorption. *Current Opinion in Toxicology*, *31*. https://doi.org/10.1016/j.cotox.2022.03.005

Tissue, B. M. (2012). Ultraviolet and Visible Absorption Spectroscopy. In *Characterization of Materials* (pp. 1–13). John Wiley & Sons, Inc. https://doi.org/10.1002/0471266965.com059.pub2

Torreggiani, M., Fois, A., Njandjo, L., Longhitano, E., Chatrenet, A., Esposito, C., Fessi, H., & Piccoli, G. B. (2021). Toward an individualized determination of dialysis adequacy: a narrative review with special emphasis on incremental hemodialysis. *Expert Review of Molecular Diagnostics*, *21*(11), 1119–1137. https://doi.org/10.1080/14737159.2021.1987216

Tuchin, V. (2007). *Tissue Optics*. SPIE. https://doi.org/10.1117/3.684093

Uhlin, F., & Fridolin, I. (2023). Optical Online Monitoring of Uremic Toxins beyond Urea. In *Updates on Hemodialysis*. IntechOpen. https://doi.org/10.5772/intechopen.110080

Uhlin, F., Fridolin, I., Magnusson, M., & Lindberg, L.-G. (2006). Dialysis dose (Kt/V) and clearance variation sensitivity using measurement of ultraviolet-absorbance (on-line), blood urea, dialysate urea and ionic dialysance. *Nephrology Dialysis Transplantation*, *21*(8), 2225–2231. https://doi.org/10.1093/ndt/gfl147

Uhlin, F., Holmar, J., Yngman-Uhlin, P., Fernström, A., & Fridolin, I. (2015). Optical Estimation of Beta 2 Microglobulin during Hemodiafiltration - Does It Work? *Blood Purification*, *40*(2), 113–119. https://doi.org/10.1159/000381797

van der Burgh, A. C., Geurts, S., Ahmad, S., Ikram, M. A., Chaker, L., Ferraro, P. M., & Ghanbari, M. (2024). Circulating metabolites associated with kidney function decline and incident CKD: a multi-platform population-based study. *Clinical Kidney Journal*, *17*(1). https://doi.org/10.1093/ckj/sfad286

van Gelder, M. K., Middel, I. R., Vernooij, R. W. M., Bots, M. L., Verhaar, M. C., Masereeuw, R., Grooteman, M. P., Nubé, M. J., van den Dorpel, M. A., Blankestijn, P. J., Rookmaaker, M. B., & Gerritsen, K. G. F. (2020). Protein-Bound Uremic Toxins in Hemodialysis Patients Relate to Residual Kidney Function, Are Not Influenced by Convective Transport, and Do Not Relate to Outcome. *Toxins*, *12*(4), 234. https://doi.org/10.3390/toxins12040234

van Oevelen, M., Bonenkamp, A. A., van Eck van der Sluijs, A., Bos, W. J. W., Douma, C. E., van Buren, M., Meuleman, Y., Dekker, F. W., van Jaarsveld, B. C., Abrahams, A. C., & DOMESTICO study group. (2024). Health-related quality of life and symptom burden in patients on haemodialysis. *Nephrology, Dialysis, Transplantation : Official Publication of the European Dialysis and Transplant Association - European Renal Association*, *39*(3), 436–444. https://doi.org/10.1093/ndt/gfad179

Vanholder, R., Boelaert, J., Glorieux, G., & Eloot, S. (2015). New Methods and Technologies for Measuring Uremic Toxins and Quantifying Dialysis Adequacy. *Seminars in Dialysis*, *28*(2), 114–124. https://doi.org/10.1111/sdi.12331

Vanholder, R., De Smet, R., Glorieux, G., Argilés, A., Baurmeister, U., Brunet, P., Clark, W., Cohen, G., De Deyn, P. P., Deppisch, R., Descamps-Latscha, B., Henle, T., Jörres, A., Lemke, H. D., Massy, Z. A., Passlick-Deetjen, J., Rodriguez, M., Stegmayr, B., Stenvinkel, P., … Zidek, W. (2003). Review on uremic toxins: Classification, concentration, and interindividual variability. *Kidney International*, *63*(5), 1934–1943. https://doi.org/10.1046/j.1523-1755.2003.00924.x

Vanholder, R., Glorieux, G., Argiles, A., Burtey, S., Cohen, G., Duranton, F., Koppe, L., Massy, Z. A., Ortiz, A., Masereeuw, R., Stamatialis, D., & Jankowski, J. (2025). Metabolomics to Identify Unclassified Uremic Toxins: A Comprehensive Literature Review. *Kidney Medicine*, *7*(3), 100955. https://doi.org/10.1016/j.xkme.2024.100955

Vanholder, R., Glorieux, G., & Eloot, S. (2015). Once upon a time in dialysis: the last days of Kt/V? *Kidney International*, *88*(3), 460–465. https://doi.org/10.1038/ki.2015.155

Vanholder, R., Hoefliger, N., De Smet, R., Ringoir, S., & Vogeleere, P. (1992). Extraction of protein bound ligands from azotemic sera: Comparison of 12 deproteinization methods. *Kidney International*, *41*(6), 1707–1712. https://doi.org/10.1038/ki.1992.244

Vanholder, R., Pletinck, A., Schepers, E., & Glorieux, G. (2018). Biochemical and Clinical Impact of Organic Uremic Retention Solutes: A Comprehensive Update. *Toxins*, *10*(1), 33. https://doi.org/10.3390/toxins10010033

Vanholder, R., Schepers, E., Pletinck, A., Nagler, E. V., & Glorieux, G. (2014). The Uremic Toxicity of Indoxyl Sulfate and p-Cresyl Sulfate. *Journal of the American Society of Nephrology*, *25*(9), 1897–1907. https://doi.org/10.1681/ASN.2013101062

Vanholder, R., Van Biesen, W., & Lameire, N. (2019). A swan song for Kt/V urea. *Seminars in Dialysis*, *32*(5), 424–437. https://doi.org/10.1111/sdi.12811

Vernooij, R. W. M., Bots, M. L., Strippoli, G. F. M., Canaud, B., Cromm, K., Woodward, M., Blankestijn, P. J., Davenport, A., Canaud, B., Barth, C., Strippoli, G., Hegbrant, J., Fischer, K., Cromm, K., Török, M., Woodward, M., Rose, M., & Bots, M. (2022). CONVINCE in the context of existing evidence on haemodiafiltration. *Nephrology Dialysis Transplantation*, *37*(6), 1006–1013. https://doi.org/10.1093/ndt/gfac019

Vivian, J. T., & Callis, P. R. (2001). Mechanisms of Tryptophan Fluorescence Shifts in Proteins. *Biophysical Journal*, *80*(5), 2093–2109. https://doi.org/10.1016/S0006-3495(01)76183-8

Wang, T., Zeng, L.-H., & Li, D.-L. (2017). A review on the methods for correcting the fluorescence inner-filter effect of fluorescence spectrum. *Applied Spectroscopy Reviews*, *52*(10), 883–908. https://doi.org/10.1080/05704928.2017.1345758

Ward, R. A., & Daugirdas, J. T. (2024). Kinetics of β-2-Microglobulin with Hemodiafiltration and High-Flux Hemodialysis. *Clinical Journal of the American Society of Nephrology*, *19*(7), 869–876. https://doi.org/10.2215/CJN.0000000000000461

Ward, R. A., Greene, T., Hartmann, B., & Samtleben, W. (2006). Resistance to intercompartmental mass transfer limits β2-microglobulin removal by post-dilution hemodiafiltration. *Kidney International*, *69*(8), 1431–1437. https://doi.org/10.1038/sj.ki.5000048

Wasung, M. E., Chawla, L. S., & Madero, M. (2015). Biomarkers of renal function, which and when? *Clinica Chimica Acta*, *438*, 350–357. https://doi.org/10.1016/j.cca.2014.08.039

Watanabe, Y., Kawanishi, H., Suzuki, K., Nakai, S., Tsuchida, K., Tabei, K., Akiba, T., Masakane, I., Takemoto, Y., Tomo, T., Itami, N., Komatsu, Y., Hattori, M., Mineshima, M., Yamashita, A., Saito, A., Naito, H., Hirakata, H., & Minakuchi, J. (2015). Japanese Society for Dialysis Therapy Clinical Guideline for “Maintenance Hemodialysis: Hemodialysis Prescriptions". *Therapeutic Apheresis and Dialysis*, *19*(S1), 67–92. https://doi.org/10.1111/1744-9987.12294

Weiner, I. D., Mitch, W. E., & Sands, J. M. (2015). Urea and Ammonia Metabolism and the Control of Renal Nitrogen Excretion. *Clinical Journal of the American Society of Nephrology : CJASN*, *10*(8), 1444–1458. https://doi.org/10.2215/CJN.10311013

Welch, A. J., & van Gemert, M. J. C. (2011). Optical-Thermal Response of Laser-Irradiated Tissue. In A. J. Welch & M. J. C. van Gemert (Eds.), *Optical-Thermal Response of Laser-Irradiated Tissue*. Springer Netherlands. https://doi.org/10.1007/978-90-481-8831-4

Yamamoto, M., Pinto-Sanchez, M. I., Bercik, P., & Britz-McKibbin, P. (2019). Metabolomics reveals elevated urinary excretion of collagen degradation and epithelial cell turnover products in irritable bowel syndrome patients. *Metabolomics*, *15*(6), 82. https://doi.org/10.1007/s11306-019-1543-0

Yang, S., Tian, X., Chen, Y., Shen, L., & Wang, J. (2022). Isotope-dilution liquid chromatography-tandem mass spectrometry method for serum beta 2-microglobulin quantification. *Journal of Chromatography B*, *1211*, 123487. https://doi.org/10.1016/j.jchromb.2022.123487

Yonemura, K., Takahira, R., Yonekawa, O., Wada, N., & Hishida, A. (2004). The diagnostic value of serum concentrations of 2-(α-mannopyranosyl)-l-tryptophan for normal renal function. *Kidney International*, *65*(4), 1395–1399. https://doi.org/10.1111/j.1523-1755.2004.00521.x

Zawada, A. M., Melchior, P., Schall, C., Erlenkötter, A., Lang, T., Keller, T., Stauss-Grabo, M., & Kennedy, J. P. (2022). Time-resolving characterization of molecular weight retention changes among three synthetic high-flux dialyzers. *Artificial Organs*, *46*(7), 1318–1327. https://doi.org/10.1111/aor.14216

Zhang, W. R., & Parikh, C. R. (2019). Biomarkers of Acute and Chronic Kidney Disease. *Annual Review of Physiology*, *81*(1), 309–333. https://doi.org/10.1146/annurev-physiol-020518-114605

Zhao, D., Sonawane, N. D., Levin, M. H., & Yang, B. (2007). Comparative transport efficiencies of urea analogues through urea transporter UT-B. *Biochimica et Biophysica Acta (BBA) - Biomembranes*, *1768*(7), 1815–1821. https://doi.org/10.1016/j.bbamem.2007.04.010

Zhao, J. (2015). Simultaneous determination of plasma creatinine, uric acid, kynurenine and tryptophan by high-performance liquid chromatography: method validation and in application to the assessment of renal function. *Biomedical Chromatography*, *29*(3), 410–415. https://doi.org/10.1002/bmc.3291

Acknowledgements

I am sincerely thankful to everyone who have contributed to the completion of this thesis with their time, knowledge and support.

My deepest gratitude goes to my supervisor, Prof. Ivo Fridolin, who has expertly guided my research and provided invaluable constructive feedback throughout my PhD studies with great patience. I am also profoundly thankful to my co-supervisor, Dr Merike Luman, for her unwavering commitment to improving patients' treatment. Together, your support and feedback have been indispensable, keeping me motivated and finding new perspectives despite setbacks and challenging outcomes.

I would like to extend my gratitude to my co-workers Dr Jürgen Arund and Dr Risto Tanner for introducing me chromatographical and spectroscopical methods and for the encouragement and thought-provoking discussions throughout the years.

I also wish to thank all my other colleagues from biofluid optics workgroup: Dr Annika Adoberg, Dr Jana Holmar, Dr Kai Lauri, Dr Liisi Leis, Dr Kristjan Pilt, engineer Denis Karai and technician Rain Kattai for the fruitful collaboration, assistance and co-authorship. Moreover, I thank my colleagues from Linköping, Gent and Madrid for conducting on-site studies, validating the ideas and providing critical feedback during the preparation of publications, which significantly enhanced their quality.

A heartfelt thanks to my family: especially my wife Maarika for her unwavering support and understanding during the countless hours spent on the research and my daughter Elli Marii for sharing your laughter, joy, and inspiration in exploring the world.

I am also grateful to students Maris Alev and Relika Toome for helping with the data collection and analysis during the studies and nurses at the North Estonia Medical Centre for assistance during the clinical experiments. Last but not least, I thank the dialysis patients who took part in the clinical experiments and made this research possible.

This work was funded partly by the European Union through the European Regional Development Fund H2020 – SMEINST – 2 – 2017, OLDIAS2 – On-line Dialysis Sensor Phase2 project with Grant Agreement nr 767572, by Estonian Centre of Excellence in IT (EXCITE) funded by European Regional Development Fund, by the Estonian Centre of Excellence of Well-Being Sciences (EstWell) by grant TK218, and by Estonian Research Council grants IUT 19-2, PSG819 and PRG2643 funded from the Estonian Ministry of Education and Research.

Abstract

Novel Spent Dialysate Based Optical Methods: Towards More Universal Dose Quantification of Haemodialysis

Haemodialysis (HD) is the most applied form of life-sustaining kidney replacement therapy for end stage of kidney disease (ESKD) patients, which is used to remove uraemic solutes and excessive fluid from patients' blood. As ESKD patients have among the highest mortality in patients with chronic diseases, improvements in HD treatment quality and adequacy are essential for improved survival.

To achieve this, usage of personalised and multidimensional dialysis dose quantification and prescription for HD has been proposed, including clearance of additional biomarkers such as prototypical middle-sized uremic retention molecule β-2-microglobulin (B2M), and residual kidney function as supplementary measures to the traditional Kt/V urea. Though, the impact of different HD treatment strategies on uraemic solutes removal is best characterized by monitoring the actual blood concentrations of patients over a period, i.e. using time-averaged concentration (TAC), or using pre-dialysis concentrations.

In practice, this requires cost-effective reliable methods and tools for monitoring these measures. Previously, accurate optical methods, utilising fluorescence and UV absorption measurements of spent dialysate, have been developed for monitoring Kt/V urea, and intradialytic removal of protein-bound and small water-soluble uraemic solutes prototypical markers, such as indoxyl sulfate (IS) and uric acid (UA). Yet, there is not a reliable optical method for monitoring B2M or residual kidney function markers, and estimation of blood concentrations of uraemic solutes using dialysate-based measurements has not been attempted.

The purpose of this thesis was to explore novel spent dialysate-based optical methods, which could be applied for more universal dose quantification of HD with the potential of ensuring more adequate HD treatment. Specifically, the thesis focused on development of predictive models, based on optical measurements of spent dialysate, to monitor removal of B2M and evaluate intradialytic levels and removal of novel endogenous kidney function marker C-mannosyl tryptophan (CMW). Furthermore, feasibility of estimating intradialytic serum TAC values from spent dialysate concentrations was studied for urea, B2M, UA and IS.

The publications of this thesis have been published based on the treatment data of 78 ESKD patients who were monitored during 312 different HD sessions. Collected blood and spent dialysate have been analysed using high performance liquid chromatography (HPLC) or clinical chemistry analyses as a reference to evaluate accuracy of optical methods and predictive models, utilising fluorescence and UV absorption measurements of spent dialysate.

The main results of the thesis are:

- Middle-sized molecules form a considerable fraction of optical signals of spent dialysate, presumably originating from intrinsic fluorescence of tryptophan in peptides and proteins, and advanced glycation end-products.
- Multiwavelength optical measurements of spent dialysate allow to estimate concentration of B2M in spent dialysate and monitor intradialytic removal of middle molecules with high accuracy.
- Endogenous kidney function biomarker CMW levels of ESKD patients are evidently over 10 times higher than in healthy subjects.

- Intradialytic removal of CMW is characteristic to small water-soluble uraemic solutes. Multiwavelength optical measurements of spent dialysate can be used to accurately monitor intradialytic levels and removal of CMW. This could help to elaborate the role of CMW in ESKD patients' health outcomes and evaluate residual kidney function in future.
- Spent dialysate concentrations and total removed solute (TRS) value of uraemic solutes are proportional to the intradialytic TAC of uraemic solutes in patient's blood. This thesis demonstrates for the first time that blood concentration of urea, UA, IS and B2M can be similarly predicted from their spent dialysate concentrations. This approach may prove useful in evaluating the impact of HD treatment on uraemic solutes levels over time.
- Spent dialysate based optical monitoring can be used to evaluate clinically relevant parameters such as TAC, TRS and reduction ratio, which make it possible to assess HD adequacy more universally. Therefore, optical monitoring of HD can be used as a non-invasive tool to potentially improve patients' health outcomes.

In conclusion, this thesis demonstrated that novel spent dialysate-based optical methods could be applied for more universal dose quantification of HD, which may provide more adequate HD treatment.

Lühikokkuvõte

Uudsed dialüsaadipõhised optilised meetodid universaalsema hemodialüüsravi doosi määramiseks

Hemodialüüsravi (HD) on neeruhaiguse lõppstaadiumis patsientide raviks enim rakendatav elusäilitav neeruasendusravi vorm, mille käigus eemaldatakse patsientide verest ureemilisi ühendeid ja liigne vedelik. Võrreldes teiste krooniliste haigetega on neeruhaiguse lõppstaadiumiga patsientide suremus üks kõrgemaid. Patsientide elumuse parendamiseks on tarvis seega suurendada HD ravikvaliteeti ja tõhusust.

Selle saavutamiseks on soovitatud HD ravidoosi hindamisel ja määramisel kasutada senisest personaalsemat ja mitmedimensionaalsemat käsitlust, mis arvestaks lisaks traditsioonilisele mõõdikule Kt/V uurea muuhulgas keskmisega suurusega ureemiliste ühendite markermolekuli β-2-mikroglobuliini (B2M) raviaegse eemaldamise efektiivsusega ja patsiendi säilinud neerufunktsiooniga. Ühtlasi on erinevate HD ravistrateegiate mõju ureemiliste ühendite eemaldamisele kõige parem hinnata nende ühendite tegeliku kontsentratsiooni järgi patsiendi veres, mis võib olla ajas keskmistatud kontsentratsioon (TAC) või HD-eelne vereproovi kontsentratsioon.

Praktikas on aga nende mõõdikute määramiseks tarvis kulutõhusaid ja töökindlaid meetodeid ning tööriistu. Seejuures on varasema töö käigus välja arendatud suure täpsusega optilised meetodid Kt/V uurea ja valkudega seonduvate ja väikeste vees lahustuvate molekulide markerite indoksüülsulfaadi (IS) ja kusihappe (UA) dialüüsiaegse eemaldamise määramiseks, mis põhinevad dialüüsiseansi käigus tekkiva dialüsaadi UV-kiirguse neelduvuse ja fluorestsentsi mõõtmisel. Samas on puudu usaldusväärne optiline meetod B2M ja neerufunktsiooni markerite määramiseks. Lisaks pole dialüsaadipõhiste mõõtmiste abil üritatud hinnata ureemiliste ühendite kontsentratsiooni patsiendi veres.

Käesoleva doktoritöö eesmärgiks oli välja töötada uudsed dialüsaadipõhised optilised meetodid, mida oleks võimalik rakendada universaalsemaks HD ravidoosi määramiseks, et tagada kvaliteetsem HD-ravi. Täpsemalt keskendus doktoritöö dialüsaadi optilistel mõõtmistel põhinevate algoritmide väljatöötamisele, et hinnata B2M-i ja uudse endogeense neerufunktsiooni markeri C-mannosüültrüptofaani (CMW) raviaegset eemaldamist ning kontsentratsioone. Lisaks hinnati markerite uurea, B2M, UA ja IS dialüüsraviaegse seerumi TAC-i määramise teostatavust dialüsaadi kontsentratsioonidest lähtuvalt.

Käesoleva doktoritöö publikatsioonid on avaldatud 78 neeruhaiguse lõppstaadiumis patsiendi raviandmete põhjal, keda jälgiti 312 erineva HD seansi ajal. Kogutud vere- ja dialüsaadiproovide analüüsimiseks kasutati referentsina kõrgsurvevedelikkromatograafiat (HPLC) või kliinilise keemia meetodeid hindamaks optiliste meetodite ja algoritmide täpsust, mis põhinevad dialüsaadi fluorestsentsi ja UV-neeldumise mõõtmisel.

Töö peamised tulemused on:

- Keskmise suurusega molekulid moodustavad märkimisväärse osa dialüsaadi optilistest signaalidest, mis arvatavasti tuleneb peptiidide ja valkude trüptofaanijääkide või glükeerimise lõpp-produktide fluorestsentsist.
- Dialüsaadi optilised mõõtmised mitmel erineval lainepikkusel võimaldavad suure täpsusega hinnata B2M-i kontsentratsiooni dialüsaadis ning hinnata keskmise suurusega ureemiliste molekulide dialüüsiaegset eemaldamist.
- Endogeense neerufunktsiooni markeri CMW kontsentratsioon on lõppstaadiumis neeruhaigusega patsientidel üle kümne korra kõrgem võrreldes tervete inimestega.

- CMW dialüüsiaegne eemaldamiskineetika on sarnane väikestele vees lahustuvatele molekulidele. Dialüsaadi optilised mõõtmised mitmel erineval lainepikkusel võimaldavad hinnata CMW dialüüsiaegset eemaldamist ning kontsentratsioone. Välja töötatud optiline meetod võib tulevikus aidata hinnata CMW mõju neerupuudulikkusega patsientide tervisele või olla kasulik neerufunktsiooni hindamisel.
- Ureemiliste ühendite kontsentratsioonid dialüsaadis ja eemaldatud ainete koguhulk on proportsionaalne patsiendi veres leiduvate ureemiliste ühendite dialüüsiaegse TAC-iga. Käesolev doktoritöö näitas esmakordselt, et uurea, UA, IS-i ja B2M-i dialüüsraviaegseid kontsentratsioone veres saab ennustada nende ühendite dialüsaadi kontsentratsioonidest lähtuvalt. Sellest võib olla abi dialüüsravi ureemiliste ühendite kehast eemaldamise efektiivsuse hindamisel.
- Dialüsaadipõhiste optiliste meetoditega saab mitteinvasiivselt hinnata kliiniliselt olulisi parameetreid nagu ureemiliste ühendite TAC, eemaldatud aine koguhulk ja suhteline eemaldamise määr, mis võimaldab hinnata HD efektiivsust ja ravidoosi universaalsemalt. HD optiline monitooring võiks seeläbi potentsiaalselt parendada HD ravikvaliteeti.

Kokkuvõtvalt näitas käesolev töö, et uudseid dialüsaadipõhised optilisi meetodeid on võimalik rakendada universaalsemaks HD ravidoosi määramiseks, et tagada potentsiaalselt efektiivsem HD-ravi.

Appendix 1 – Overview of the clinical set-up

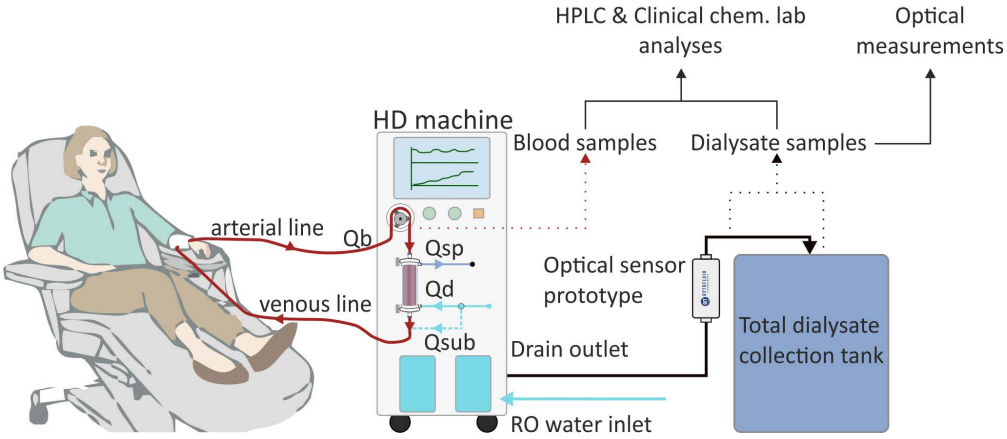

Figure 8. Overview of the clinical set-up during the studies. In case of zero net ultrafiltration, ultrafiltration rate is equal to substitution fluid's flow rate (Qsub) and spent dialysate flow rate (Qsp) is the sum of Qsub and dialysate flow rate (Qd) in post-dilution haemodiafiltration regime; with Qb marking the blood flow rate.

Appendix 2 – Publication I

Publication I

Paats, J., Adoberg, A., Arund, J., Fridolin, I., Lauri, K., Leis, L., Luman, M., Tanner, R. (2021). Optical Method and Biochemical Source for the Assessment of the Middle-Molecule Uremic Toxin β2-Microglobulin in Spent Dialysate. *Toxins*, *13*, 255. https://doi.org/10.3390/toxins13040255.

toxins

MDPI

Article

Optical Method and Biochemical Source for the Assessment of the Middle-Molecule Uremic Toxin β2-Microglobulin in Spent Dialysate

Joosep Paats [1,*], Annika Adoberg [2], Jürgen Arund [1], Ivo Fridolin [1], Kai Lauri [1,3], Liisi Leis [2], Merike Luman [1,2] and Risto Tanner [1]

[1] Department of Health Technologies, Tallinn University of Technology, 19086 Tallinn, Estonia; Jurgen.Arund@taltech.ee (J.A.); Ivo.Fridolin@taltech.ee (I.F.); Kai.Lauri@synlab.ee (K.L.); Merike.Luman@regionaalhaigla.ee (M.L.); Risto.Tanner@taltech.ee (R.T.)
[2] Centre of Nephrology, North Estonia Medical Centre, 13419 Tallinn, Estonia; Annika.Adoberg@regionaalhaigla.ee (A.A.); Liisi.Leis@regionaalhaigla.ee (L.L.)
[3] SYNLAB Eesti OÜ, 10138 Tallinn, Estonia
* Correspondence: Joosep.Paats@taltech.ee

Abstract: Optical monitoring of spent dialysate has been used to estimate the removal of water-soluble low molecular weight as well as protein-bound uremic toxins from the blood of end stage kidney disease (ESKD) patients. The aim of this work was to develop an optical method to estimate the removal of β2-microglobulin (β2M), a marker of middle molecule (MM) uremic toxins, during hemodialysis (HD) treatment. Ultraviolet (UV) and fluorescence spectra of dialysate samples were recorded from 88 dialysis sessions of 22 ESKD patients, receiving four different settings of dialysis treatments. Stepwise regression was used to obtain the best model for the assessment of β2M concentration in the spent dialysate. The correlation coefficient 0.958 and an accuracy of 0.000 ± 0.304 mg/L was achieved between laboratory and optically estimated β2M concentrations in spent dialysate for the entire cohort. Optically and laboratory estimated reduction ratio (RR) and total removed solute (TRS) of β2M were not statistically different ($p > 0.35$). Dialytic elimination of MM uremic toxin β2M can be followed optically during dialysis treatment of ESKD patients. The main contributors to the optical signal of the MM fraction in the spent dialysate were provisionally identified as tryptophan (Trp) in small peptides and proteins, and advanced glycation end-products.

Keywords: β2-microglobulin; hemodialysis; dialysis adequacy; middle molecule uremic toxins; optical monitoring; ultraviolet absorbance; fluorescence

Key Contribution: Middle molecule (MM) uremic toxins have considerable contribution to the overall optical properties of spent dialysate, which allows to optically monitor removal of MM toxins like β2-microglobulin. Future research should address identifying specific MM uremic toxins behind the optical properties of MM fraction.

Citation: Paats, J.; Adoberg, A.; Arund, J.; Fridolin, I.; Lauri, K.; Leis, L.; Luman, M.; Tanner, R. Optical Method and Biochemical Source for the Assessment of the Middle-Molecule Uremic Toxin β2-Microglobulin in Spent Dialysate. *Toxins* **2021**, *13*, 255. https://doi.org/10.3390/toxins13040255

Received: 12 February 2021
Accepted: 29 March 2021
Published: 31 March 2021

1. Introduction

The largest number of the end stage kidney disease (ESKD) patients are treated using hemodialysis (HD), which has remained one of the most expensive and time-consuming methods among the treatments of chronic diseases. Therefore, the monitoring of HD quality, related to the removal efficiency of the uremic solutes in dialysis, is important to ensure adequacy and cost-efficiency of the HD procedure [1,2]. Optical monitoring of the spent dialysate on the outflow from the dialysis machine is a promising alternative to dialysis adequacy estimation based on blood sampling [3]. While ultraviolet (UV) absorbance monitoring of the spent dialysate [4–6] enables determining urea-based dialysis quality parameters [7,8], the potential of optical dialysis monitoring is wider. Earlier

research has shown the potential of optical monitoring of the spent dialysate to estimate the removal of low molecular weight uremic toxins [9–14], elimination of electrolytes, such as phosphate and calcium, [15,16], and possibly for nutrition assessment [17]. As a result, the UV monitoring of the removal of low molecule weight uremic solutes by HD treatment has become commonly applied in the treatment practice worldwide [18–20]. Furthermore, fluorescence of spent dialysate has proved to be well applicable for on-line removal monitoring of protein-bound uremic toxins [21–23]. However, many recent publications have confirmed the essential role of middle molecule (MM) group of uremic toxins in pathology and mortality of ESKD patients [24–28]. Despite promising works exploring the correlation between optical properties of spent dialysate and MM molecules, the biochemical origin of the MM toxins' optical contribution to the optical signal has not yet been revealed [29–31]. Still, the optimization of the removal of MM uremic solutes has remained an unsolved problem in the treatment of ESKD patients [32].

The aim of this study was to develop an improved optical method based on the UV absorbance and fluorescence of the spent dialysate for the assessment of the concentration of β2-microglobulin (β2M) in the spent dialysate as the specific marker of MM uremic toxins in dialysate, and to explore the methods' biochemical origins.

2. Results

2.1. Correlations between Optical Data and Concentration of β2M in Dialysate

Correlations between UV absorbance of spent dialysate at different wavelengths and concentration of β2M in spent dialysate can be seen in Figure 1 based on the data from all three hemodiafiltration (HDF) modalities (including the tank samples). The best correlation was observed at the UV wavelengths around 222 nm (R^2 = 0.881). The range of UV absorption of aromatic amino acids at 275–280 nm exhibited a slightly weaker correlation (R^2 = 0.862); surprisingly, quite a good correlation became evident at the wavelength of 311 nm (R^2 = 0.865).

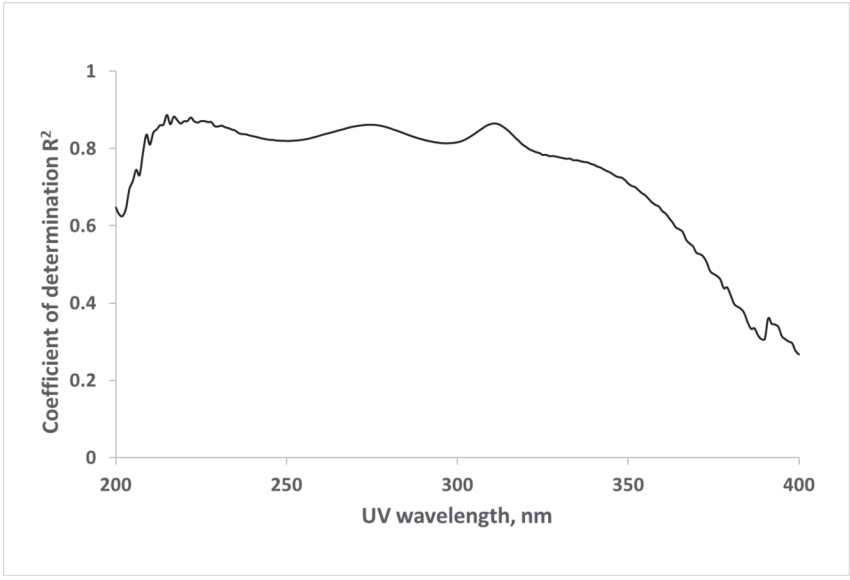

Figure 1. Wavelength dependence of the correlation between ultraviolet (UV)-absorbance of spent dialysate and concentration of β2-microglobulin (β2M) in spent dialysate for hemodiafiltration (HDF) modalities (N = 375).

The best correlation between the fluorescence of spent dialysate and the concentration of β2M in spent dialysate was found in the wavelength region Ex350–370/Em500–555 nm with the coefficient of determination R^2 up to 0.859 (Figure 2).

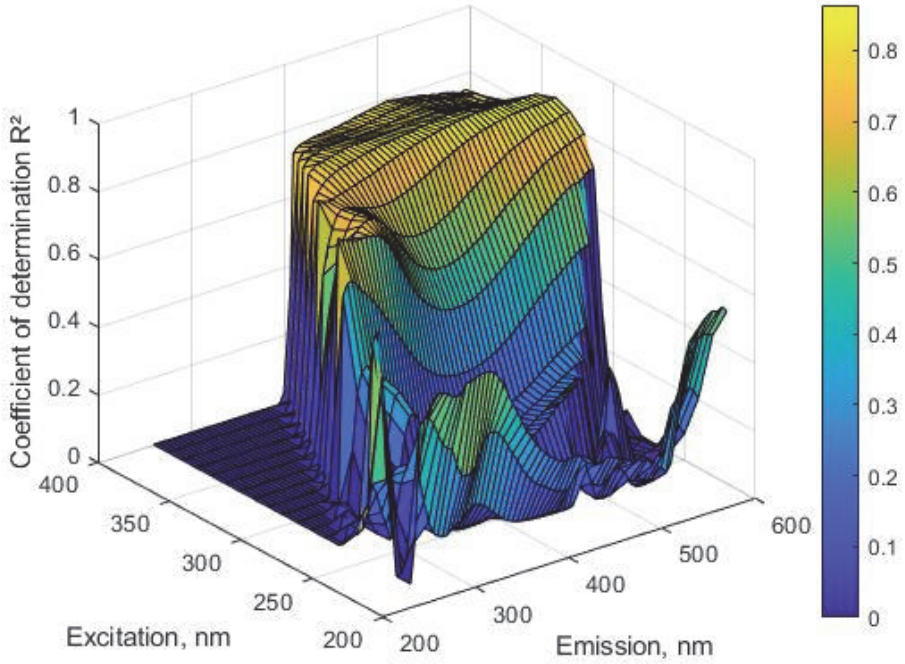

Figure 2. Wavelength dependence of the correlation between fluorescence intensity and concentration of β2M in spent dialysate for HDF modalities (N = 375).

The highest correlation between the spectral data of the dialysate and the concentration of β2M was observed in the case of combined UV absorbance with the fluorescence. The best correlations between UV absorbance, the excitation/emission of spent dialysate and the concentration of the β2M in spent dialysate were selected using multiple regression analysis yielding a model including the following optical parameters; UV absorbance at 280 nm, fluorescence Ex280/Em325 and Ex350/Em555 (adjusted R 0.958, accuracy (BIAS ± SE) 0.000 ± 0.304, N = 375).

The identity and Bland Altman plots of the calibration and the validation groups comparing β2M determined at the clinical laboratory (Lab) and predicted optically (Opt), can be seen in Figure 3. The concentration of β2M in the dialysate for both groups was calculated with the algorithm, derived from regression data of the calibration group using optical parameters showing the best correlation combination. The correlation coefficient 0.966 with the accuracy of 0.000 ± 0.272 mg/L was achieved for the calibration group, and the correlation coefficient 0.953 with the accuracy of 0.061 ± 0.340 mg/L was achieved for the validation group between the laboratory estimated β2M concentration in spent dialysate and the corresponding values predicted by the optical model, respectively.

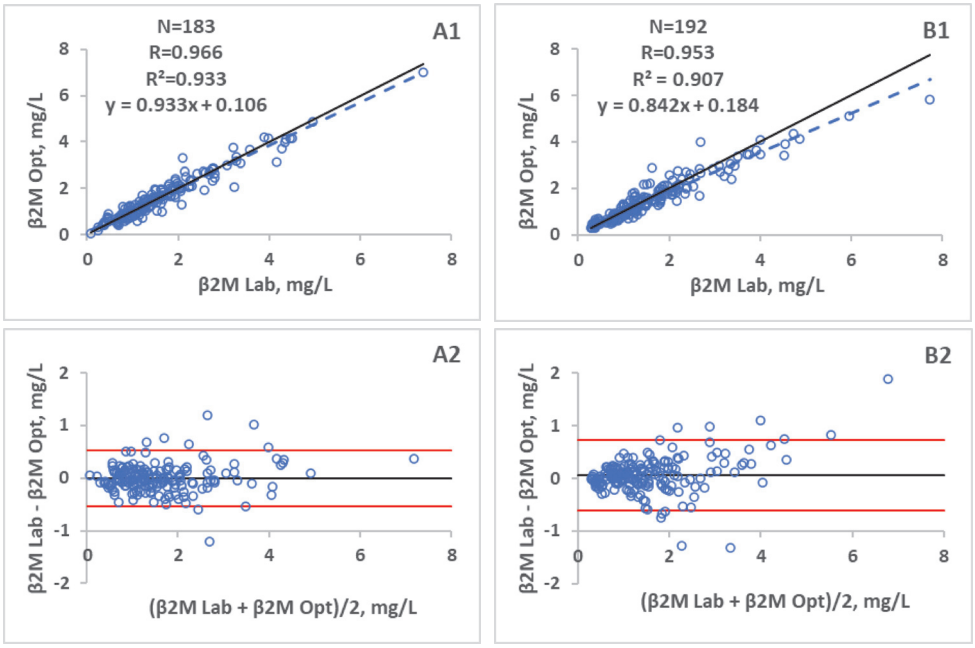

Figure 3. Identity plots of the β2M concentration in spent dialysate determined at the clinical laboratory (Lab) and predicted optically (Opt), and Bland-Altman plots of the differences between Lab and Opt concentrations. **A**—Calibration set, **B**—Validation set, 1—Regression plot, 2—Bland-Altman plot.

Figure 4 shows average changes of β2M concentration in the spent dialysate during the dialysis treatments estimated in parallel at the laboratory and optically for the validation set. The optically derived β2M concentration time profile corresponds well with the lab data.

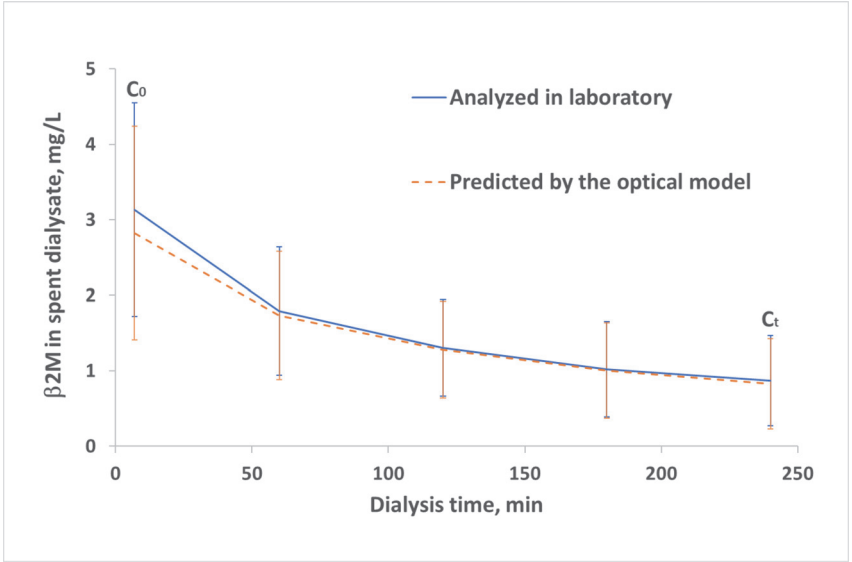

Figure 4. Time-series of changing β2M concentration (mean ± SD) in the spent dialysate during HDF dialysis sessions (N = 29) for patients of the validation set.

Corresponding clinical output for the validation set as the reduction ratio (RR) and total removed solute (TRS) values for β2M are presented in Table 1 using the best multi-regression model (Figure 3) for β2M concentration prediction from the optical measurements. Optically and laboratory estimated values of RR and TRS were not statistically different ($p > 0.34$ and $p > 0.35$, respectively).

Table 1. Clinical output of β2M removal by HDF dialysis as the average reduction ratio (RR) and the total removed solute (TRS) for the validation set.

Clinical Parameter	β2M Lab Mean ± SD	β2M Opt Mean ± SD	*p*	Accuracy (BIAS ± SE)	Pearson Correlation
RR (%, N = 31)	73.37 ± 10.39	72.06 ± 7.77	0.35	−1.31 ± 5.41	0.894
TRS (mg, N = 33)	234.5 ± 72.8	228.6 ± 83.9	0.35	−5.95 ± 36.09	0.904

2.2. UV and Fluorescence Spectra of the MM Fraction

Figure 5 shows the average UV spectra measured as the difference between untreated spent dialysate samples and filtrates, containing solutes < 1kDa of the corresponding dialysate from standard HDF (stHDF) and low flux HD (LF HD) modalities (see Table 4 for dialysis settings). The most noticeable difference in UV absorbance referable to compounds with MW > 1 kDa seems to be in the wavelength region of 210–230 nm. Differences between the spectra of dialysate and corresponding filtrates, referable to compounds with MW > 1 kDa, were considered as characteristics of "MM fraction" hereinafter.

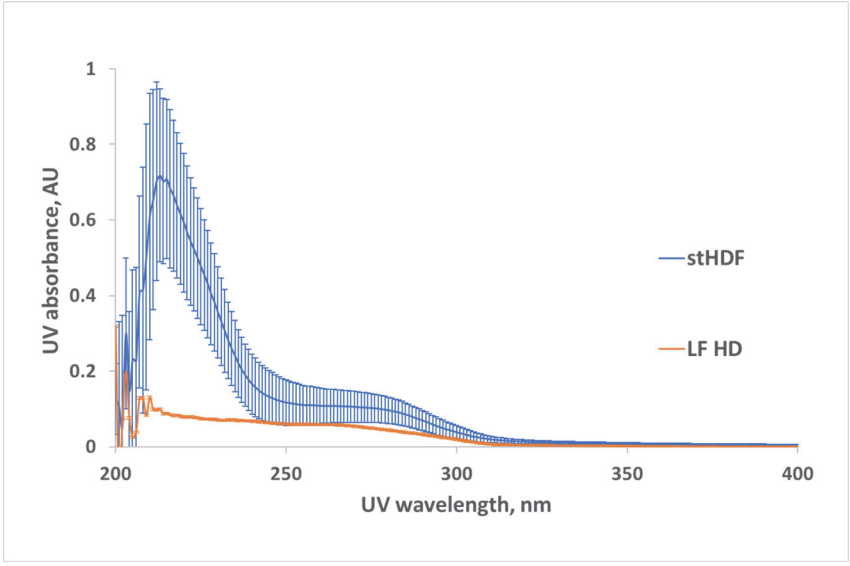

Figure 5. UV spectra (mean ± SD, N = 9) of middle molecule (MM) fractions of 7 min dialysate from low flux HD (LF HD) and standard HDF (stHDF) modality. The untreated dialysate was measured against corresponding filtrate containing solutes < 1 kDa for a subset of samples.

Figure 6 shows the interrelationship between UV absorbance of untreated spent dialysate samples and corresponding filtrates, containing solutes < 1 kDa, from LF HD and stHDF modalities. The very high R^2 value indicates that variation between optical signals of dialysate samples and corresponding filtrates, caused by the MM fraction, is negligible in the UV region > 230 nm.

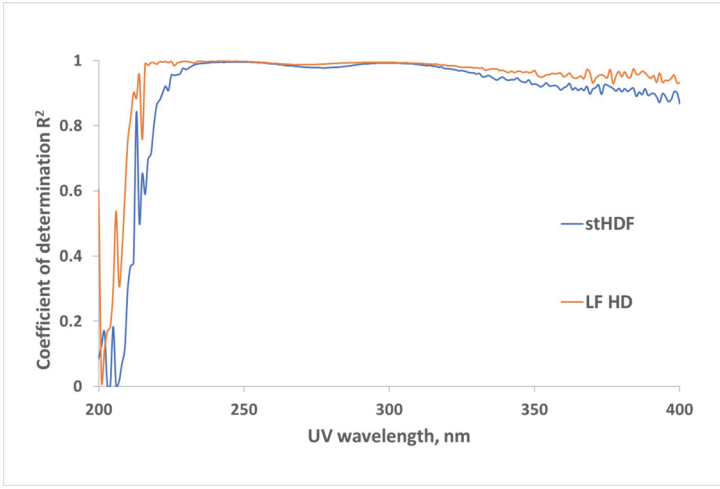

Figure 6. Correlation between UV-absorbance of untreated spent dialysate samples and UV-absorbance of corresponding filtrates, containing solutes < 1 kDa, from LF HD and the stHDF modalities sampled 7 min after the start of the dialysis from a subset of samples (N = 17).

The mean fluorescence emission spectra of MM fractions with characteristic wavelengths of excitation, where the largest difference between MM fractions of LF HD and stHDF can be seen, are shown in Figure 7. Emission wavelengths are presented starting with the lowest meaningful excitation wavelength (i.e., for Ex220 nm emission starts from 230 nm; for Ex280 nm Em starts from 290 nm, and for Ex350 nm Em starts from 360 nm). The predominant maximum emission of the expected MM fraction is evident in the wavelength region Ex280/Em325–335 nm. The fluorescence characteristic to advanced glycation end-products (AGEs) Ex350/Em430–550 nm is present in Figure 7, but with ~10 times weaker intensity compared to fluorescence at Ex280/Em325–335 nm.

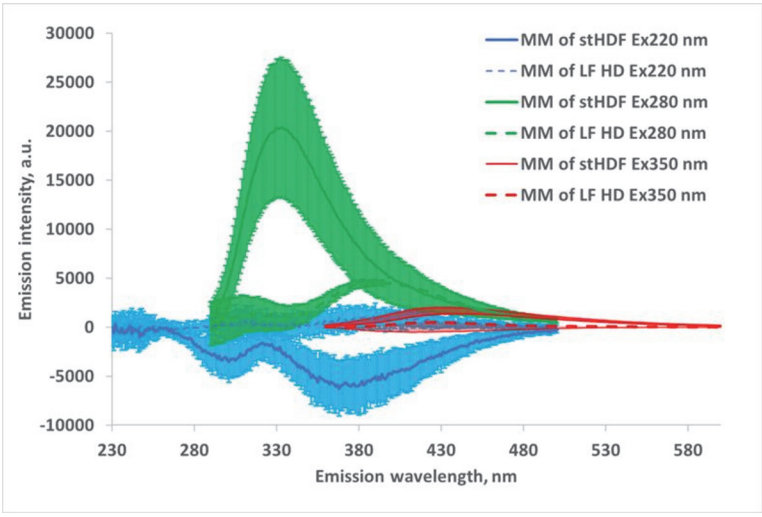

Figure 7. Fluorescence emission spectra (mean ± SD, N = 17) of MM fractions of dialysate measured as the difference between untreated dialysate and corresponding filtrates, containing solutes < 1 kDa, from LF HD and the stHDF modalities sampled 7 min after the start of the dialysis at some characteristic wavelengths from a subset of samples.

For a subset of the stHDF samples collected 7 min after the start (N = 17), MM fraction contributed on average 26.09 ± 6.68% at Ex280/Em325 nm to overall fluorescence of the spent dialysate.

Figure 8 shows that the correlation between the optical signals of dialysate samples and corresponding filtrates is lowest in the wavelength region Ex280/Em320–330 nm due to removal of the MM fraction by filtration. This coincides with the predominant maximum emission region of the MM fraction in Figure 7. The lowest correlation is seen at Ex280/Em325 nm, with the coefficient of determination R^2 equal to 0.76.

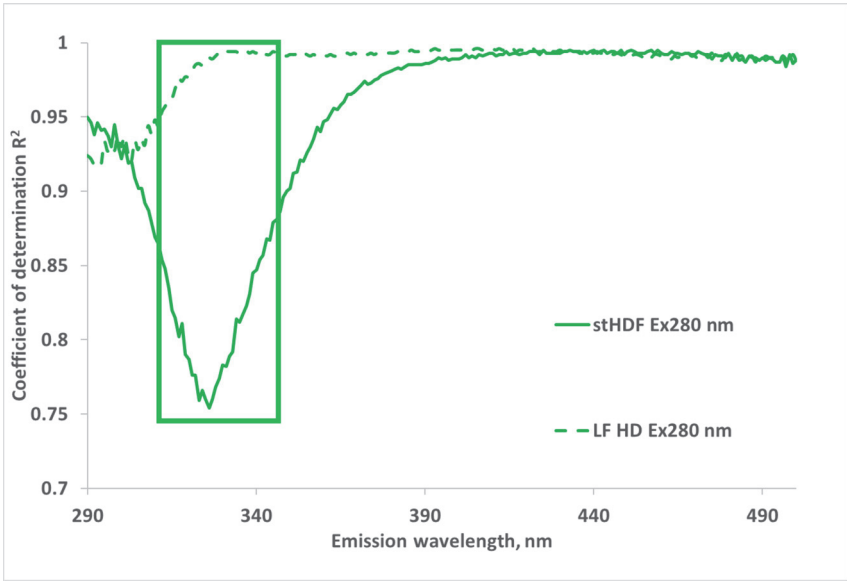

Figure 8. Correlation between fluorescence emission spectra of untreated spent dialysate and corresponding filtrates, containing uremic solutes < 1 kDa, from LF HD and the stHDF modalities sampled 7 min after the start of the dialysis at Ex280 nm from a subset of samples (N = 17). Emission region with the highest correlation between β2M in the spent dialysate, used in the final regression model, is marked with a rectangle.

3. Discussion

The main findings of the study were: (1) concentration of MM uremic toxin β2M in spent dialysate can be assessed using the UV absorbance and fluorescence of the spent dialysate; (2) β2M concentration prediction from the optical measurements can be used for intradialytic β2M removal assessment as the RR and the TRS; (3) the main contributions to the optical signal of the MM fraction arise apparently from the fluorescence of tryptophan (Trp) in small proteins and peptides and the fluorescence of AGEs, whereas UV absorbance of the peptide bond and aromatic side chains of amino acids seems to have a smaller contribution.

Strong correlation and high accuracy were achieved in comparing the biochemically and optically estimated concentration of the MM uremic toxin β2M in spent dialysate using multiple regression analysis based on the data from all three HDF modalities (R value 0.966 and 0.953, accuracy 0.000 ± 0.272 mg/L and 0.061 ± 0.340 mg/L for the calibration and the validation group, respectively). This enabled visualizing the changing β2M concentration in the spent dialysate during dialysis (Figure 4) and calculating the intradialytic β2M removal by HDF dialysis as RR and TRS from the optical signal (Table 1). The biochemically and optically assessed RR and TRS values were not statistically different ($p > 0.34$ and $p > 0.35$, respectively). Although the removal of β2M is limited by intercompartmental mass transfer, an RR of 68 ± 2% was achieved in an earlier study of 10 patients with HDF in

the post-dilution mode, calculated from pre- and post-treatment serum levels of β2M [33]. Our result of an optically estimated RR of 72.06 ± 7.77% is comparable, considering that two modalities besides the standard HDF were aimed to achieve the maximal removal of middle molecules in our settings. A mean total single session removal of β2M 204.9 ± 53.4 mg was observed by Brunati et al., using standard high-flux bicarbonate dialysis [34], which is similar to the value 228.6 ± 83.9 mg, achieved in this work using optical assessment technology combined with the total dialysate collection.

A comparison of both UV absorbance and fluorescence spectra of untreated HDF dialysate with corresponding filtrates, containing solutes < 1kDa (Figures 5 and 7), as well as the corresponding comparison of HDF and LF HD spent dialysate strongly supports the idea that optical properties of dialysate provide a potential for on-line monitoring of eliminating not only small and protein-bound molecules, but also middle molecule uremic toxins from the blood of ESKD patients [29–31]. The highest absorbance in the short wavelength region of UV light could be expected in the light of present knowledge about the peptide nature and amino acid composition of the MM uremic toxins [35]. The most widely used features of the absorbance spectra of proteins are attributed to chromophores present in the sidechains of aromatic amino acids like Trp around 280 nm ($\varepsilon \sim 5600\ M^{-1}\ cm^{-1}$), tyrosine around 275 nm ($\varepsilon \sim 1420\ M^{-1}\ cm^{-1}$) and phenylalanine around 257 nm ($\varepsilon \sim 197\ M^{-1}\ cm^{-1}$) [36]. Our results from LF and stHDF modalities (Figure 6) confirm that the MM fraction does not have considerable contribution to the overall UV absorbance of spent dialysate in relation to other chromophores in spent dialysate [12] at corresponding wavelengths. The peptide bond in proteins has a strong absorbance at around 190 nm ($\varepsilon \sim 7000\ M^{-1}\ cm^{-1}$) and a weaker absorbance between 210 and 220 nm ($\varepsilon \sim 100\ M^{-1}\ cm^{-1}$) [37]. As dialysate has a very high absorbance below 230 nm [38,39], and upper absorbance measurement limit of a spectrophotometer was exceeded for some of the samples, which caused noisy data below 230 nm; the cuvette with a shorter optical path length or dilution of spent dialysate samples must be used for a more detailed search of usability of this UV absorbance region for the assessment of MM removal by dialysis as it enables distinguishing the variation caused by the noise and MM fraction more clearly.

The abovementioned three amino acids are mainly responsible for the inherent fluorescence properties of proteins, with Trp being the dominant intrinsic fluorophore in proteins (Table 2). The deep negative emission of the peak at Ex220/Em370–380 nm (Figure 7) is evidently caused by excitation light absorbance in the short UV wavelength region (so-called inner filter effect) observed also in many other mixtures of fluoro- and chromophores in solutions [40,41].

Table 2. The fluorescent properties of aromatic amino acids in water at neutral pH [42].

Amino Acid	Excitation Wavelength (nm)	Emission Wavelength (nm)	Bandwidth (nm)	Quantum Yield
Tryptophan	295	353	60	0.13
Tyrosine	275	304	34	0.14
Phenylalanine	260	282	-	0.02

In addition to the intrinsic fluorescence of these amino acids, a set of UV-absorbing and fluorescent post-translational modifications, including AGEs, has been described, where free amino groups of aliphatic amino acids are involved [43–46]. Such types of chromo- and fluorophores are known to accumulate in chronic hemodialysis patients [47–50] and have a large variety of toxic effects for dialysis patients [51]. Only a small part of AGEs has a fluorescence excitation region in the usual absorption wavelength of proteins [46]. Still, the fluorescence of deproteinized serum, specific to AGEs (Ex370/Em440 nm), has been found to predict mortality in hemodialysis patients [52]. AGE pentosidine, which is a crosslink between arginine and lysine residues in proteins [53], has an absorption at 335 nm and a maximum emission at about 375–385 nm [54,55]. Among other typical fluorescent

AGEs, argpyrimidine has high absorbance between 320 and 335 nm, and a fluorescence emission maximum of about 400 nm [56]; the vesperlysine A, a crosslink between two lysine residues, has a maxima of absorption at 302 and 263 nm and maxima of emission at 380 and 440 nm [57]. The crossline, another crosslink between two lysine residues, has an emission maximum at 440 nm with excitation at 380 nm [56]. The human β2M modified by glycation is the major component of hemodialysis-associated amyloidosis and has an emission maximum at 450 nm with an excitation at 360 nm [58]. This coincides with the higher emission intensity above 400 nm of an MM fraction at an excitation of 350 nm measured in the spent dialysate from HDF (Figure 7). Moreover, the fluorescence in the same Ex/Em wavelength region exhibited a high degree of correlation with the concentration of β2M in our experiments (Figure 2), with the highest correlation at even higher emission wavelengths of up to 555 nm. This agreement indicates that the fluorescence of AGEs may be the main source of fluorescence of the MM fraction of spent dialysate at least in the longer excitation wavelength region, where aromatic amino acids of MM fraction do not exhibit fluorescent properties. An emission maximum around 450 nm as well as a clear difference between HD and HDF dialysate in this region (Figure 7) supports the essential role of AGEs in the formation of the fluorescence of the MM fraction. Some shifts in highest correlation values between β2M and emission toward longer wavelengths above 450 nm (Figure 2) may be explained to some degree by the energy transfer between different fluorophores in the dialysate (e.g., Förster resonance energy transfer) [59,60] as well as by re-absorbance by different fluorophores and re-emission in longer wavelength regions.

Some weak emissions of non-modified β2M can be achieved with excitation at 220 nm, but such emissions of spent dialysate were found to be independent of the concentration of β2M in the dialysate leading to the conclusion that the β2M in spent dialysate cannot be directly monitored by spectrophotometric measurements [61]. Our spectra of the MM fraction of dialysate (Figure 7) confirm this statement regarding that neither the emission of glycated nor normal β_2M are evidently dominant in the total fluorescence of spent dialysate at shorter excitation wavelengths when not corrected for the primary inner filter effect. However, correction of the inner filter effect is crucial to achieve a linear relationship between the fluorophore's concentration and fluorescence in highly absorbing samples [40,41] such as spent dialysate [38,39].

The most essential role in the formation of fluorescence of MM fraction seems to originate from the emission region 320–340 nm, with the average maximum at 332 nm, if excited at 280 nm (Figures 7 and 8), which is common for fluorescence of Trp residues in hydrophobic environment of peptides and proteins [62]. This is also close to intrinsic Trp fluorescence of β2M under native condition with the peak at ~337 nm [63]. MM fractions contributed on average 26.09 ± 6.68% to the overall fluorescence of spent dialysate at Ex280/Em325 nm at the beginning of dialysis from the stHDF modality. Interestingly, for the same dataset, the correlation between optical signals of dialysate samples and the corresponding filtrates, containing solutes < 1 kDa, was lowest in the wavelength region Ex280/Em320–330 nm due to the removal of the MM fraction (R^2 = 0.76), which confirms the high contribution of the MM fraction to the overall fluorescence signal of spent dialysate. In addition, a good correlation was found between the emission intensity at Ex280/Em325 nm, corrected for the inner filtering effect, and the concentration of β2M in spent dialysate from different HDF modalities and timepoints (R^2 = 0.838, N = 375).

Apart from aromatic amino acids, pyridoxin and typical enzyme cofactors such as pyridoxal phosphate, pyridoxamine phosphate, nicotinamide adenine dinucleotide and flavin adenine dinucleotide are listed as the main natural intrinsic fluorophores in living tissues [42], which evidently may be adsorbed to proteins with the dimensions of "middle molecules".

In future, specific MM uremic toxins behind the optical properties of MM fraction could be identified by separating the MM fraction to individual chromo- and fluorophores. This could provide additional information about differences between patients and validate the method more extensively.

4. Conclusions

The present work suggests that multicomponent regression analysis proved to be a useful tool for the combination of absorbance and fluorescence at different wavelength regions for concentration and elimination assessment of the MM uremic toxin β2M during dialysis treatment. Including more independent variables (e.g., patient- and diagnosis-specific) into the multiparameter regression analysis may be the next step. The main contributors in the formation of optical properties of the MM fraction are apparently the fluorescence of Trp in small proteins and peptides and the fluorescence of AGEs; whereas UV absorbance of peptide bond and aromatic side chains of amino acids seems to have smaller contribution. Complicated mutual influences of chromophores and fluorophores in dialysate do not allow to attribute distinct excitation/emission wavelength pairs to specific fluorophores in the complex mixture of chromo- and fluorophores present in dialysate. Some presumptive assessments resulting from the phenomenon of the correlations found in this work allow evaluating the optical technology as promising for on-line optical monitoring of eliminating not only β2M but also all of the MM fraction during dialysis treatment.

5. Materials and Methods

In total, 22 ESKD patients were enrolled into the study from the Centre of Nephrology at the North Estonia Medical Centre, Tallinn, Estonia. The study was approved by the Tallinn Medical Research Ethics Committee in Estonia (decision no. 2205, 27. Dec. 2017) and conducted in accordance with the Declaration of Helsinki. Inclusion criteria were the following: over 18 years old patients on chronic hemodialysis, HD procedures via AV fistula or graft (catheters were not used) for 4 h thrice weekly, blood access capable to manage blood flow of at least 300 mL/min, absence of clinical signs of infection or other active acute clinical complications and an estimated life expectancy over 6 months. Clinical data of the participants monitored for a total of 88 HD sessions is presented in Table 3.

Table 3. Clinical data of the end stage kidney disease (ESKD) patients. Numerical values are given as a mean ± SD or as a median and interquartile range (Q1–Q3).

Entity of the Data	Specification
Cause of ESKD	Diabetes (4); Hypertension (8); Glomerulonephritis (3); Tubulointerstitial nephritis (3); Renal carcinoma (2); Other (2)
Age (years)	55 ± 17
Gender	M (17), F (=5)
Race, Caucasian (%)	100
BMI, kg/m^2 [a]	26.8 ± 5.8
BW, kg [a]	81.5 ± 21.3
Ultrafiltration volume, mL	2565 ± 1190
Urinary volume, mL	0 (14 patients) 700 (335–825) (8 patients)
Serum total protein, g/L	62.8 ± 5.5
Hematocrit, % [a]	34.4 (3.5)
Serum calcium, mmol/L [a]	2.25 (0.16)
Serum phosphorus, mmol/L [a]	1.92 (1.63–2.29)
Serum parathyroid hormone, pmol/L [a]	28.7 (16.8–41.9)
Dialysis access	native fistula (15); graft (7)
Dialysis vintage, months [a]	23 (11–83)
spKt/Vurea [a]	1.47 (1.23–1.67)

Abbreviations: M—male; F—female; BMI—body mass index; BW—body weight; spKt/V—single-pool criterion of the dose of dialysis, stHDF—standard HDF. [a] Based on data of stHDF.

Each patient was observed during four midweek dialysis sessions, using Fresenius 5008 dialysis machines (Fresenius Medical Care, Bad Homburg v. d. Höfe, Germany). In order to include large variety of treatment settings, the following dialysis modalities, dialyzers and machine settings were applied (Table 4): (1) standard HDF dialysis with

standard settings (stHDF), as previously prescribed for the patient in routine clinical care. This provided a baseline and introduced patients more smoothly into the study; (2) low flux HD (LF HD) with minimal dialysis settings to provide conditions for minimal uremic toxin removal; (3) medium HDF with maximum dialyzer surface area and highest dialysate (d) blood (b) flow ratio (Qd/Qb); (4) high HDF with maximum dialysis settings in terms of dialyzer surface area, dialysate and blood flow, and the substitution volume expected to increase removal of MM.

Table 4. Dialysis treatment settings of hemodiafiltration (HDF) and hemodialysis (HD). Numerical values are given as mean ± SD.

Entity of the Data	Standard HDF	Low Flux HD	Medium HDF	High HDF
Volume substituted (Vs, L)	21.1 ± 3.1	0 ± 0	15.3 ± 1.4	25.3 ± 2.8
Dialysis time, min.	240	240	240	240
Blood flow, mL/min (Qb)	300.8 ± 12.7	200 ± 0	299.7 ± 1.0	364.2 ± 27.1
Dialysate flow, ml/min (Qd)	470.8 ± 105.4	300 ± 0	799.8 ± 0.9	800.0 ± 0.0
Dialyzer area [a], m^2	2.0 ± 0.2	1.5 ± 0.0	2.2 ± 0.0	2.2 ± 0.0
Number of dialyses (N)	22	22	22	22

[a] Specification of dialyzers: Standard: FX800 (N = 8), FX1000 (N = 14), Low flux: Lo15 (N = 22), Medium: FX1000 (N = 22), High: FX1000 (N = 22). All dialyzers had polysulfone-based membranes with the following effective membrane area: 1.8 m^2 (Helixone®, FX800), 2.2 m^2 (Helixone®, FX1000), 1.5 m^2 (Amembris®, Xevonta Lo 15).

Spent dialysate samples were taken from the dialysate outlet of the dialysis machine before dialysis, at 7, 60, 120 and 180 min after the start of the session and at the end of the session (240 min). In addition, the waste dialysate was collected into a large tank during the whole procedure. After the end of the procedure, the dialysate collection tank was weighed, and one sample was taken from it after careful stirring. All dialysate samples were divided into three sets: the first set of samples were directly sent to a clinical laboratory for analysis of β2M; another two sets of samples were separated for the analytical laboratory analyses. Prior to transportation, the samples were processed as follows: (A) spent dialysate samples for the clinical laboratory were collected into 120 mL Becton Dickinson Vacutainer urine collection cups (Franklin Lakes, NJ, USA) and drawn thereafter into the Becton Dickinson Vacutainer SST II Advanced 5 mL (Franklin Lakes, NJ, USA) vacuum tubes; (B) one set of samples for analytical chemistry analysis were transported into the lab in 120 mL Becton Dickinson Vacutainer urine collection cups; (C) the third set of samples were subjected to centrifugation. 12 mL of dialysate were loaded into the centrifugal filter tube with MW cut-off limit 1 kDa (Pall Laboratory Macrosep® type MAP001C37, Pal Corp., Ann Arbor, MI, USA) and centrifuged at 37 °C for 40 min with the speed of 5000 rpm (2375.75× *g*, type 2–16 KL centrifuge with the rotor 11,192 from the Sigma Laborzentrifugen GmbH, Osterode am Harz, Germany). Filtrates were pipetted into standard laboratory vials with Teflon-tightened screw caps and transported into the lab together with the non-filtered samples.

The set A of samples was analyzed for β2M by the clinical laboratory (SYNLAB Eesti OÜ, Tallinn, Estonia) using standard sandwich type immunochemical system "Immulite 2000 Beta-2 Microglobulin" (Siemens Healthineers AG, Erlangen, Germany). Sets B and C of samples were subjected to optical analyses during the day of sampling at room temperature, as follows: UV spectra were recorded with the UV-3600 spectrophotometer (Shimadzu, Kyoto, Japan) in the wavelength range of 190–400 nm with the increment of 1 nm using a quartz cuvette with optical path length of 10 mm. An untreated pure dialysis buffer, sampled from the outflow of the dialysis machine prior to switching on the blood flow, was used as the reference solution in UV measurements (separately for each dialysis session) or the filtrate of the measurement of dialysate for the same patient. Fluorescence spectra were recorded with the spectrofluorometer RF-6000 (Shimadzu, Kyoto, Japan) using the excitation wavelength range of 200–400 nm with the increment of 10 nm and the emission wavelength range of 210–600 nm with the increment of 1 nm. The bandwidths of 5 nm were used in both monochromators and the used quartz cuvette had an optical

path length of 4 mm. Differences between the spectra of the dialysate and corresponding filtrates, referable to compounds with MW > 1 kDa, were considered as characteristics of the "MM fraction" and their possible biochemical origin was examined based on data available in the literature. Additionally, a regression analysis was used to analyze the variation of optical signals at different wavelengths, caused by the MM fraction, when comparing the spectra of dialysate samples and corresponding filtrates. Correction of emission intensity in relation to inner filtering of the excitation beam was used in the case of excitation at 280 nm when included into the final regression model [40,41].

Forward stepwise regression was used to obtain regression models for the assessment of the β2M concentration through optical parameters of spent dialysate. Independent variables included UV absorbance and fluorescence with selected excitation/emission wavelength pairs as specified below. The final choice of the best combination of optical parameters was validated by dividing HDF data into a calibration set (50% of the material, i.e., 11 patients with even number of registration, 33 HDF sessions) and a validation set (50% of the material, 11 patients with odd number of registration, 33 HDF sessions).

Systematic error (BIAS) was calculated for the models as follows:

$$\mathrm{BIAS} = \frac{\sum_{i=1}^{\mathrm{N}} e_i}{\mathrm{N}} \tag{1}$$

where e_i is the i-th residual (difference between the lab and modelled β2M) and N is the number of observations [64].

Standard error of performance corrected for BIAS was calculated for the two models as follows [64].

$$\mathrm{SE} = \sqrt{\frac{\sum_{i=1}^{\mathrm{N}} (e_i - \mathrm{BIAS})^2}{\mathrm{N} - 1}} \tag{2}$$

Removal of β2M during dialysis sessions was described by a reduction ratio % (RR) in dialysate:

$$\mathrm{RR} = \frac{\mathrm{C}_0 - \mathrm{C}_\mathrm{t}}{\mathrm{C}_0} \times 100\% \tag{3}$$

where C_0 is the concentration of β2M in a spent dialysate sample taken after 7 min from the start of the dialysis procedure and C_t is the concentration of β2M in a spent dialysate sample taken at the end of the dialysis procedure.

The total removed solute (TRS) of β2M was calculated based on the total dialysate collection (TDC) as follows:

$$\mathrm{TRS} = \mathrm{C}_\mathrm{T} \times \mathrm{W}_\mathrm{T} \tag{4}$$

where C_T is the final substance concentration in the dialysate collection tank and W_T is the weight of the dialysate collection tank [kg]. It was assumed that the average density of spent dialysate is 1.008 ± 0.001 kg/L [65]. Both RR and TRS were calculated based on β2M concentration in dialysate estimated in the laboratory as well as by the best optical multiparameter model. Excel MS 365 (Microsoft, Redmond, WA, USA) and MATLAB R2019b (MathWorks, Natick, MA, USA) software were used for statistical analyses. All results were assessed for possible errors and data conformity. Twenty-one data points from the total of 396 were omitted from the data set due to errors related to sample drawing, clinical laboratory analysis and due to self-tests of the HD machine. Individual differences in the laboratory and optically estimated results were examined using a Bland and Altman analysis [66], and a parametric paired t-test (two-tailed) was used to determine the statistical difference between laboratory and optical methods. A p-value of <0.05 was considered statistically significant.

Author Contributions: Conceptualization, A.A., J.A., I.F., L.L., M.L., J.P., R.T.; data curation, J.P., J.A., K.L., L.L., R.T.; formal analysis, J.P., J.A., I.F., R.T.; funding acquisition: I.F.; investigation, J.P., A.A., J.A., K.L., L.L., R.T.; methodology, A.A., J.A., I.F., K.L., L.L., M.L., J.P., R.T.; project administration: J.A., M.L.; validation, J.A., J.P., and I.F.; visualization, J.P., and R.T.; writing—original draft preparation, J.P., R.T., A.A., J.A., I.F., L.L., M.L.; writing—review and editing, J.P., A.A., J.A., I.F., K.L., L.L., M.L., R.T.; All authors have read and agreed to the published version of the manuscript.

Funding: The research was funded partly by the European Union through the European Regional Development Fund H2020-SMEINST-2-2017, OLDIAS2—Online Dialysis Sensor Phase2 project, Grant Agreement nr 767572, the Estonian Ministry of Education and Research under institutional research financing, grant nr IUT 19-2, and by Estonian Centre of Excellence in IT (EXCITE) funded by European Regional Development Fund.

Institutional Review Board Statement: The study was conducted according to the guidelines of the Declaration of Helsinki, and approved by the Tallinn Medical Research Ethics Committee in Estonia (decision no. 2205, 27 December 2017).

Informed Consent Statement: Informed consent was obtained from all subjects involved in the study.

Data Availability Statement: Data sharing is not applicable due to legal and privacy issues.

Acknowledgments: The authors wish to thank all dialysis patients who participated in the experiments, and nurses at the Centre of Nephrology, North Estonia Medical Centre for assistance during the clinical experiments. The authors greatly acknowledge technical help of the students M. Alev, M. Lukner, L. Rannamäe and R. Toome in sample and data processing.

Conflicts of Interest: The authors declare no conflict of interest. The funders had no role in the design of the study; in the collection, analyses, or interpretation of data; in the writing of the manuscript, or in the decision to publish the results.

References

1. Tattersall, J.; Martin-Malo, A.; Pedrini, L.; Basci, A.; Canaud, B.; Fouque, D.; Haage, P.; Konner, K.; Kooman, J.; Pizzarelli, F.; et al. EBPG guideline on dialysis strategies. *Nephrol. Dial. Transplant.* **2007**, *22*, ii5–ii21. [CrossRef]
2. Tattersall, E.; Ward, R.; Canaud, B.; Blankestijn, P.J.; Bots, M.; Covic, A.; Davenport, A.; Grooteman, M.; Gura, V.; Hegbrant, J.; et al. Online haemodiafiltration: Definition, dose quantification and safety revisited. *Nephrol. Dial. Transplant.* **2013**, *28*, 542–550. [CrossRef]
3. Daugirdas, J.T.; Depner, T.A.; Inrig, J.; Mehrotra, R.; Rocco, M.V.; Suri, R.S.; Weiner, D.E.; Greer, N.; Ishani, A.; MacDonald, R.; et al. KDOQI Clinical Practice Guideline for Hemodialysis Adequacy: 2015 Update. *Am. J. Kidney Dis.* **2015**, *66*, 884–930. [CrossRef]
4. Gál, G.; Gróf, J. Continuous Uv Photometric Monitoring of the Efficiency of Hemodialysis. *Int. J. Artif. Organs* **1980**, *3*, 338–341. [CrossRef] [PubMed]
5. Fridolin, I.; Magnusson, M.; Lindberg, L.-G. Measurement of solutes in dialysate using UV absorption. *BiOS 2001 Int. Symp. Biomed. Opt.* **2001**, *4263*, 40–48. [CrossRef]
6. Fridolin, I.; Magnusson, M.; Lindberg, L.-G. On-Line Monitoring of Solutes in Dialysate Using Absorption of Ultraviolet Radiation: Technique Description. *Int. J. Artif. Organs* **2002**, *25*, 748–761. [CrossRef]
7. Uhlin, F.; Fridolin, I.; Magnusson, M.; Lindberg, L.-G. Dialysis dose (Kt/V) and clearance variation sensitivity using measurement of ultraviolet-absorbance (on-line), blood urea, dialysate urea and ionic dialysance. *Nephrol. Dial. Transplant.* **2006**, *21*, 2225–2231. [CrossRef]
8. Castellarnau, A.; Werner, M.; Günthner, R.; Jakob, M. Real-time Kt/V determination by ultraviolet absorbance in spent dialysate: Technique validation. *Kidney Int.* **2010**, *78*, 920–925. [CrossRef] [PubMed]
9. Umimoto, K.; Tatsumi, Y.; Kanaya, H.; Jokei, K. *Analysis of Uremic Substances in Dialysate by Visible Ultraviolet Spectroscopy*; Springer: Berlin, Germany, 2007; pp. 3205–3207.
10. Umimoto, K.; Kanaya, Y.; Kawanishi, H.; Kawai, N. *Measuring of Uremic Substances in Dialysate by Visible Ultraviolet Spectroscopy*; Springer: Berlin, Germany, 2009; pp. 42–45.
11. Vasilevskiy, A.M.; Konoplev, G.A. Polycomponental monitoring of process of effluent dialyzate by a method of uf of spectrometry. *Biotekhnosfera* **2009**. Available online: https://scholar.google.com/scholar?cluster=6506178806057926161 (accessed on 23 December 2020).
12. Arund, J.; Tanner, R.; Uhlin, F.; Fridolin, I. Do Only Small Uremic Toxins, Chromophores, Contribute to the Online Dialysis Dose Monitoring by UV Absorbance? *Toxins* **2012**, *4*, 849–861. [CrossRef] [PubMed]
13. Holmar, J.; Fridolin, I.; Uhlin, F.; Lauri, K.; Luman, M. Optical Method for Cardiovascular Risk Marker Uric Acid Removal Assessment during Dialysis. *Sci. World J.* **2012**, *2012*, 1–8. [CrossRef] [PubMed]
14. Tomson, R.; Fridolin, I.; Uhlin, F.; Holmar, J.; Lauri, K.; Luman, M. Optical measurement of creatinine in spent dialysate. *Clin. Nephrol.* **2013**, *79*, 107–117. [CrossRef]

15. Enberg, P.; Fridolin, I.; Holmar, J.; Fernström, A.; Uhlin, F. Utilization of UV Absorbance for Estimation of Phosphate Elimination during Hemodiafiltration. *Nephron* **2012**, *121*, c1–c9. [CrossRef]
16. Holmar, J.; Uhlin, F.; Fernström, A.; Luman, M.; Jankowski, J.; Fridolin, I. An Optical Method for Serum Calcium and Phosphorus Level Assessment during Hemodialysis. *Toxins* **2015**, *7*, 719–727. [CrossRef] [PubMed]
17. Luman, M.; Jerotskaja, J.; Lauri, K.; Fridolin, I. Dialysis dose and nutrition assessment by optical on-line dialysis adequacy monitor. *Clin. Nephrol.* **2009**, *72*, 303–311. [CrossRef] [PubMed]
18. Uhlin, F.; Fridolin, I. *Optical Monitoring of Dialysis Dose*; Springer Science and Business Media LLC: New York, NY, USA, 2013; pp. 867–928.
19. Adimea Real-Time Monitoring Process. Available online: https://www.bbraun.com/content/dam/catalog/bbraun/bbraunProductCatalog/S/AEM2015/en-01/b3/adimea.pdf (accessed on 23 December 2020).
20. Kt/v Measurement. Dialysis Dose Monitor Measuring the Delivered Dialysis Dose. Available online: http://nikkisomedical.com/wp-content/uploads/2017/06/DDM_english_2013-03_vers04.pdf (accessed on 23 December 2020).
21. Arund, J.; Luman, M.; Uhlin, F.; Tanner, R.; Fridolin, I. Is Fluorescence Valid to Monitor Removal of Protein Bound Uremic Solutes in Dialysis? *PLoS ONE* **2016**, *11*, e0156541. [CrossRef]
22. Holmar, J.; Arund, J.; Uhlin, F.; Tanner, R.; Fridolin, I. Quantification of Indoxyl Sulphate in the Spent Dialysate Using Fluorescence Spectra. In Proceedings of the 1st World Congress on Electroporation and Pulsed Electric Fields in Biology, Medicine and Food & Environmental Technologies, Portorož, Slovenia, 6–10 September 2011; pp. 45–48.
23. Holmar, J.; Uhlin, F.; Ferenets, R.; Lauri, K.; Tanner, R.; Arund, J.; Luman, M.; Fridolin, I. Estimation of removed uremic toxin indoxyl sulphate during hemodialysis by using optical data of the spent dialysate. In Proceedings of the 2013 35th Annual International Conference of the IEEE Engineering in Medicine and Biology Society (EMBC), Institute of Electrical and Electronics Engineers (IEEE), Osaka, Japan, 3–7 July 2013; pp. 6707–6710.
24. Masakane, I.; Sakurai, K. Current approaches to middle molecule removal: Room for innovation. *Nephrol. Dial. Transplant.* **2018**, *33*, 12–21. [CrossRef]
25. Yamamoto, S. Molecular mechanisms underlying uremic toxin-related systemic disorders in chronic kidney disease: Focused on β2-microglobulin-related amyloidosis and indoxyl sulfate-induced atherosclerosis—Oshima Award Address 2016. *Clin. Exp. Nephrol.* **2019**, *23*, 151–157. [CrossRef] [PubMed]
26. Clark, W.R.; Dehghani, N.L.; Narsimhan, V.; Ronco, C. Uremic Toxins and their Relation to Dialysis Efficacy. *Blood Purif.* **2019**, *48*, 299–314. [CrossRef]
27. Blankestijn, P.J.; Fischer, I.K.; Barth, C.; Cromm, K.; Canaud, B.; Davenport, A.E.; Grobbee, D.; Hegbrant, J.; Roes, K.C.; Rose, M.; et al. Benefits and harms of high-dose haemodiafiltration versus high-flux haemodialysis: The comparison of high-dose haemodiafiltration with high-flux haemodialysis (CONVINCE) trial protocol. *BMJ Open* **2020**, *10*, e033228. [CrossRef]
28. Kirsch, A.H.; Lyko, R.; Nilsson, L.-G.; Beck, W.; Amdahl, M.; Lechner, P.; Schneider, A.; Wanner, C.; Rosenkranz, A.R.; Krieter, D.H. Performance of hemodialysis with novel medium cut-off dialyzers. *Nephrol. Dial. Transplant.* **2016**, *32*, 165–172. [CrossRef]
29. Lauri, K.; Luman, M.; Holmar, J.; Tomson, R.; Kalle, S.; Arund, J.; Uhlin, F.; Fridolin, I. *Can Removal of Middle Molecular Uremic Retention Solutes be Estimated by UV-absorbance Measurements in Spent Dialysate?* Springer: Toronto, ON, Canada, 2015; pp. 1297–1300.
30. Uhlin, F.; Holmar, J.; Yngman-Uhlin, P.; Fernström, A.; Fridolin, I. Optical Estimation of Beta 2 Microglobulin during Hemodiafiltration-Does It Work? *Blood Purif.* **2015**, *40*, 113–119. [CrossRef] [PubMed]
31. Lauri, K.; Arund, J.; Holmar, J.; Tanner, R.; Kalle, S.; Luman, M.; Fridolin, I. Removal of Urea, β2-Microglobulin, and Indoxyl Sulfate Assessed by Absorbance and Fluorescence in the Spent Dialysate During Hemodialysis. *ASAIO J.* **2019**, *66*, 698–705. [CrossRef] [PubMed]
32. Wolley, M.J.; Hutchison, C.A. Large uremic toxins: An unsolved problem in end-stage kidney disease. *Nephrol. Dial. Transplant.* **2018**, *33*, iii6–iii11. [CrossRef]
33. Ward, A.R.; Greene, T.W.; Hartmann, B.; Samtleben, W. Resistance to intercompartmental mass transfer limits β2-microglobulin removal by post-dilution hemodiafiltration. *Kidney Int.* **2006**, *69*, 1431–1437. [CrossRef] [PubMed]
34. Brunati, C.C.M.; Gervasi, F.; Cabibbe, M.; Ravera, F.; Menegotto, A.; Querques, M.; Colussi, G. Single Session and Weekly Beta 2-Microglobulin Removal with Different Dialytic Procedures: Comparison between High-Flux Standard Bicarbonate Hemodialysis, Post-Dilution Hemodiafiltration, Short Frequent Hemodialysis with NxStage Technology and Automated Peritoneal Dialysis. *Blood Purif.* **2019**, *48*, 86–96. [CrossRef]
35. Krochmal, M.; Schanstra, J.P.; Mischak, H. Urinary peptidomics in kidney disease and drug research. *Expert Opin. Drug Discov.* **2017**, *13*, 259–268. [CrossRef] [PubMed]
36. Prasad, S.; Mandal, I.; Singh, S.; Paul, A.; Mandal, B.; Venkatramani, R.; Swaminathan, R. Near UV-Visible electronic absorption originating from charged amino acids in a monomeric protein. *Chem. Sci.* **2017**, *8*, 5416–5433. [CrossRef]
37. Rosenheck, K.; Doty, P. The Far Ultraviolet Absorption Spectra of Polypeptide and Protein Solutions and Their Dependence on Conformation. *Proc. Natl. Acad. Sci. USA* **1961**, *47*, 1775–1785. [CrossRef]
38. Jerotskaja, J.; Lauri, K.; Tanner, R.; Luman, M.; Fridolin, I. Optical dialysis adequacy sensor: Wavelength dependence of the ultra violet absorbance in the spent dialysate to the removed solutes. In Proceedings of the 2006 International Conference of the IEEE Engineering in Medicine and Biology Society, New York, NY, USA, 30 August–3 September 2006; pp. 2960–2963.

39. Fridolin, I.; Lindberg, L.-G. On-line monitoring of solutes in dialysate using wavelength-dependent absorption of ultraviolet radiation. *Med. Biol. Eng. Comput.* **2003**, *41*, 263–270. [CrossRef]
40. Fonin, A.V.; Sulatskaya, A.I.; Kuznetsova, I.M.; Turoverov, K.K. Fluorescence of Dyes in Solutions with High Absorbance. Inner Filter Effect Correction. *PLoS ONE* **2014**, *9*, e103878. [CrossRef] [PubMed]
41. Wang, T.; Zeng, L.-H.; Li, D.-L. A review on the methods for correcting the fluorescence inner-filter effect of fluorescence spectrum. *Appl. Spectrosc. Rev.* **2017**, *52*, 883–908. [CrossRef]
42. Lakowicz, J.R. Fluorophores. In *Principles of Fluorescence Spectroscopy*, 3rd ed.; Lakowicz, J.R., Ed.; Springer US: Boston, MA, USA, 2006; pp. 63–95.
43. Ulrich, P. Protein Glycation, Diabetes, and Aging. *Recent Prog. Horm. Res.* **2001**, *56*, 1–22. [CrossRef] [PubMed]
44. Stirban, A.; Gawlowski, T.; Roden, M. Vascular effects of advanced glycation endproducts: Clinical effects and molecular mechanisms. *Mol. Metab.* **2014**, *3*, 94–108. [CrossRef]
45. Gugliucci, A. Formation of Fructose-Mediated Advanced Glycation End Products and Their Roles in Metabolic and Inflammatory Diseases. *Adv. Nutr.* **2017**, *8*, 54–62. [CrossRef]
46. Perrone, A.; Giovino, A.; Benny, J.; Martinelli, F. Advanced Glycation End Products (AGEs): Biochemistry, Signaling, Analytical Methods, and Epigenetic Effects. *Oxidative Med. Cell. Longev.* **2020**, *2020*, 1–18. [CrossRef] [PubMed]
47. Thornalley, P.J.; Rabbani, N. Highlights and Hotspots of Protein Glycation in End-Stage Renal Disease. *Semin. Dial.* **2009**, *22*, 400–404. [CrossRef]
48. Mallipattu, S.K.; Uribarri, J. Advanced glycation end product accumulation. *Curr. Opin. Nephrol. Hypertens.* **2014**, *23*, 547–554. [CrossRef]
49. Yamamoto, S.; Kazama, J.J.; Wakamatsu, T.; Takahashi, Y.; Kaneko, Y.; Goto, S.; Narita, I. Removal of uremic toxins by renal replacement therapies: A review of current progress and future perspectives. *Ren. Replace. Ther.* **2016**, *2*, 43. [CrossRef]
50. Rabbani, N.; Thornalley, P.J. Advanced glycation end products in the pathogenesis of chronic kidney disease. *Kidney Int.* **2018**, *93*, 803–813. [CrossRef]
51. Stinghen, A.E.; Massy, Z.A.; Vlassara, H.; Striker, G.E.; Boullier, A. Uremic Toxicity of Advanced Glycation End Products in CKD. *J. Am. Soc. Nephrol.* **2015**, *27*, 354–370. [CrossRef] [PubMed]
52. Roberts, M.A.; Thomas, M.C.; Fernando, D.; Macmillan, N.; Power, D.A.; Ierino, F.L. Low molecular weight advanced glycation end products predict mortality in asymptomatic patients receiving chronic haemodialysis. *Nephrol. Dial. Transplant.* **2006**, *21*, 1611–1617. [CrossRef] [PubMed]
53. Miyata, T.; Taneda, S.; Kawai, R.; Ueda, Y.; Horiuchi, S.; Hara, M.; Maeda, K.; Monnier, V.M. Identification of pentosidine as a native structure for advanced glycation end products in beta-2-microglobulin-containing amyloid fibrils in patients with dialysis-related amyloidosis. *Proc. Natl. Acad. Sci. USA* **1996**, *93*, 2353–2358. [CrossRef] [PubMed]
54. Meerwaldt, R.; Links, T.; Graaff, R.; Thorpe, S.R.; Baynes, J.W.; Hartog, J.; Gans, R.; Smit, A. Simple Noninvasive Measurement of Skin Autofluorescence. *Ann. N. Y. Acad. Sci.* **2005**, *1043*, 290–298. [CrossRef]
55. Kalle, S.; Tanner, R.; Luman, M.; Fridolin, I. Free Pentosidine Assessment Based on Fluorescence Measurements in Spent Dialysate. *Blood Purif.* **2018**, *47*, 85–93. [CrossRef]
56. Schmitt, A.; Schmitt, J.; Münch, G.; Gasic-Milencovic, J. Characterization of advanced glycation end products for biochemical studies: Side chain modifications and fluorescence characteristics. *Anal. Biochem.* **2005**, *338*, 201–215. [CrossRef] [PubMed]
57. Tessier, F.; Obrenovich, M.; Monnier, V.M. Structure and Mechanism of Formation of Human Lens Fluorophore LM-1. *J. Biol. Chem.* **1999**, *274*, 20796–20804. [CrossRef]
58. Miyata, T.; Oda, O.; Inagi, R.; Iida, Y.; Araki, N.; Yamada, N.; Horiuchi, S.; Taniguchi, N.; Maeda, K.; Kinoshita, T. beta 2-Microglobulin modified with advanced glycation end products is a major component of hemodialysis-associated amyloidosis. *J. Clin. Investig.* **1993**, *92*, 1243–1252. [CrossRef]
59. Förster, T. Experimentelle und theoretische Untersuchung des zwischenmolekularen Übergangs von Elektronenanregungsenergie. *Z. Nat. A* **1949**, *4*, 321–327. [CrossRef]
60. Förster, T. *Delocalized Excitation and Excitation Transfer*; Florida State University: Tallahassee, FL, USA, 1965.
61. Donadio, C.; Calia, D.; Ghimenti, S.; Onor, M.; Colombini, E.; Fuoco, R.; Di Francesco, F. The Removal of β2-Microglobulin in Spent Dialysate Cannot Be Monitored by Spectrophotometric Analysis. *Blood Purif.* **2015**, *40*, 109–112. [CrossRef]
62. Vivian, J.T.; Callis, P.R. Mechanisms of Tryptophan Fluorescence Shifts in Proteins. *Biophys. J.* **2001**, *80*, 2093–2109. [CrossRef]
63. Narang, D.; Sharma, P.K.; Mukhopadhyay, S. Dynamics and dimension of an amyloidogenic disordered state of human β2-microglobulin. *Eur. Biophys. J.* **2013**, *42*, 767–776. [CrossRef] [PubMed]
64. Esbensen, K. *Multivariate Data Analysis –in Practice. Introduction to Multivariate Data Analysis and Experimental Design*, 5th ed.; CAMO Software: Oslo, Norway, 2009.
65. Eloot, S.; Dhondt, A.; Vierendeels, J.; De Wachter, D.; Verdonck, P.; Vanholder, R. Temperature and concentration distribution within the Genius(R) dialysate container. *Nephrol. Dial. Transplant.* **2007**, *22*, 2962–2969. [CrossRef] [PubMed]
66. Giavarina, D. Understanding Bland Altman analysis. *Biochem. Med.* **2015**, *25*, 141–151. [CrossRef] [PubMed]

Appendix 3 – Publication II

Publication II

Paats, J., Adoberg, A., Arund, J., Dhondt, A., Fernström, A., Fridolin, I., Glorieux, G., Gonzalez Parra, E., Holmar, J., Leis, L., Luman, M., Perez-Gomez, V. M., Sanchez-Ospina, D., Segelmark, M., Uhlin, F., Ortiz, A. (2023). Time-averaged concentration estimation of uraemic toxins with different removal kinetics: a novel approach based on intradialytic spent dialysate measurements. *Clinical Kidney Journal*, *16*(4), 735–744. https://doi.org/10.1093/ckj/sfac273.

Clinical Kidney Journal, 2023, vol. 16, no. 4, 735–744

https://doi.org/10.1093/ckj/sfac273
Advance Access Publication Date: 20 December 2022
Original Article

ORIGINAL ARTICLE

Time-averaged concentration estimation of uraemic toxins with different removal kinetics: a novel approach based on intradialytic spent dialysate measurements

Joosep Paats [1], Annika Adoberg [2], Jürgen Arund [1], Annemieke Dhondt [3], Anders Fernström [4], Ivo Fridolin [1], Griet Glorieux [3], Emilio Gonzalez-Parra [5], Jana Holmar [1], Liisi Leis [2], Merike Luman [1,2], Vanessa Maria Perez-Gomez [5], Kristjan Pilt [1], Didier Sanchez-Ospina [5], Mårten Segelmark [4], Fredrik Uhlin [1,4] and Alberto Ortiz [5]

[1]Department of Health Technologies, Tallinn University of Technology, Tallinn, Estonia, [2]Centre of Nephrology, North Estonia Medical Centre, Tallinn, Estonia, [3]Nephrology Division, Ghent University Hospital, Ghent, Belgium, [4]Department of Nephrology and Department of Health, Medicine and Caring Sciences, Linköping University, Linköping, Sweden and [5]Fundación Jiménez Díaz University Hospital Health Research Institute, Madrid, Spain

Correspondence to: Joosep Paats; E-mail: joosep.paats@taltech.ee

ABSTRACT

Background. Kt/V_{urea} is the most used marker to estimate dialysis adequacy; however, it does not reflect the removal of many other uraemic toxins, and a new approach is needed. We have assessed the feasibility of estimating intradialytic serum time-averaged concentration (TAC) of various uraemic toxins from their spent dialysate concentrations that can be estimated non-invasively online with optical methods.

Methods. Serum and spent dialysate levels and total removed solute (TRS) of urea, uric acid (UA), indoxyl sulphate (IS) and β2-microglobulin (β2M) were evaluated with laboratory methods during 312 haemodialysis sessions in 78 patients with four different dialysis treatment settings. TAC was calculated from serum concentrations and evaluated from TRS and logarithmic mean concentrations of spent dialysate ($M_{ln}D$).

Results. Mean (± standard deviation) intradialytic serum TAC values of urea, UA, β2M and IS were 10.4 ± 3.8 mmol/L, 191.6 ± 48.1 µmol/L, 13.3 ± 4.3 mg/L and 82.9 ± 43.3 µmol/L, respectively. These serum TAC values were similar and highly correlated with those estimated from TRS [10.5 ± 3.6 mmol/L ($R^2 = 0.92$), 191.5 ± 42.8 µmol/L ($R^2 = 0.79$), 13.0 ± 3.2 mg/L ($R^2 = 0.59$) and 82.7 ± 40.0 µmol/L ($R^2 = 0.85$)] and from $M_{ln}D$ [10.7 ± 3.7 mmol/L ($R^2 = 0.92$), 191.6 ± 43.8 µmol/L ($R^2 = 0.80$), 12.9 ± 3.2 mg/L ($R^2 = 0.63$) and 82.2 ± 38.6 µmol/L ($R^2 = 0.84$)], respectively.

Received: 2.9.2022; Editorial decision: 12.12.2022

Conclusions. Intradialytic serum TAC of different uraemic toxins can be estimated non-invasively from their concentration in spent dialysate. This sets the stage for TAC estimation from online optical monitoring of spent dialysate concentrations of diverse solutes and for further optimization of estimation models for each uraemic toxin.

Keywords: chronic haemodialysis, dialysis adequacy, time-averaged concentration, urea, uraemic toxin

INTRODUCTION

Adequate dialysis treatment improves survival and reduces morbidity in haemodialysis (HD) patients. Conventionally, dialysis adequacy is assessed by the clearance of the small molecular weight molecule urea and quantified as Kt/V_{urea} or URR, which is calculated from urea concentrations in pre-dialysis and post-dialysis blood samples [1]. Kt/V_{urea} has helped to standardize HD treatment and define the minimum dose of dialysis needed to avoid morbidity and mortality related to inadequate dialysis, although the Kt/V_{urea} concept has several shortcomings [2–4].

Kt/V_{urea} may be inaccurate for dialysis patients with divergent body compositions [3, 5, 6]. In addition, Kt/V_{urea} does not easily allow comparison of adequacy for patients who receive different dialysis prescriptions with varying duration and frequency [4, 7, 8] and for patients who have acceptable residual renal function [3], as this has a major impact on solute removal [9, 10]. Furthermore, Kt/V_{urea} poorly reflects the removal of solutes other than urea, which are associated with clinical outcomes, such as middle molecules and protein-bound molecules [3, 11–13].

Despite these limitations, Kt/V_{urea} remains the most frequent measure of dialysis adequacy [1], even as high cut-off membranes are available and convective strategies have become common that aim to increase the clearance of middle molecules and protein-bound uraemic toxins [3, 13]. New approaches are therefore needed to quantify the HD dose that also represents removal of uraemic toxins other than urea and can be applied to dialysis sessions with varying settings (modality, frequency, duration) to optimize patient survival and quality of life [3, 14].

Alternative measures of dialysis adequacy have been proposed, e.g. the equivalent renal urea clearance [15], the time-averaged concentration (TAC)/time-averaged deviation concept [16], ionic dialysance [17] and fractional solute removal [18], among other indices. However, a key issue is the existence of many types of uraemic toxins that should be removed by HD but are not assessed by Kt/V_{urea}. The TAC of individual solutes, which strongly depends on the total dialysis time per week and on the weekly dialytic frequency, may provide insights into the clearance of diverse solutes [7, 16, 19]. TAC evaluates changes in uraemic toxin levels over time, even if they have different size and removal characteristics, and allows comparing the effect of different dialysis strategies on individual uraemic toxins [7, 16, 19]. Moreover, TAC integrates the impact of patient parameters, such as residual renal clearance and the rate of generation of uraemic toxins [16]. Indeed, TAC was historically used to assess dialysis adequacy, but it was replaced by the simpler Kt/V_{urea} due to cumbersome calculations [16].

TAC is usually estimated from repeated blood sampling and calculated as the area under the concentration curve over the period of interest. In other words, TAC is the mean concentration of the solute of interest over a period of time, which can be one treatment cycle, e.g. a week, or one intradialytic period, i.e. an individual dialysis session time [7, 15, 18, 20]. However, evaluating intradialytic TAC from repeated blood samples obtained during the dialysis session is more complex than assessing Kt/V_{urea}, which usually requires only pre- and post-dialysis sampling [7, 20, 21]. This problem becomes more prominent for solutes with higher intercompartmental resistance [20].

Online optical monitoring methods that do not require blood sampling allow the simultaneous monitoring of multiple uraemic toxins in the outflow of effluent dialysate from dialysis machines (spent dialysate) [22–24]. As the mass of toxins removed from blood to the dialysate is proportional to the dialysate flow/dialyzer clearance ratio [21, 25] in the case of using membranes with negligible adsorption capacity, such as polysulfone-based membranes [26], we hypothesized that the concentration of uraemic toxins in spent dialysate could be used to precisely estimate blood TAC values from each dialysis session. So far, dialysate-based methods have enabled evaluation of Kt/V_{urea}, the removal ratio and the total mass of removed solutes, providing additional information about treatment quality [22, 23, 27, 28].

The aim of this work was to estimate intradialytic serum TAC of urea, uric acid (UA), indoxyl sulphate (IS) and β2-microglobulin (β2M) from their concentrations in spent dialysate. Urea, UA, IS and β2M were considered as markers for the three general uraemic toxin groups based on different physicochemical characteristics and removal kinetics, namely small water-soluble compounds, protein-bound compounds and middle molecules [27].

MATERIALS AND METHODS

Clinical data were acquired from four separate dialysis centres from countries with diverse life expectancies, renal replacement therapy incidences and kidney transplant rates: North Estonia Medical Centre, Tallinn, Estonia (22 patients); Linköping University Hospital, Linköping, Sweden (21 patients); Ghent University Hospital, Ghent, Belgium (15 patients) and Fundación Jiménez Díaz University Hospital Health Research Institute, Madrid, Spain (20 patients). The clinical characteristics of the 78 participants monitored for a total of 312 dialysis procedures have been described [28] and are summarized in Supplementary Table 1. All studies were performed in accordance with the Declaration of Helsinki after approval of the study protocol by local ethics committees. Informed consent was obtained from all subjects involved in the study [28].

Inclusion criteria were age >18 years; chronic HD; thrice weekly HD procedures for 3.5–4.5 hours, preferably via arteriovenous fistula or graft; achievable blood flow of at least 300 ml/min; absence of clinical signs of infection or other active acute clinical complications and an estimated life expectancy >6 months.

Each patient underwent four HD sessions, each time using a different HD setting, as summarized in Supplementary Table 2 and described in detail previously [28]. Blood and spent dialysate samples were collected during each dialysis session [28]. Serum and spent dialysate concentrations of uraemic toxins were determined in clinical or analytical laboratories as described earlier [28, 29]. In short, urea, UA and β2M were assessed in

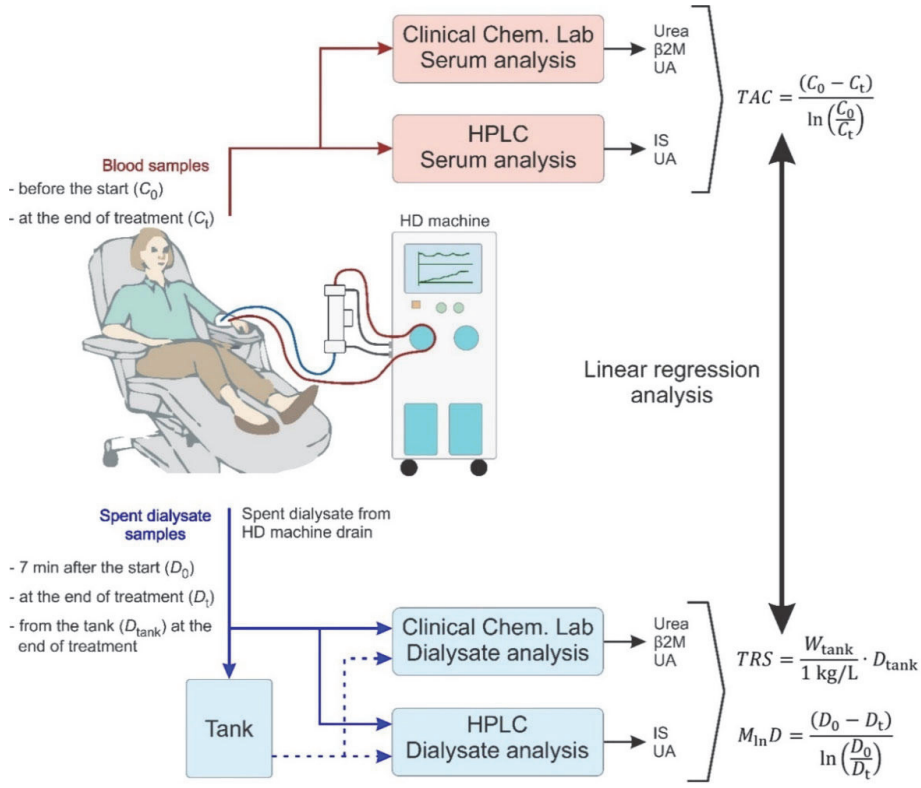

Figure 1: Clinical set-up, sample collection and analysis. The same set-up was repeated four times for each patient, each time using a different HD setting.

clinical biochemistry labs and IS and UA were assessed by high-performance liquid chromatography (HPLC), as shown in Fig. 1. For UA, HPLC results were used in subsequent calculations.

For each dialysis session, the TAC over dialysis sessions was estimated for urea, UA, IS and β2M from serum concentrations, total removed solute (TRS) from total dialysate collection and the mean concentration of uraemic toxins in spent dialysate during dialysis, which was calculated from spent dialysate concentrations.

Values of average effective blood flow (Q_b) during dialysis sessions, dialysate flow, ultrafiltration rate, total ultrafiltration volume and total substitution volume were read from the dialysis machine's screen at the end of the treatment session. The mass of the total waste dialysate collected during the session was measured. It was assumed that the average density of spent dialysate is equal to the density of water at room temperature (1 kg/L). The effective spent dialysate flow rate (Q_d) was calculated from the weight of spent dialysate (W_{tank}) collected during the session, divided by the dialysis session time (240 min), multiplied by the average density of spent dialysate:

$$Qd = \frac{W_{tank}}{1\text{kg/L} \cdot 240\,\text{min}}. \quad (1)$$

The TAC of uraemic retention solutes in serum over dialysis sessions was calculated by the following equation [29], where the denominator is a simplified single-pool Kt/V:

$$TAC = \frac{(C_0 - C_t)}{\ln\left(\frac{C_0}{C_t}\right)}, \quad (2)$$

where C_0 is the serum concentration of uraemic solutes before the dialysis session and C_t is the serum concentration of uraemic solutes at the end of the dialysis session.

Serum TAC values were normalized to a 300 ml/min effective blood flow rate to robustly compensate for dialyzer clearance.

$$TAC_n = TAC \cdot \frac{Q_b}{300\,\text{mL/min}}, \quad (3)$$

where Q_b is the effective blood flow rate for the particular dialysis session.

The mean concentration of uraemic toxins in spent dialysate during the dialysis session was calculated as the logarithmic mean concentration ($M_{ln}D$) using equation (3):

$$M_{ln}D = \frac{(D_0 - D_t)}{\ln\left(\frac{D_0}{D_t}\right)}, \quad (4)$$

where D_0 is the spent dialysate concentration of uraemic solutes in samples taken 7 min after the start of the dialysis session and

D_t is the spent dialysate concentration of uraemic solutes at the end of the dialysis session.

For comparability of dialysis sessions with different treatment settings, spent dialysate $M_{ln}D$ values were subsequently normalized to a 300 ml/min effluent dialysate flow rate to compensate for flow rate–dependent dilution of dialysate samples using equation (5), where Q_d is the effluent dialysate flow rate for the particular dialysis session:

$$M_{ln}D_n = M_{ln}D \cdot \frac{Q_d}{300\ \mathrm{mL/min}}. \quad (5)$$

The TRS of each solute was calculated from the total dialysate collection (TDC) as follows:

$$TRS = \frac{W_{tank}}{1\ \mathrm{kg/L}} \cdot D_{tank}, \quad (6)$$

where D_{tank} is the concentration of uraemic solute in the total dialysate collection and W_{tank} is the weight of total waste dialysate in the dialysate collection tank (kg).

All the results were assessed for possible errors and data conformity. The stability of blood and dialysate flow rates were monitored online (shown in Supplementary Figure 1) throughout each dialysis session, similarly as described before [30]. Dialysis sessions were excluded from the analysis when the sampling of spent dialysate had occurred during notably different flow rates relative to the other sampling points or during self-tests of the HD machine. In addition, data points in which analyte concentrations were below the quantification limit of clinical laboratory methods were omitted.

Linear regression analysis was used to investigate the relationship between TAC values in serum and TRS and $M_{ln}D_n$ values in spent dialysate. Afterwards, obtained linear regression equations were used to estimate TAC values in serum. Confidence intervals were estimated for regression lines using the predict function in MATLAB R2020b (MathWorks, Natick, MA, USA).

Systematic error (BIAS) was calculated for the results as follows:

$$BIAS = \frac{\sum_{i=1}^{N} e_i}{N}, \quad (7)$$

where e_i is the ith residual (difference between the results) and N is the number of observations [31].

The standard error (SE) of performance corrected for BIAS was calculated as follows [31]:

$$SE = \sqrt{\frac{\sum_{i=1}^{N} (e_i - BIAS)^2}{N-1}}. \quad (8)$$

Individual differences between the TAC of uraemic toxins in serum and corresponding values estimated from TRS or $M_{ln}D$ values in spent dialysate were examined using Bland–Altman analysis [32]. MATLAB R2020b was used for data analysis and data visualization.

RESULTS

Overall, clinical data were available for 78 participants from four HD units from four different countries monitored for a total of 312 dialysis procedures. Clinical characteristics have been described earlier [28] and are summarized in Supplementary Table 1. TAC values were calculated from intradialytic serum and $M_{ln}D$ values were calculated from spent dialysate concentrations for different uraemic retention solutes and normalized by effective blood or spent dialysate flow rates, respectively. TRS was evaluated based on TDC.

There was a generally strong correlation between TRS and intradialytic TAC ($R^2 > 0.59$) values (shown in Fig. 2) and $M_{ln}D$ ($R^2 > 0.89$) values (shown in Supplementary Fig. 2) for different uraemic retention solutes, normalized by effective blood or spent dialysate flow rates, respectively. The lowest R^2 values were found for β2M, a solute with the highest intercompartmental resistance and molecular weight.

There was also good correlation between intradialytic TAC and $M_{ln}D$ values in all cases, regardless of treatment modality (shown in Fig. 3). The correlation was higher for urea (molecular mass 60 g/mol, $R^2 = 0.92$), intermediate for UA and IS (molecular mass 168 g/mol, $R^2 = 0.80$ and molecular mass 213 g/mol, $R^2 = 0.84$, respectively) and lower for β2M (molecular weight 11.8 kDa, $R^2 = 0.63$). For haemodiafiltration and HD modality separately, the strongest correlation was seen for urea [$R^2 = 0.91$ ($n = 152$), $R^2 = 0.96$ ($n = 63$)] and the weakest correlation for β2M [$R^2 = 0.62$ ($n = 168$), $R^2 = 0.83$ ($n = 37$)], respectively.

Table 1 shows the intradialytic TAC values for urea, UA, β2M and IS and the corresponding TAC values calculated from TRS or $M_{ln}D_n$ in spent dialysate. TAC values estimated from TRS were calculated by the linear regression equations shown in Fig. 2 and TAC values estimated from spent dialysate $M_{ln}D_n$ values were calculated by the linear regression equations shown in Fig. 3.

Bland–Altman plots comparing intradialytic TAC values and TAC values estimated from spent dialysate $M_{ln}D_n$ normalized by flow rates or estimated from TRS are shown in Fig. 4. It can be seen from the plot that random error between TAC values and estimated TAC values remains similar over the whole concentration scale, while systematic error is negligible.

DISCUSSION

To our knowledge, serum TAC of uraemic toxins have not been previously estimated from spent dialysate. The main finding of the present report is that the concentration of diverse uraemic solutes in spent dialysate can be used to estimate serum TAC values for multiple uraemic solutes, minimizing blood sampling needs and blood loss. This finding sets the stage for online optical monitoring of serum TAC from spent dialysate concentrations of multiple uraemic toxins that would allow real-time, point-of-care decision making regarding HD adequacy [23, 24, 30].

The high correlation coefficients found between intradialytic TAC and spent dialysate $M_{ln}D$ or TRS values support the potential to estimate the intradialytic TAC of uraemic solutes with different removal kinetics from their concentrations in spent dialysate.

It is noteworthy that the midweek mean intradialytic serum TAC value of urea (10.4 ± 3.8 mmol/L) was well aligned with the average equivalent measures of the HEMO study standard and high-dose arm, corresponding to a HEMO high weekly TAC value ≤11.6 mmol/L [33], very similar to the median TAC values presented by Kloppenburg *et al.* [34], and the plasma TAC (11.7 mmol/L) for a study exploring increasing HD frequency versus HD duration [7], respectively. Furthermore, the achieved serum urea TAC was very close to the lowest TAC value (≈10 mmol/L) for the most efficient treatment modes in the 'Lopot plot' [35] modelled from data with varying duration, frequency and spacing of treatments based on a study using a

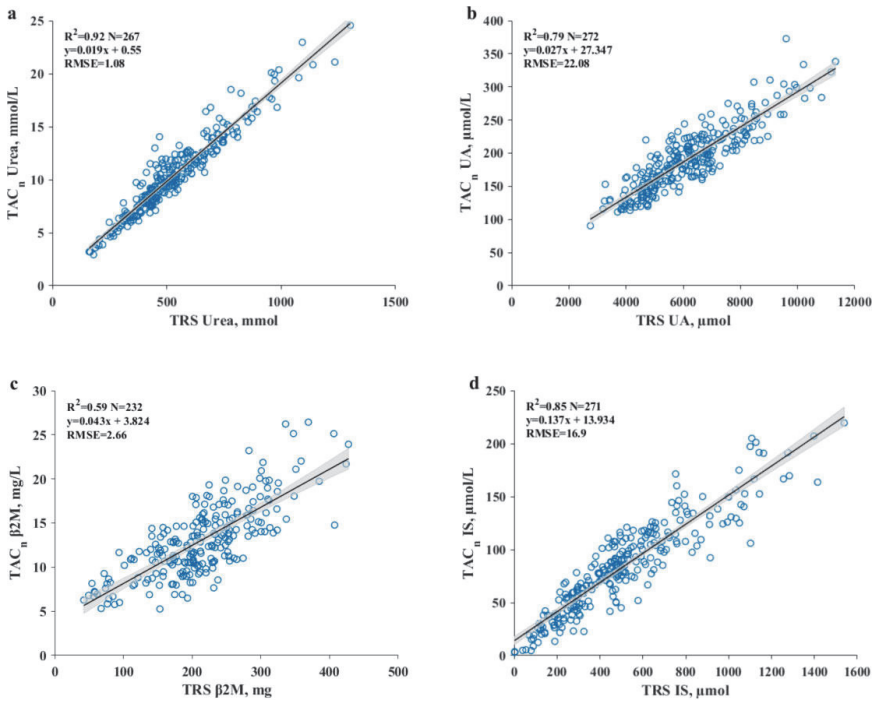

Figure 2: Correlation between total dialysate collection based on TRS and intradialytic TACs of **(a)** urea, **(b)** UA, **(c)** β2M and **(d)** IS in serum (TAC_n) normalized by effective blood flow rate. Black line indicates the regression line and grey area indicates the 95% CI of the slope.

variable-volume two-pool urea kinetic model [8]. Even so, serum urea TAC values remained higher than those obtained with high-efficiency daily HD, which are close to those of healthy kidneys, in which serum urea TAC is <4 mmol/L [36].

The strongest correlation between intradialytic TAC and spent dialysate $M_{ln}D$ values was observed for urea ($R^2 = 0.92$) and the weakest for β2M ($R^2 = 0.63$). The main reason for the different correlation coefficients of different uraemic solutes is probably related to the solute-dependent kinetic behaviour. Urea has negligible resistance to intercompartmental shifts compared with other solutes, which are therefore more difficult to remove by dialysis [4, 12, 13]. This causes a rapid decline of the serum concentration of other solutes at the beginning of the HD session, especially for solutes with slow intercompartment clearance such as β2M, and therefore double-pool kinetics should be used to describe the removal of such solutes [12, 37].

As serum TAC values over the dialysis session were calculated in the current work using equation (2), where the denominator is a simplified single-pool Kt/V [38], serum TAC of uraemic toxins with slower intercompartment clearance was probably overestimated due to the pronounced decrease of serum levels at the start of dialysis [12, 37]. The divergence between serum TAC and corresponding values estimated from $M_{ln}D$ was likely further amplified by the difference in the timing of the sampling time of blood and spent dialysate. While the first serum samples were taken prior to the start of dialysis when serum and extracellular compartments were equilibrated, the first spent dialysate samples were taken 7 minutes after starting the dialysis session, when an intercompartmental concentration gradient had already been developed to some extent. This effect even overestimates intradialytic serum urea TAC when using only pre-dialysis and post-dialysis serum samples to calculate TAC [7, 20, 21], but a larger effect can be expected for solutes with higher intercompartmental resistance.

These inaccuracies can be avoided by measuring intradialytic serum and spent dialysate concentrations with higher frequency to accurately describe the concentration profile and TAC or $M_{ln}D$ of solutes. While additional blood sampling is inconvenient and burdensome for patients, continuous monitoring of different uraemic toxins simultaneously in spent dialysate can be achieved non-invasively with online optical monitoring methods [22–24]. Continuous monitoring of uraemic toxin concentrations in spent dialysate could be used to obtain precise TAC values from TRS [23, 30, 39].

In addition, online monitoring of effluent dialysate concentrations can help to detect interruptions in treatment, sudden changes of dialysate and blood flows and clinical alarms and determine effective dialysis time [30, 40] more accurately, which could reduce errors in TAC estimation. Furthermore, the accuracy of TAC estimation could be increased by using real-time values of dialysis machine treatment settings and considering dialyzer specifications in the modelling of dialyzer clearance. Whereas in this study membranes with negligible adsorption capacity were used, it is important to note that the use of

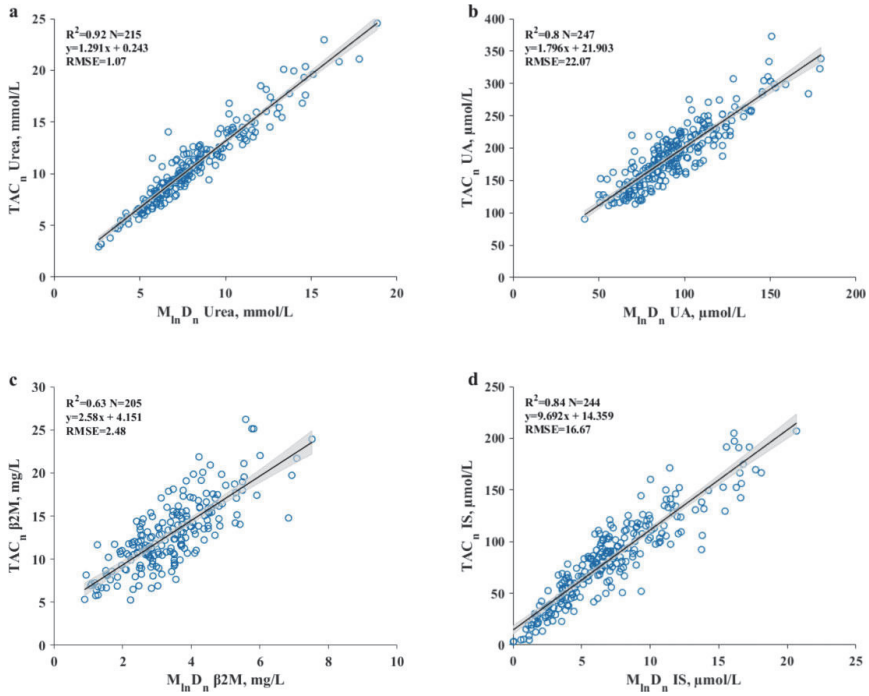

Figure 3: Correlation between intradialytic TACs of **(a)** urea, **(b)** UA, **(c)** β2M and **(d)** IS in serum (TAC_n) and logarithmic mean concentration ($M_{ln}D_n$) in spent dialysate normalized by effective blood or spent dialysate flow rates, respectively. Black line indicates the regression line and grey area indicates the 95% CI of the slope.

Table 1: Mean ± SD values of intradialytic TACs (TAC_n) normalized by blood flow rate and estimated from TRS and $M_{ln}D_n$ in spent dialysate normalized by spent dialysate flow rate for urea, UA, β2M and total IS).

	TAC_n	TAC_n from TRS	TAC_n from $M_{ln}D_n$
Urea (mmol/L)	10.4 ± 3.8 ($n = 274$)	10.5 ± 3.6 ($n = 267$)	10.7 ±3.7 ($n = 215$)
UA (µmol/L)	191.6 ± 48.1 ($n = 273$)	191.5 ± 42.8 ($n = 272$)	191.6 ± 43.8 ($n = 247$)
β2M (mg/L)	13.3 ± 4.3 ($n = 264$)	13.0 ± 3.2 ($n = 232$)	12.9 ± 3.2 ($n = 205$)
IS (µmol/L)	82.9 ± 43.3 ($n = 273$)	82.7 ± 40.0 ($n = 271$)	82.2 ± 38.6 ($n = 244$)

negatively charged adsorptive membranes such as polymethyl methacrylate or adsorbent columns can additionally adsorb uraemic toxins before passing across the membrane into spent dialysate. This may cause additional errors in the dialysate-based readings and the commonly used set-up of optical sensors should be modified to take this effect into account.

Also, patient-specific parameters such as dialyzer recirculation [41] and haematocrit [4] influence the clearance of uraemic toxins and thus proportionality [25, 42] between serum concentration of uraemic toxins and their concentration in spent dialysate [30]. In this regard, urea is removed from both erythrocytes and plasma water as blood passes through the dialyzer, but this is not the case for other uraemic toxins that are only removed from plasma, and thus their clearance depends on haematocrit and cannot exceed plasma flow [4]. Therefore, for uraemic toxins without facilitated transport in and out of erythrocytes, i.e. other than urea [4], plasma concentrations should be used in the estimation of TAC [4]. This can additionally explain why the strongest correlation between serum and spent dialysate TAC values was observed for urea, as we used serum concentrations, and clearance of urea is mainly limited by extracorporeal blood and dialysate flows [12].

Notwithstanding these limitations, the study demonstrates the feasibility of obtaining reasonable estimates of serum TAC values from spent dialysate. Moreover, preliminary (unpublished) data show that the modality does not affect the accuracy of optical estimation of uraemic toxin concentrations in spent dialysate in the tested range including higher dialysate and substitution flow rates. Before clinical implementation, these general models should be optimized for each uraemic toxin, considering treatment settings, dialyzer membrane specifications, patients' body parameters and using plasma values, which would allow a more precise estimation of serum TAC values from spent dialysate concentration values. Additionally,

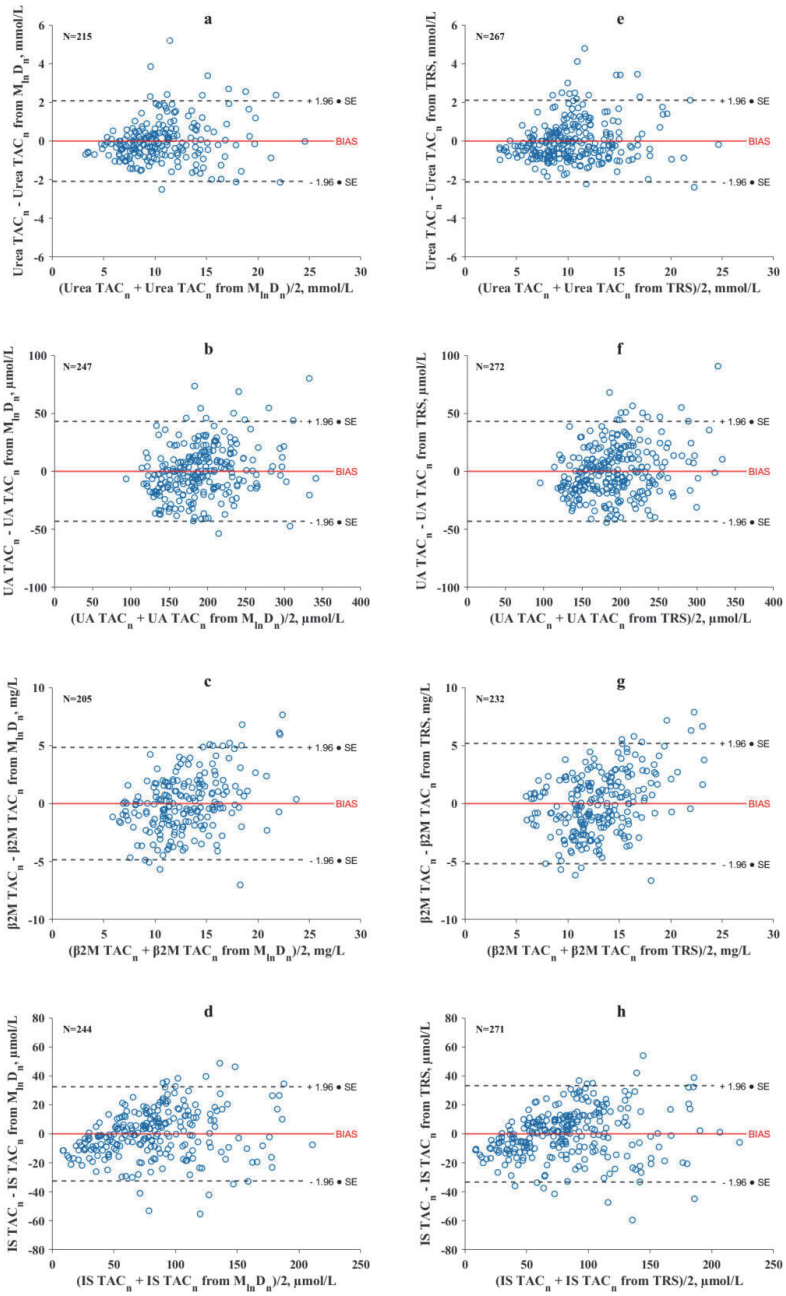

Figure 4: Bland–Altman plots comparing intradialytic TAC values in serum normalized by effective blood flow rate (TAC_n) and corresponding TAC_n values estimated from logarithmic mean concentrations ($M_{ln}D_n$) in spent dialysate normalized by spent dialysate flow or from TRS for **(a, e)** urea, **(b, f)** UA, **(c, g)** β2M and **(d, h)** total IS.

clinical implementation would be facilitated by estimating uraemic toxin concentrations in spent dialysate from continuous optical online monitoring of spent dialysate, providing a more convenient, less labour-intensive method [22–24, 30], which may allow optimization of the HD prescription.

Although the TAC concept offers additional information on HD adequacy, HD adequacy should be multitargeted and cover all patient needs and clinical goals that improve outcomes [14, 43, 44]. Kt/V has been criticized for ignoring the question of how much uraemic toxin is left in the patient [4]. The serum TAC concept can address this question. Moreover, Kt/V does not consider fluid management nor residual kidney function [45]. The latter should also be reflected in TAC values, which has been illustrated for β2M [46]. TAC is therefore a good parameter for comparison of the status of patients with varying residual kidney functions and diets on different dialysis strategies.

In conclusion, the present study demonstrates the feasibility of evaluating serum TAC of uraemic toxins from uraemic toxin concentrations in spent dialysate. In the future, automatic evaluation of intradialytic serum TAC values from optical online monitoring of spent dialysate could provide a more convenient and precise measure of the impact of treatment on TAC values and allow a real-time, point-of-care adjustment of the dialysis prescription. In this regard, for clinical implementation, the general models described herein should be optimized for each uraemic toxin considering treatment settings and patient parameters.

SUPPLEMENTARY DATA

Supplementary data are available at *ckj* online.

ACKNOWLEDGEMENTS

The authors wish to thank all the dialysis patients who participated in the experiments, Rain Kattai and Deniss Karai for their skilful technical assistance; Maris Alev, Mihkel Fridolin, Risto Tanner and Relika Toome for helping with the data collection and analysis; Kai Lauri for coordinating biochemical analyses in SYNLAB Eesti OÜ; nurses at the Centre of Nephrology, North Estonia Medical Centre for assistance during the clinical experiments; the research nurses Kelly Stjernfelt and Micael Gylling for data collection; Mattias Ekström and Mats Torvaldsson Tränk for technical assistance at the Department of Nephrology, University Hospital, Linköping, Sweden; the research nurses Isabelle Dewettinck, Sabine Inion and Elsie De Man for their assistance during the experimental dialysis sessions and data collection, and Tom Mertens, Sophie Lobbestael and Bart Vaeyens for their technical assistance at the Department of Nephrology, Ghent University Hospital, Ghent, Belgium; and the research nurse Monica Pereira at the Fundación Jiménez Díaz University Hospital Health Research Institute in Madrid, Spain.

FUNDING

This research was funded partly by the European Union through the European Regional Development Fund (H2020-SMEINST-2-2017), OLDIAS2—Online Dialysis Sensor Phase2 project (grant agreement 767572), the Estonian Ministry of Education and Research under institutional research financing (grant IUT 19-2) and the Estonian Centre of Excellence in IT (EXCITE) funded by the European Regional Development Fund. Financial support for some of the Swedish portion of the study came from the Njurfonden (2017 and 2018), Sweden. M.V.P.G. was funded by Programa Rio Hortega ISCIII FEDER funds. A.O. was funded by PI19/00588, PI19/00815, DTS18/00032, ERA-PerMed-JTC2018 (KIDNEY ATTACK AC18/00064 and PERSTIGAN AC18/00071, ISCIII-RETIC REDinREN RD016/0009 FEDER funds, Sociedad Española de Nefrología, Fundacion Renal Iñigo Álvarez de Toledo (FRIAT), Comunidad de Madrid CIFRA2 B2017/BMD-3686.

AUTHORS' CONTRIBUTIONS

A.F., I.F., G.G., M.L., M.S., F.U. and A.O. were responsible for conceptualization. A.A., J.A., A.D., A.F., I.F., G.G., L.L., M.L., J.P., E.G.-P., V.M.P.-G., M.S., F.U. and A.O. were responsible for the methodology. J.P., A.A., J.A., J.H., A.D., G.G., L.L., V.M.P.-G., D.S.-O., E.G.-P. and F.U. were responsible for the investigation. J.P., A.A., J.A., A.D., L.L., V.M.P.-G., D.S.-O., K.P. and F.U. were responsible for data curation. J.A., J.P. and I.F. were responsible for validation. J.P., J.A., I.F. and K.P. were responsible for formal analysis. J.P., A.A., J.A., A.D., A.F., E.G.-P., J.H., I.F., G.G., J.H., L.L., M.L., V.M.P.-G., M.S., K.P., F.U. and A.O. were responsible for original draft preparation. J.P., A.A., J.A., A.D., A.F., E.G.-P., J.H., I.F., G.G., J.H., L.L., M.L., V.M.P.-G., M.S., K.P., F.U. and A.O. were responsible for review and editing. J.P. and K.P. were responsible for visualization.

DATA AVAILABILITY STATEMENT

The data are owned by a third party. The data underlying this article were provided by OÜ Optofluid Technologies by permission. Data will be shared upon request to the corresponding author with permission of OÜ Optofluid Technologies.

CONFLICT OF INTEREST STATEMENT

A.F. has received consultancy or speaker fees from Otsuka, AstraZeneca, Vifor Pharma and Alnylam. A.O. is the former CKJ Editor-in-Chief and has received grants from Sanofi and consultancy or speaker fees or travel support from Advicciene, Astellas, AstraZeneca, Amicus, Amgen, Fresenius Medical Care, GlaxoSmithKline, Bayer, Sanofi-Genzyme, Menarini, Kyowa Kirin, Alexion, Idorsia, Chiesi, Otsuka, Novo Nordisk and Vifor Fresenius Medical Care Renal Pharma and is director of the Catedra Mundipharma-UAM of diabetic kidney disease and the Catedra AstraZeneca-UAM of chronic kidney disease and electrolytes. V.M.P.-G. has received grants from Catedra Mundipharma-UAM and Catedra AstraZeneca-UAM and consultancy or speaker fees or travel support from Kyowa Kirin, Alexion and Otsuka AstraZeneca and Sanofi-Genzyme. M.S. has received grants from Hansa Biopharma and consulting fees from Hansa Biopharma, Chemocentryx, AstraZeneca and Vifor Pharma. All other authors declare no conflicts of interest. The funders had no role in the design of the study; in the collection, analyses or interpretation of data; in the writing of the manuscript or in the decision to publish the results.

REFERENCES

1. Steyaert S, Holvoet E, Nagler E *et al*. Reporting of "dialysis adequacy" as an outcome in randomised trials conducted in adults on haemodialysis. *PLoS One* 2019;**14**:e0207045. https://doi.org/10.1371/journal.pone.0207045
2. Saran R, Canaud BJ, Depner TA *et al*. Dose of dialysis: key lessons from major observational studies and clinical trials. *Am J Kidney Dis* 2004;**44**:47–53. https://doi.org/10.1053/j.ajkd.2004.08.011

3. Vanholder R, Van Biesen W, Lameire N. A swan song for Kt/V urea. *Semin Dial* 2019;**32**:424–37. https://doi.org/10.1111/sdi.12811
4. Meyer TW, Sirich TL, Hostetter TH. Dialysis cannot be dosed. *Semin Dial* 2011;**24**:471–9. https://doi.org/10.1111/j.1525-139X.2011.00979.x
5. Spalding EM, Chandna SM, Davenport A *et al.* Kt/V underestimates the hemodialysis dose in women and small men. *Kidney Int* 2008;**74**:348–55. https://doi.org/10.1038/ki.2008.185
6. Daugirdas JT, Hanna MG, Becker-Cohen R *et al.* Dose of dialysis based on body surface area is markedly less in younger children than in older adolescents. *Clin J Am Soc Nephrol* 2010;**5**:821–7. https://doi.org/10.2215/CJN.08171109
7. Eloot S, van Biesen W, Dhondt A *et al.* Impact of increasing haemodialysis frequency versus haemodialysis duration on removal of urea and guanidino compounds: a kinetic analysis. *Nephrol Dial Transplant* 2009;**24**:2225–32. https://doi.org/10.1093/ndt/gfp059
8. Daugirdas JT, Tattersall J. Effect of treatment spacing and frequency on three measures of equivalent clearance, including standard Kt/V. *Nephrol Dial Transplant* 2010;**25**:558–61. https://doi.org/10.1093/ndt/gfp446
9. Marquez IO, Tambra S, Luo FY *et al.* Contribution of residual function to removal of protein-bound solutes in hemodialysis. *Clin J Am Soc Nephrol* 2011;**6**:290–6. https://doi.org/10.2215/CJN.06100710
10. Eloot S, Van Biesen W, Glorieux G *et al.* Does the adequacy parameter Kt/Vurea reflect uremic toxin concentrations in hemodialysis patients? *PLoS One* 2013;**8**:e76838. https://doi.org/10.1371/journal.pone.0076838
11. Eloot S, Torremans AN, De Smet R *et al.* Kinetic behavior of urea is different from that of other water-soluble compounds: the case of the guanidino compounds. *Kidney Int* 2005;**67**:1566–75. https://doi.org/10.1111/j.1523-1755.2005.00238.x
12. Eloot S, Schneditz D, Vanholder R. What can the dialysis physician learn from kinetic modelling beyond Kt/Vurea? *Nephrol Dial Transplant* 2012;**27**:4021–9. https://doi.org/10.1093/ndt/gfs367
13. Vanholder R, Glorieux G, Eloot S. Once upon a time in dialysis: the last days of Kt/V? *Kidney Int* 2015;**88**:460–5. https://doi.org/10.1038/ki.2015.155
14. Perl J, Dember LM, Bargman JM *et al.* The use of a multidimensional measure of dialysis adequacy—moving beyond small solute kinetics. *Clin J Am Soc Nephrol* 2017;**12**:839–47. https://doi.org/10.2215/CJN.08460816
15. Casino FG, Lopez T. The equivalent renal urea clearance: a new parameter to assess dialysis dose. *Nephrol Dial Transplant* 1996;**11**:1574–81. https://doi.org/10.1093/ndt/11.8.1574
16. Lopot F, Nejedlý B, Sulková S. Physiology in daily hemodialysis in terms of the time average concentration/time average deviation concept. *Hemodial Int* 2004;**8**:39–44. https://doi.org/10.1111/j.1492-7535.2004.00073.x
17. Locatelli F, Buoncristiani U, Canaud B *et al.* Haemodialysis with on-line monitoring equipment: tools or toys? *Nephrol Dial Transplant* 2005;**20**:22–33. https://doi.org/10.1093/ndt/gfh555
18. Waniewski J, Debowska M, Lindholm B. Theoretical and numerical analysis of different adequacy indices for hemodialysis and peritoneal dialysis. *Blood Purif* 2006;**24**:355–66. https://doi.org/10.1159/000093199
19. Mineshima M. Intensive hemodialysis: effects of treatment time and frequency on time-averaged concentrations of solutes. In: Nakamoto H, Nitta K, Tsuchiya K *et al.*, eds. *Recent Advances in Dialysis Therapy in Japan*. Basel: Karger, 2018:184–7. https://doi.org/10.1159/000485720
20. Kanagasundaram NS, Greene T, Larive AB *et al.* Dosing intermittent haemodialysis in the intensive care unit patient with acute renal failure—estimation of urea removal and evidence for the regional blood flow model. *Nephrol Dial Transplant* 2008;**23**:2286–98. https://doi.org/10.1093/ndt/gfm938
21. Garred LJ. Dialysate-based kinetic modeling. *Adv Ren Replace Ther* 1995;**2**:305–18. https://doi.org/10.1016/S1073-4449(12)80029-X
22. Castellarnau A, Werner M, Günthner R *et al.* Real-time Kt/V determination by ultraviolet absorbance in spent dialysate: technique validation. *Kidney Int* 2010;**78**:920–5. https://doi.org/10.1038/ki.2010.216
23. Lauri K, Arund J, Holmar J *et al.* Removal of urea, β2-microglobulin, and indoxyl sulfate assessed by absorbance and fluorescence in the spent dialysate during hemodialysis. *ASAIO J* 2020;**66**:698–705. https://doi.org/10.1097/MAT.0000000000001058
24. Luman M, Jerotskaja J, Lauri K *et al.* Dialysis dose and nutrition assessment by optical on-line dialysis adequacy monitor. *Clin Nephrol* 2009;**72**:303–11. https://doi.org/10.5414/CNP72303
25. Garred LJ, DiGiuseppe B, Chand W *et al.* KT/V and protein catabolic rate determination from serial urea measurement in the dialysate effluent stream. *Artif Organs* 1992;**16**:248–55. https://doi.org/10.1111/j.1525-1594.1992.tb00305.x
26. Ficheux A, Gayrard N, Szwarc I *et al.* The use of SDS-PAGE scanning of spent dialysate to assess uraemic toxin removal by dialysis. *Nephrol Dial Transplant* 2011;**26**:2281–9. https://doi.org/10.1093/ndt/gfq709
27. Vanholder R, Pletinck A, Schepers E *et al.* Biochemical and clinical impact of organic uremic retention solutes: a comprehensive update. *Toxins (Basel)* 2018;**10**:33. https://doi.org/10.3390/toxins10010033
28. Paats J, Adoberg A, Arund J *et al.* Serum levels and removal by haemodialysis and haemodiafiltration of tryptophan-derived uremic toxins in ESKD patients. *Int J Mol Sci* 2020;**21**:1522. https://doi.org/10.3390/ijms21041522
29. Paats J, Adoberg A, Arund J *et al.* Optical method and biochemical source for the assessment of the middle-molecule uremic toxin β2-microglobulin in spent dialysate. *Toxins (Basel)* 2021;**13**:255. https://doi.org/10.3390/toxins13040255
30. Uhlin F, Fridolin I, Magnusson M *et al.* Dialysis dose (Kt/V) and clearance variation sensitivity using measurement of ultraviolet-absorbance (on-line), blood urea, dialysate urea and ionic dialysance. *Nephrol Dial Transplant* 2006;**21**:2225–31. https://doi.org/10.1093/ndt/gfl147
31. Esbensen K. *Multivariate Data Analysis – In Practice: an introduction to multivariate data analysis and experimental design*, 5th ed. Oslo: Camo Software, 2009.
32. Giavarina D. Understanding Bland Altman analysis. *Biochem Med (Zagreb)* 2015;**25**:141–51. https://doi.org/10.11613/BM.2015.015
33. Vartia A. Effect of treatment frequency on haemodialysis dose: comparison of EKR and stdKt/V. *Nephrol Dial Transplant* 2009;**24**:2797–803. https://doi.org/10.1093/ndt/gfp177
34. Kloppenburg WD, Stegeman CA, Hooyschuur M *et al.* Assessing dialysis adequacy and dietary intake in the individual hemodialysis patient. *Kidney Int* 1999;**55**:1961–9. https://doi.org/10.1046/j.1523-1755.1999.00412.x
35. Korohoda P, Pietrzyk JA, Schneditz D. Quantifying the discontinuity of haemodialysis dose with time-averaged

concentration (TAC) and time-averaged deviation (TAD). *Nephrol Dial Transplant* 2010;**25**:1011–2. https://doi.org/10.1093/ndt/gfp656
36. Misra M, Nolph KD. Adequacy in dialysis: intermittent versus continuous therapies. *Nefrologia* 2000;**20**:25–32. http://www.ncbi.nlm.nih.gov/pubmed/10835874
37. Ward RA, Greene T, Hartmann B *et al.* Resistance to intercompartmental mass transfer limits β2-microglobulin removal by post-dilution hemodiafiltration. *Kidney Int* 2006;**69**:1431–7. https://doi.org/10.1038/sj.ki.5000048
38. Lim PS, Lin Y, Chen M *et al.* Precise quantitative assessment of the clinical performances of two high-flux polysulfone hemodialyzers in hemodialysis: validation of a blood-based simple kinetic model versus direct dialysis quantification. *Artif Organs* 2018;**42**:E55–66. https://doi.org/10.1111/aor.13011
39. Keshaviah PR, Ebben JP, Emerson PF. On-line monitoring of the delivery of the hemodialysis prescription. *Pediatr Nephrol* 1995;**9**(Suppl 1):S2–8. https://doi.org/10.1007/BF00867675
40. Ross EA, Paugh-Miller JL, Nappo RW. Interventions to improve hemodialysis adequacy: protocols based on real-time monitoring of dialysate solute clearance. *Clin Kidney J* 2018;**11**:394–9. https://doi.org/10.1093/ckj/sfx110
41. Mohan S, Madhrira M, Mujtaba M *et al.* Effective ionic dialysance/blood flow rate ratio: an indicator of access recirculation in arteriovenous fistulae. *ASAIO J* 2010;**56**:427–33. https://doi.org/10.1097/MAT.0b013e3181e743eb
42. Fridolin I, Magnusson M, Lindberg LG. On-line monitoring of solutes in dialysate using absorption of ultraviolet radiation: technique description. *Int J Artif Organs* 2002;**25**:748–61. https://doi.org/10.1177/039139880202500802
43. Canaud B, Stuard S, Laukhuf F *et al.* Choices in hemodialysis therapies: variants, personalized therapy and application of evidence-based medicine. *Clin Kidney J* 2021;**14**:i45–i58. https://doi.org/10.1093/ckj/sfab198
44. Canaud B, Wabel P, Tetta C. Dialysis prescription: a modifiable risk factor for chronic kidney disease patients. *Blood Purif* 2010;**29**:366–74. https://doi.org/10.1159/000309422
45. Fernández Lucas M, Ruíz-Roso G, Merino JL *et al.* Initiating renal replacement therapy through incremental haemodialysis: protocol for a randomized multicentre clinical trial. *Trials* 2020;**21**:206. https://doi.org/10.1186/s13063-020-4058-0
46. Roumelioti ME, Nolin T, Unruh ML *et al.* Revisiting the middle molecule hypothesis of uremic toxicity: a systematic review of beta 2 microglobulin population kinetics and large scale modeling of hemodialysis trials in silico. *PLoS One* 2016;**11**:e0153157. https://doi.org/10.1371/journal.pone.0153157

Appendix 4 – Publication III

Publication III

Paats, J., Adoberg, A., Leis, L., Arund, J., Lauri, K., Luman, M., Tanner, R., Holmar, J., Pilt, K., Fridolin, I. (2025). Intradialytic optical assessment of C-mannosyl tryptophan removal using spent dialysate. Scientific Reports, 15(1), 20052. https://doi.org/10.1038/s41598-025-01844-z.

scientific reports

Check for updates

OPEN

Intradialytic optical assessment of C-mannosyl tryptophan removal using spent dialysate

Joosep Paats[1]✉, Annika Adoberg[1,2], Liisi Leis[1,2], Jürgen Arund[1], Kai Lauri[1,3], Merike Luman[1,2], Risto Tanner[1], Jana Holmar[1], Kristjan Pilt[1] & Ivo Fridolin[1]

C-mannosyl tryptophan (CMW), also known as C-glycosyltryptophan, is a novel biomarker that is strongly correlated to chronic kidney disease (CKD) incidence and progression risk and mortality among earlier stages of CKD patients prior to end stage kidney disease. This study determined concentrations of CMW in blood and spent dialysate of CKD patients on chronic hemodialysis (HD) for the first time, and investigated the possibility for optical estimation of CMW concentrations in spent dialysate, its intradialytic removal and time-averaged concentration (TAC) of CMW based on optical measurements of spent dialysate. In total, 264 pre- and postdialysis blood samples, and 528 spent dialysate samples from 88 HD sessions of 22 patients were analyzed using high pressure liquid chromatography and spectrophotometry. We identified that CMW concentrations in CKD patients on chronic HD are over 10 times higher compared to earlier reported CMW concentrations in healthy subjects. The concentration of CMW in spent dialysate can be monitored based on spectrophotometric analysis of spent dialysate ($r > 0.939$, standard error: 0.07 µmol/L) and it is possible to evaluate CMW-based HD adequacy parameters, such as reduction ratio, mass of total removed solute, and TAC without blood sampling. In future, optical monitoring of CMW could be potentially used to improve clinical management of hemodialysis patients.

Keywords C-mannosyl tryptophan, C-glycosyltryptophan, Hemodialysis, End stage kidney disease, Uremic solutes, Spectrophotometric analysis

Chronic kidney disease (CKD) affects approximately 10% of the global population[1]. CKD is a progressive disease, and if uncontrolled, CKD can progress to end stage kidney disease (ESKD). In case of ESKD, kidney replacement therapy (KRT) is required to prevent death from uremic syndrome, caused mainly by uremic solutes that accumulate to the body in ESKD[2]. The most applied form of KRT is hemodialysis (HD), accounting for approximately 69% of all forms of KRT that were applied to treatment of 3.9 million ESKD patients in 2017[3]. During HD metabolic waste products, termed as uremic solutes, and excessive water are removed from ESKD patients' bodies, and balance of electrolytes is restored. By the year 2015, over 270 different uremic solutes had been identified of which many are considered to exert toxic effect based on experimental or observational studies and randomized controlled trials[4,5]. Since retention of uremic solutes in CKD arises from impaired kidney function through decreased filtration, secretion, reabsorption, generation or metabolic breakdown of solutes, efforts have been taken to identify reliable metabolite biomarker for diagnostic purposes and for improving health outcomes of CKD[6–9]. However, as biomarker levels can be influenced by anthropometric parameters, nutritional status, gut microbiome in addition to impaired kidney function and etiology[9], it can be challenging to characterize status of patients from different populations and stages of CKD based on the concentration of individual metabolite, such as in case of using creatinine for glomerular filtration rate (GFR) estimation[6,9–11].

Among uremic solutes[5], monomeric C-mannosyl tryptophan (CMW) with monoisotopic molecular weight of 366.14 Da, also known as C-glycosyltryptophan, is a clinically promising biomarker that has been shown to be independently and strongly correlated with health outcomes and estimated GFR (eGFR) in healthy subjects and patients in different stages of CKD from populations of European and non-European ancestry independent of age[12–15]. Particularly, CMW is a degradation product of C-mannosylatated proteins[16], which have undergone a unique post-translational modification that features attachment of a single α-mannose to the tryptophan residue of a substrate protein via C–C bond, the only known form of protein C-linked glycosylation in humans[17–19].

[1]Department of Health Technologies, Tallinn University of Technology, 19086 Tallinn, Estonia. [2]Centre of Nephrology, North Estonia Medical Centre, Sütiste Tee 19, 13419 Tallinn, Estonia. [3]SYNLAB Eesti OÜ, Veerenni 53a, 10138 Tallinn, Estonia. ✉email: joosep.paats@taltech.ee

In contrast to the O-glycosidic and N-glycosidic bonds, C-glycosyl bond that connects the carbohydrate to target molecule is generally resistant to hydrolysis and exhibits more metabolic stability[20]. Specifically, C-mannosylation is mediated by C-mannosyltransferases in endoplasmic reticulum that transfer a mannose from dolichol phosphate mannose usually to the first tryptophan in the motif Trp-Xaa-Xaa-Trp of a substrate proteins[18,21,22]. So far, approximately 30 different C-mannosylated proteins, mostly from thrombospondin type I repeat superfamily and cytokine receptor type I family, have been experimentally verified in humans[18]. However, 18% of all human secreted or transmembrane proteins have been predicted to be C-mannosylated[21], which appears to be essential for proper folding, stability, transportation, and function of the C-mannosylated proteins[18]. Eventually, during the proteolytic degradation of C-mannosylated proteins, a monomeric CMW is generated that is thought to be not further catabolized in the body[16,18]. Consequently, CMW is excreted from the body via urine[23,24], reportedly with the clearance of CMW close to that of inulin[25].

Concerning clinical relevance, several researchers from different workgroups have shown that blood concentration of CMW is a good indicator of eGFR[12,25,26] and a predictor of eGFR decline[12,13,27]. A recently published study of Burgh et al., which enrolled over 4800 participants, found that among the total of 1381 studied metabolites, CMW was the most strongly associated metabolite with CKD risk and progression[13]. While serum concentration of CMW increases exponentially with the decline of eGFR[25], urine CMW levels are also altered with CKD and provide information about CKD outcomes similarly[14]. In a metabolome-wide association study enrolling 5087 CKD patients, with measurements of 1487 metabolites in urine, higher levels of CMW in urine were significantly associated with all of the adverse outcomes of interest, such as progression to ESKD, a combined progression to ESKD and acute kidney injury, and death[14]. Notably, out of the 55 identified urine metabolites that were significantly associated with at least one of the endpoints in that study, CMW was the only metabolite related to all of the examined outcomes, disregarding the unknown metabolite X-12117[14]. Moreover, some studies have shown that concentration of CMW is more strongly correlated to measured GFR compared to established serum creatinine–based parameters, regardless of the age and muscle mass of the subject[12,25,26].

Although CMW is a clinically promising biomarker and an endogenous uremic solute with potential intrinsic toxicity, the dialytic removal characteristics of CMW and the relationship between clinical outcomes and CMW have not been assessed so far for ESKD patients who are receiving HD. Additionally, biochemical methods have not been developed to determine CMW concentrations yet, and quantification of CMW with mass spectrometry or chromatographical methods remains time consuming and expensive.

The aim of this study was to determine the levels of CMW in ESKD patients' blood and spent dialysate using high pressure liquid chromatography (HPLC), and investigate the possibility for optical estimation of CMW concentrations in spent dialysate, and assess time-averaged concentration (TAC) of CMW and its intradialytic removal as reduction ratio (RR) and total removed solute (TRS) based on spectrophotometric analysis of spent dialysate without blood sampling.

Methods

Ethics

The study protocol was approved by the Tallinn Medical Research Ethics Committee at the National Institute for Health Development in Estonia (decision no. 2205). A written informed consent was obtained from all patients involved in the study and the study was conducted in accordance with the Declaration of Helsinki.

Subjects and hemodialysis treatments settings

Twenty-two ESKD patients on chronic HD treatment (thrice weekly) were enrolled into the study from the Centre of Nephrology, North Estonia Medical Centre, Estonia as part of the multicenter OLDIAS2—Online Dialysis Sensor Phase 2 project, encompassing patients from diverse European countries[28]. All patients fulfilled the following criteria: over 18 years old with vascular access (arteriovenous fistula/ arteriovenous graft) capable of managing blood flow of at least 300 mL/min, without clinical signs of infection or other active acute clinical complications and an estimated life expectancy over 6 months. Of the patients, 17 were male and 5 were female, with an average age (± SD) of 55 ± 17 years, who had spKt/Vurea of 1.47 (1.23–1.67), given as median (interquartile range), in routine treatment. Detailed description of demographic and clinical data of patients has been presented in Table 1.

During the study period, each patient received four midweek dialysis sessions with predefined settings (Table 2) to vary dialytic removal of uremic toxins using Fresenius 5008 dialysis machine (Fresenius Medical Care, Bad Homburg v. d. Höfe, Germany). On the remaining days of the week, patients received their standard treatment regimen as prescribed in their routine clinical care. The predefined HD settings included: one low flux hemodialysis with minimal settings and three different post-dilution haemodiafiltration (HDF) treatments with the prescribed duration of 4 hours. Three different dialyzers with polysulphone-based membranes: Xevonta® Lo15 (B. Braun Medical, Melsungen, Germany), Helixone® FX800 and Helixone® FX1000 (Fresenius Medical Care, Bad Homburg v. d. Höfe, Germany) with effective membrane areas of 1.5 m^2, 1.8 m^2 and 2.2 m^2 were used, respectively. Treatment settings were kept constant during each dialysis session: the applied blood flow ranged from 200 to 400 mL/min and dialysate flow from 300 to 800 mL/min, respectively. Substitution volume over all HDF sessions varied from 11.7 to 31.2 L per session. In the end of each treatment, the effective average treatment settings of each session were recorded from the screen of dialysis machine (Table 2) for the following calculations.

Sample collection and analysis

During each treatment session, blood samples were collected from the arterial blood line and spent dialysate samples from the drain outlet tube of HD machine at discrete sampling times.

Entity of the Data	Specifications
Cause of ESKD	Diabetes (4); Hypertension (8); Glomerulonephritis (3); Tubulointerstitial nephritis (3); Renal carcinoma (2); Other (2)
Age [years]	55 ± 17
Gender	M 17; F 5
Race, Caucasian [%]	100
BMI [kg/m2]	26.8 ± 5.8
BW [kg]	81.5 ± 21.3
Ultrafiltration volume [mL]	2565 ± 1190
Urinary volume [mL]	0 [14 patients]; 700 (335–825) [8 patients]
Serum total protein [g/L]	62.8 ± 5.5
Hematocrit [%]	34.4 ± 3.5
Serum calcium [mmol/L]	2.25 ± 0.16
Serum phosphorus [mmol/L]	1.92 (1.63–2.29)
Serum parathyroid hormone [pmol/L]	28.7 (16.8–41.9)
Vascular access	AVF 15; AVG 7
Dialysis vintage [months]	23 (11–83)
spKt/Vurea	1.47 (1.23–1.67)

Table 1. Clinical data of the 22 end stage kidney disease (ESKD) patients monitored during total of 88 hemodialysis sessions. Numerical values are given as a mean ± standard deviation or as a median and interquartile range (Q1–Q3). M, male; F, female; BMI, body mass index; BW, body weight; spKt/V, single-pool criterion of the dose of dialysis; AVF, arteriovenous fistula, AVG, arteriovenous graft.

Entity of the Data	Standard HDF	Low Flux HD	Medium HDF	High HDF
Effective blood flow, mL/min (Qb)	296 (295–297)	199 (198–199)	297 (296–298)	368 (356–377)
Effective dialysate flow, mL/min (Qd)	359 (355–493)	297 (297–298)	789 (788–795)	791 (788–796)
Substitution volume (Vs, L)	22.0 (20.0–23.0)	0	14.9 (14.9–15)	25.2 (23–27.9)
Substitution rate, mL/min	95.5 (87–99)	0	66 (65–66)	112 (100–123)
Ultrafiltration rate, mL/min	9.0 (6.3–14.6)	12.6 (8.3–16.4)	11.6 (6.3–13.8)	11.25 (7.5–16.7)
Dialyzer model[a]	FX800; FX1000	Lo15	FX1000	FX1000
Number of dialyses (N)	22	22	22	22

Table 2. The effective dialysis treatment settings of the predefined hemodiafiltration (HDF) and hemodialysis (HD) sessions. Standard HDF marks treatment settings that were prescribed to the patients in routine clinical care. Numerical values of each modality are given as median and interquartile range (Q1–Q3). [a]Specification of dialyzers and effective membrane areas: Helixone® FX800 1.8 m^2, Helixone® FX1000 2.2 m^2 (Fresenius Medical Care, Bad Homburg v. d. Höfe, Germany), Xevonta® Lo 15 1.8 m^2 (B. Braun Medical, Melsungen, Germany).

Blood samples were drawn immediately before the start, and immediately at the end of the dialysis session using the slow pump method, i.e. blood flow was decreased to 50 mL/min 2 min prior of the sampling to avoid any effects of recirculation. Additionally, one blood sample was taken 30 min postdialysis. Blood samples were collected into 3.5 mL and 5 mL Becton Dickinson Vacutainer SST II Advance (Franklin Lakes, NJ, USA) tubes, kept still for 30 min to allow clotting and were thereafter centrifuged for 20 min with swing-out buckets at 3000 g. After centrifugation, serum was separated from the blood cells and subjected to further analyses.

Spent dialysate samples were collected from the drain outlet of the dialysis machine 7, 60, 120, 180 min after the start, and at the end of dialysis session (240 min) before initiating the slow pump method. Additionally, the total spent dialysate from the whole procedure was collected to a large tank. After the procedure, the tank was weighted with DE 300K50DL platform scale (Kern & Sohn GmbH, Balingen, Germany) and after carefully mixing, a sample was taken from the tank to estimate mass of total removed solute. All dialysate samples were first collected into 120 mL Becton Dickinson Vacutainer urine collection cups (Franklin Lakes, NJ, USA) and aliquoted afterwards into 5 mL Brand cryogenic tubes (Brand GMBH & CO KG, Wertheim, Germany) for analytical chemistry analyses.

A total of 264 blood samples (including 176 pre- and immediate postdialysis, and 88 blood samples taken 30 min postdialysis) and 528 spent dialysate samples of 22 patients from 88 different dialysis sessions were collected and subjected to further analysis on the same day. One set of serum samples was sent to the clinical chemistry laboratory (SYNLAB Eesti OÜ, Tallinn, Estonia) to determine concentration of most used dialysis dose marker molecule urea in serum using standardized methods. Furthermore, a second set of samples were analyzed in analytical chemistry laboratory of Tallinn University of Technology to determine concentration of CMW in the collected serum and dialysate samples using HPLC.

Prior to HPLC analysis serum samples were filtered by centrifugation using Sartorius Vivacon 30 kDa cut-off filters (Göttingen, Germany) at 14.000 g for 3 h at 37 °C. Before serum filtration, cut-off filters were washed through with 400 µL type I ultrapure water (Millipore Synergy UV, Burlington, MA, USA) by centrifugation at 14.000 g for 15 min at 37 °C. To stabilize uric acid to undissociated form, 1 µL of formic acid (Sigma-Adrich, St. Louis, MO, USA) was added to the serum filtrate and likewise 10 µL of formic acid was added to unprocessed spent dialysate samples before HPLC analysis.

The HPLC analysis was carried out with Ultimate 3000 Series HPLC system from Dionex, a division of Thermo Scientific company (Sunnyvale, CA, USA) equipped with a quaternary gradient pump unit (DGP-3600RS), a thermostated autosampler (WPS-3000TSL analytical), a column oven (TCC-3000RS), a diode array spectrophotometric detector (DAD-3000RS), and a fluorescence detector (FLD-3400RS). Separation was performed using two continuous columns of Poroshell 120 C18 4.6 × 150 mm with a security guard Poroshell 120 C18 4.6 × 5 mm from Agilent Instruments (Santa Clara, CA, United States) with the temperature of columns at 40 °C and autosampler at 4 °C. A three-step linear gradient elution program was employed with the total flow rate of 0.6 mL/min as described earlier[29]. The eluent consisted of a mixture of 0.05 M formic acid adjusted to pH 4.25 with ammonium hydroxide (A), and organic solvent of HPLC grade methanol and HPLC-S grade acetonitrile, both from Honeywell (Charlotte, NC, USA) in ratio of 9:1 containing 0.05 M ammonium formiate salt (B). The obtained chromatographic data were processed with Chromeleon 7.1 software by Thermo Scientific (Waltham, MA, USA).

Chromatographic peak of CMW on the serum and the spent dialysate samples' chromatograms was identified based on the comparison of the retention time and fluorescence spectra with those of the standard solution of CMW and further confirmed by the MS/MS mass spectra of the peak specific to CMW[24,30]. Mass spectra were registered with a quadrupole time-of-flight mass spectrometer micrOTOF-Q II with an electrospray ionization (ESI) source (Bruker, Billerica, USA) that was coupled to HPLC system. Mass spectrometer was used in negative ion mode and the operating conditions were as follows: mass range of m/z 50–700; ion source temperature of 200 °C, ESI voltage of 4.5 kV, ESI nebulization gas flow of 8.0 L/min, drying gas flow of 1.2 bar, detector voltage of 2.03 kV, acquisition rate of 1 Hz as described earlier by Arund et al.[29]. Mass calibration was carried out using a solution of sodium formate (10 mmol/L) in the range of m/z 50 to 700. Data were acquired with Compass HyStar (version 3.2) and processed with Compass DataAnalysis (version 4.0 SP1) software (both Bruker, Billerica, USA).

Aqueous calibration standard solutions of CMW were prepared from reference substance purchased from Toronto Research Chemicals Inc (Toronto, Ontario, Canada) with purity of assay > 98% (thin layer chromatography) diluted in type I ultrapure water (Millipore Synergy UV, Burlington, MA, USA) and followed by treatment in ultrasonic bath for 30 min to ensure complete dissolution of the compound. The standard solutions with different known concentrations were analyzed with the same HPLC method as the serum and the spent dialysate samples to calibrate the HPLC system for determination of CMW concentration based on the acquired fluorescence signals (excitation: 280 nm; emission 360 nm). The linearity of the fluorescence signal was investigated in the concentration range of 0.017–10.5 µmol/L with 6 points (3 replicate injections each) achieving Pearson correlation coefficient of > 0.999 and inter-day precision (relative standard deviation) < 0.26% over a given range.

In addition, an extra set of spent dialysate samples were analyzed separately with ultraviolet (UV)- and fluorescence spectroscopy using UV-3600 spectrophotometer and RF-6000 spectrofluorometer, both from Shimadzu (Kyoto, Japan). UV absorption spectra were recorded over a wavelength range of 200–400 nm with sampling interval of 1 nm (spectral bandwidth of 2 nm) and quartz cuvette with optical path length of 5 mm using pure dialysis solution as a reference. Fluorescence spectra were measured over the excitation wavelength range of 200–400 nm with the increment of 10 nm and the emission wavelength range of 210–600 nm with the increment of 1 nm at room temperature. A quartz cuvette with an optical path length of 4 mm were used and bandwidths of both excitation and emission monochromators were set to 5 nm. Emission spectra were corrected for inner filtering of the excitation beam as described earlier based on the measured absorbance values at excitation wavelength[31,32]. Thereafter, the emission spectra were smoothed using moving average filter with the window size of 10.

In parallel to spent dialysate sampling, on-line fluorescence and UV absorption measurements were carried out during each dialysis session in real-time with an optical sensor prototype (Optofluid Technologies OÜ, Tallinn, Estonia) connected to the drain outlet of the dialysis machine. Measurement results of the sensor prototype were compared to laboratory results to detect possible errors related to the sample drawing during the self-tests of the HD machine[33] or incorrect sample labelling. As a result, the data of one serum and 33 spent dialysate samples were excluded during the data preprocessing from the following analysis due to aforementioned errors.

Data analysis and CMW removal evaluation

Forward stepwise regression was used to create a model for predicting concentration of CMW in spent dialysate samples using data of UV absorption and fluorescence of dialysate samples. For this purpose, the patients' data were equally partitioned to a calibration and validation datasets based on the patients' pseudonymised identification numbers, which were used to develop and validate the model, respectively. The exclusion of samples' data due to the self-tests of haemodialysis machine resulted in final sizes of datasets for calibration N = 244 and validation N = 251 as the excluded datapoints were not equally distributed. The fluorescence intensity with excitation in range of 240–400 nm and UV absorbance at a single wavelength (based on linear regression analysis between concentration of CMW and UV absorbance in spent dialysate samples of calibration dataset) were included as predictor variables of training data. The upper limit of the selectable variables was limited to three during model training to avoid overfitting. During the model training, a variable was included into the model in case the *p*-value was less than 0.05 for an F-test of the change in the sum of squared error that resulted from adding the variable.

Subsequently, the accuracy of the created model was evaluated on the calibration and validation data using Bland Altman[34] and regression analysis. Systematic error (BIAS) was calculated for the models as follows:

$$BIAS = \frac{\sum_{i=1}^{N} e_i}{N}$$

where e_i is the i-th residual (difference between HPLC determined and modelled CMW) and N is the number of observations[35].

Standard error of performance corrected for BIAS was calculated for the model as follows[35].

$$SE = \sqrt{\frac{\sum_{i=1}^{N} (e_i - BIAS)^2}{N-1}}$$

In order to assess removal of CMW during HD sessions, dialysis adequacy parameters, such as RR, TRS and TAC were estimated. The parameters were calculated based on HPLC determined CMW concentrations in serum and spent dialysate samples, and optical model-predicted CMW concentrations in spent dialysate samples to evaluate possibility of estimating these parameters non-invasively.

The RR of CMW during each dialysis session was calculated based on serum samples as follows:

$$RR_{\text{serum}} = \frac{C_{\text{pre}} - C_{\text{post}}}{C_{\text{pre}}} \times 100\% \quad , \tag{1}$$

where C_{pre} and C_{post} are HPLC determined pre- and immediate postdialysis concentrations of CMW in serum samples, respectively. Moreover, effective RR was additionally calculated using serum samples taken predialysis and 30 min postdialysis to assess extent of rebound effect caused by postdialysis redistribution of CMW in body compartments[36]. Furthermore, RR was similarly found for urea to compare removal dynamics of CMW with kinetic behavior of urea.

To calculate spent dialysate-based RR of CMW, concentrations of CMW in spent dialysate samples determined with HPLC or estimated with optics-based model were used:

$$RR_{\text{dialysate}} = \frac{D_7 - D_{240}}{D_7} \times 100\%, \tag{2}$$

where D_7 and D_{240} are the concentrations of CMW in spent dialysate samples taken at 7 min after the start and at the end (240 min) of the dialysis procedure, respectively.

The TRS of CMW was calculated based on total dialysate collection as follows:

$$TRS = D_{\text{T}} \cdot W_{\text{T}} \quad , \tag{3}$$

where D_T is the concentration of CMW in the dialysate collection tank determined with HPLC or estimated with optics-based model and W_T is the weight of the dialysate collection tank. The density of spent dialysate was assumed to be 1 kg/L.

To compare concentrations of CMW in serum and spent dialysate directly, spent dialysate concentrations of CMW (D_t) were normalized by spent dialysate and blood flow rates ($D_{t\,\text{norm}}$), thereby roughly compensating for dialyzer clearance[37,38]:

$$D_{t\ \text{norm}} = D_t \cdot \frac{Qd + Qsubs + UF}{Qb} \quad , \tag{4}$$

where Q_b is effective blood flow and the numerator "dialysate flow rate (Q_d) + substitution rate ($Qsubs$) + ultrafiltration rate (UF)" marks the total flow rate of spent dialysate.

TAC of CMW in blood over dialysis sessions was calculated from HPLC determined CMW concentrations as the logarithmic mean concentration, as proposed by Lim et al.[39]:

$$TAC = \frac{(C_{\text{pre}} - C_{\text{post}})}{\ln\left(\frac{C_{\text{pre}}}{C_{\text{post}}}\right)} \quad , \tag{5}$$

where C_{pre} and C_{post} are pre- and immediate postdialysis concentrations of CMW determined with HPLC, respectively.

In parallel, TAC of CMW was estimated (TAC_{opt}) from optical model-predicted CMW spent dialysate concentrations:

$$TAC_{\text{opt}} = a \cdot \frac{(D_{7\ \text{norm}} - D_{240\ \text{norm}})}{\ln\left(\frac{D_{7\ \text{norm}}}{D_{240\ \text{norm}}}\right)}, \tag{6}$$

where $D_{7\ norm}$ and $D_{240\ norm}$ mark optically estimated CMW concentrations in spent dialysate samples taken 7 and 240 min after the start of dialysis, respectively, which have been normalized by spent dialysate and blood flow rates (Table 2) according to Eq. 4. The regression coefficient "a" was determined based on calibration dataset.

All data analysis was done using MATLAB R2020b (MathWorks, Natick, MA, USA) software. Individual differences of serum and dialysate based dialysis adequacy parameters were compared using Bland Altman analysis[34]. The Anderson–Darling test was employed to assess the normality of the datasets, which determined

the appropriate statistical tests for subsequent analysis. For normally distributed data, Student's two-tailed paired t-test was used to compare differences between related samples from the same patient, while the unpaired two-tailed t-test was applied to compare differences between treatment modalities. For non-normally distributed data, the Wilcoxon test was utilized. In all statistical tests, a p-value of < 0.05 was considered significant.

Results

In total, 264 serum samples and 528 spent dialysate samples were analyzed with HPLC. Figure 1 shows an example of a characteristic chromatogram of a spent dialysate sample and overlaid chromatogram of a standard solution, including reference substances.

The fluorescence and relative abundance peak of ion m/z^{-1} 365.14 ± 0.03 with retention time of 20.01 min on the spent dialysate chromatogram was identified as a CMW based on the mass spectrum (Supplementary Fig. S1), fluorescence spectrum and the retention time of the peak that were identical to the standard solution of CMW. The concentration of CMW in the serum and spent dialysate samples was quantified based on the acquired fluorescence signals as described in the Methods section. The HPLC analysis showed that the median (interquartile range) predialysis concentration of CMW in serum samples was 2.78 (2.20–3.22) µmol/L and 0.52 (0.38–0.73) µmol/L at the end of treatment, and in spent dialysate samples 0.64 (0.52–0.79) µmol/L and 0.13 (0.08–0.22) µmol/L, respectively.

Figure 2 compares average RRs of CMW and urea during dialysis sessions calculated from serum and spent dialysate concentrations for different dialysis modalities and settings.

It can be seen from the Fig. 2 that the RR of CMW is higher in comparison with RR of urea (> 6.7 percentage points) for all modalities ($p < 0.001$) and that the removal efficacy of CMW and urea are similarly affected by the treatment settings, calculated based on serum samples. What stands out is that the RRs of both solutes are significantly higher ($p < 0.001$) for most efficient HD modality (High HDF) in comparison with Low Flux HD with RR (± SD) of 84.8 ± 6.1% vs 66.4 ± 8.9% for CMW and RR (± SD) of 78.1 ± 5.8% vs 58.9 ± 7.0% for urea (see Supplementary Fig. S2 for inter-modality statistical differences). Whereas the differences between RRs of HDF sessions are smaller. A comparison of the RR results of CMW calculated based on serum and spent dialysate samples showed that values found from spent dialysate samples were slightly lower (4.3 percentage points) than serum-based values for Low Flux HD sessions with relatively low blood and dialysate flow rates ($p < 0.001$), but not for HDF sessions ($p > 0.15$). The median (interquartile range) RR over all sessions based on predialysis and immediately taken postdialysis serum sample was 80.1 (72.3–86.0)% for CMW, and for urea 71.3 (63.0–78.0)%, respectively. The rebound effect significantly affected the RRs of both solutes ($p < 0.01$). Namely, effective RR, which was calculated based on predialysis and 30 min postdialysis serum samples was lower: 74.7 (66.6–81.2)% for CMW and 66.2 (58.2–73.3)% for urea. Furthermore, the extent of rebound effect was not statistically different between CMW and urea ($p = 0.530$).

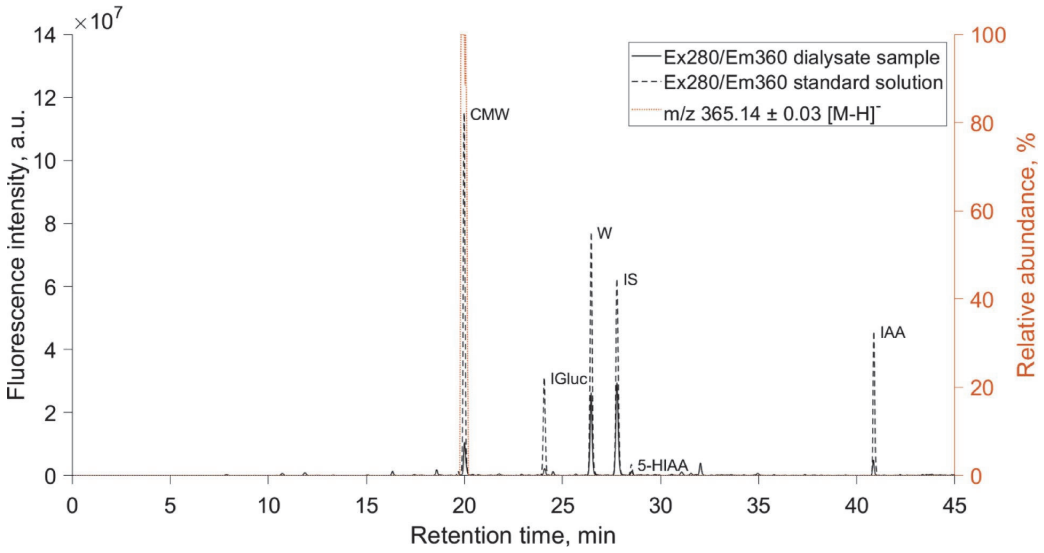

Fig. 1. A characteristic chromatogram of a spent dialysate sample and superimposed chromatogram of a standard solution, including C-mannosyl tryptophan (CMW), indoxyl glucuronide (IGluc), tryptophan (W), indoxyl sulfate (IS), 5-hydroxyindole-3-acetic acid (5-HIAA), indole-3-acetic acid (IAA). Extracted ion chromatogram of a spent dialysate sample in negative ion mode characteristic for CMW (m/z^{-1} 365.14 ± 0.03) is marked as (…), and fluorescence signals at excitation (Ex) 280 nm/Emission (Em) 360 nm are marked as (–) for dialysate sample, and as (--) for the standard solution.

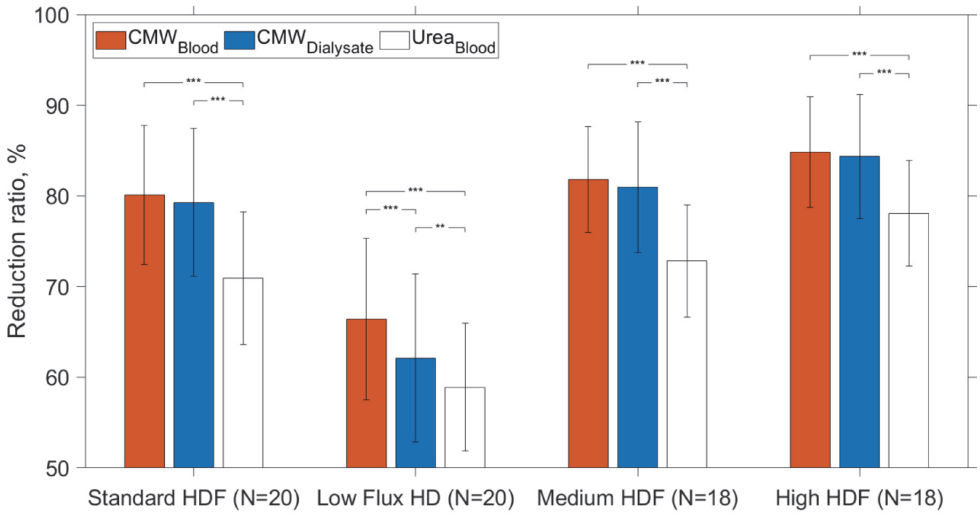

Fig. 2. Reduction ratios (average ± SD) of C-mannosyl tryptophan (CMW) and urea for hemodialysis (HD) and different hemodiafiltration (HDF) modalities (see Table 2 in Methods section) evaluated based on serum and spent dialysate samples collected from the start and end (240 min) of the dialysis sessions; statistical intra-modality differences, evaluated using paired two-tailed t-tests, are denoted as follows: *** ($p < 0.001$), ** ($p < 0.01$), * ($p < 0.05$).

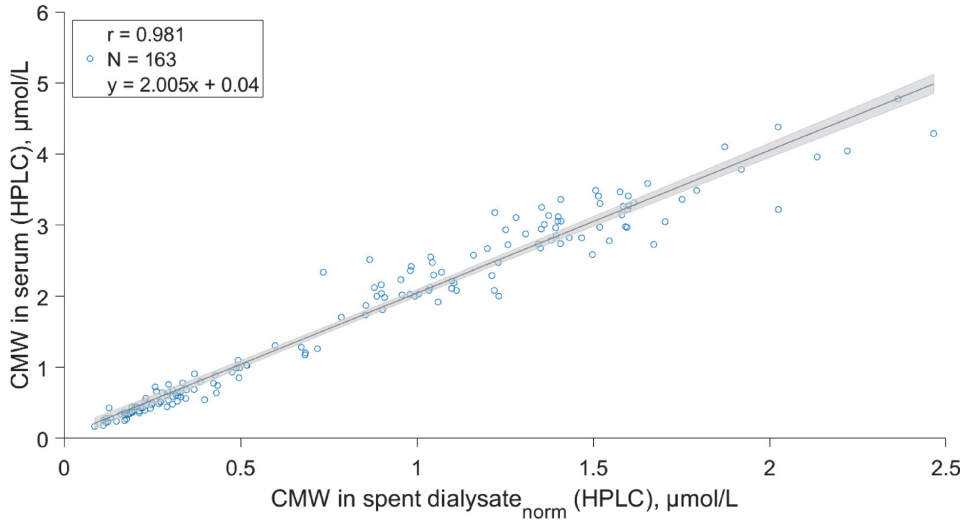

Fig. 3. Correlation between C-mannosyl tryptophan (CMW) concentration determined with high pressure liquid chromatography (HPLC) in serum and CMW in spent dialysate normalized (norm) by spent dialysate flow rate and effective blood flow rate based on Eq. 4 (see Methods section). Black continuous line indicates the regression line and grey area indicates the 95% CI of the slope.

Figure 3 shows a scatter plot of the relationship between the concentration of CMW in serum and CMW concentration in spent dialysate samples normalized by blood and spent dialysate flow rates using Eq. 4; with exclusion of 13 paired spent dialysate datapoints due to the HD machines' self-tests from the total of 176 pre- and postdialysis blood samples. It is evident from the figure that blood and spent dialysate concentrations of CMW are strongly correlated after normalization by treatment settings ($r = 0.981$, $p < 0.001$).

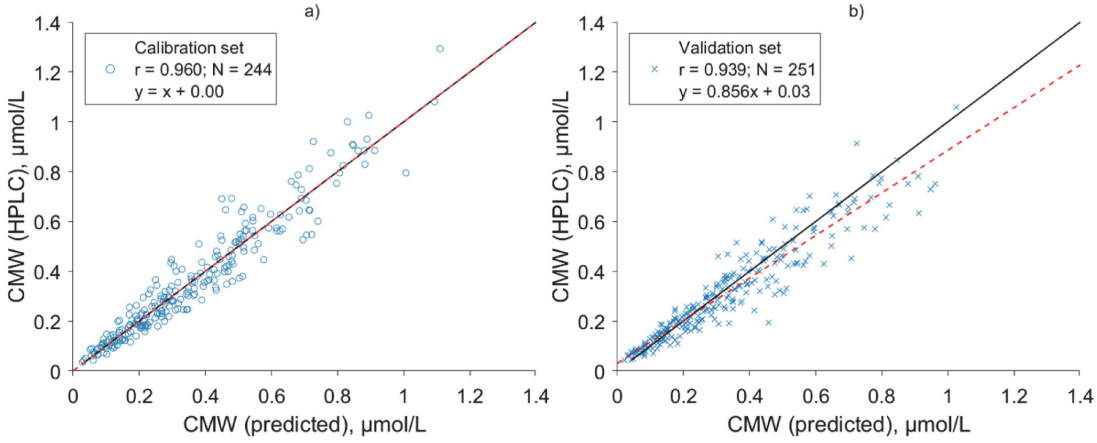

Fig. 4. Scatter plots of the relationship of C-mannosyl tryptophan (CMW) concentration in spent dialysate determined with high pressure liquid chromatography (HPLC) and estimated with optics-based predictive model for (**a**) calibration set and (**b**) validation set. Black continuous line indicates the identity line and dashed red line marks the regression line.

Clinical parameter	CMW HPLC median (Q1-Q3)	CMW Opt median (Q1-Q3)	*p*-value	Accuracy (BIAS ± SE)	Pearson correlation coefficient
$RR_{dialysate}$ (%, N = 74)	78.7 (68.6–85.7)	78.5 (67.0–84.6)	0.811	0.7 ± 3.7	0.958
RR_{serum} (%, N = 72)	80.3 (72.3–85.9)	77.8 (66.1–84.5)	0.347	2.4 ± 4.9	0.939
TRS (µmol, N = 86)	40.25 (34.29–47.89)	43.84 (36.75–52.12)	0.213	− 1.72 ± 7.95	0.792
TAC (µmol/L, N = 72)	1.34 (1.13–1.54)	1.39 (1.17–1.59)	0.442	0.00 ± 0.25	0.717

Table 3. Hemodialysis performance parameters for all modalities combined based on reduction ratio (RR), total removed solute (TRS) and time averaged concentration (TAC) of C-mannosyl tryptophan (CMW). Results based on high pressure liquid chromatography (HPLC) analysis of serum or spent dialysate samples were compared with the results calculated from the output of the optical (Opt) model using Wilcoxson test. Numerical values are given as median and interquartile range (Q1–Q3).

In addition to fluorescence data at excitation from 240 to 400 nm, UV absorbance at 295 nm was included as predictor variable of model training data, based on linear regression analysis between concentration of CMW and UV absorbance in spent dialysate samples (Supplementary figure S3). The linear regression model that was created based on calibration dataset to estimate concentration of CMW in spent dialysate from the optical spent dialysate measurements included Ex250Em380 and Ex260Em349, and UV absorbance at 295 nm as variables with the highest predictive power. The scatter plots of the calibration and the validation groups comparing CMW determined with HPLC and predicted based on the optical measurements are shown on Fig. 4.

The model yielded high accuracy (BIAS ± SE) on both calibration and validation set. Pearson correlation coefficient of 0.960 ($p < 0.001$) with the accuracy of 0.00 ± 0.07 µmol/L was achieved for the calibration group (Fig. 4a), and Pearson correlation coefficient of 0.939 ($p < 0.001$) with the accuracy of − 0.02 ± 0.07 µmol/L was achieved for the validation group (Fig. 4b) between the CMW concentration in spent dialysate determined with HPLC and the corresponding values predicted using the model, respectively.

Table 3 compares the HD performance parameters, such as RR, TRS and TAC of CMW evaluated based on HPLC analysis of serum or spent dialysate samples and using output from the optics-based predictive model (Fig. 4) for all data; with exclusion of 14 RR dialysate, 16 RR serum; 16 TAC and 2 TRS values, which were removed prior data analysis due to the HD machines' self-tests and incorrect sample labelling.

RR values of CMW based on HPLC analysis of dialysate samples were strongly correlated with the optically estimated RR values (r = 0.958, $p < 0.001$) and similar (Table 3). Likewise, RR values of CMW based on HPLC analysis of serum samples were strongly correlated with spent dialysate-based optically estimated RR values (r = 0.939, $p < 0.001$) and similar ($p = 0.347$). Whereas the correlation was somewhat weaker between HPLC based and optically estimated CMW for TRS (r = 0.792, $p < 0.001$) and TAC (r = 0.717, $p < 0.001$).

Discussion

Previous research has established that CMW is an endogenous metabolite, and a highly potential biomarker related to the health outcomes and CKD progression in earlier stages of CKD patients prior to ESKD. To our

knowledge, CMW levels in ESKD patients and its hemodialytic removal have not been previously studied, although CMW has a potential intrinsic toxicity, and the concentration of CMW has been shown to rise in CKD patients. In this study, we filled this gap, and additionally created an optics-based predictive model for estimating hemodialytic removal and TAC of CMW non-invasively from spectrophotometric analysis of spent dialysate.

The main findings of this study were: (1) predialysis serum CMW concentrations of studied ESKD patients were presumably over 10 times higher compared to previously published CMW levels of healthy subjects; (2) in comparison to traditional maintenance HD adequacy marker-molecule urea, CMW is removed more efficiently (RR higher more than 6.7 percentage points) during HD; (3) CMW concentration in spent dialysate can be estimated optically with good accuracy (4) spent dialysate based optical monitoring allows to evaluate hemodialytic removal of CMW from patients' blood and TAC of patients.

In the present study, the concentration of CMW in the collected samples was determined with a HPLC method earlier described by Arund et al. (2016) for analyzing the main fluorescent solutes, which are removed from ESKD patients' blood into dialysis solution during HD[29]. Besides other identified tryptophan metabolites, Arund et al. found an unidentified fluorophore that was a significant constituent of the fluorescence signal (excitation: 280 nm; emission 360 nm) of spent dialysate samples, with a relative contribution to the fluorescence signal ranging between 2 and 16% in the analyzed spent dialysate samples[29]. The researchers hypothesized this compound, labeled as Unknown 1, to be glycoconjugate of tryptophan[29]. Here, we confirm that this previously unidentified uremic retention solute is CMW (Fig. 1) based on the comparison of mass spectra (Supplementary Fig. S1), fluorescence spectra and retention time of reference substance to that of CMW peak on chromatograms. Concerning HPLC analysis, a very good symmetry of the CMW peak on the chromatogram (Fig. 1) and full separation from the peaks of other fluorescent metabolites present in dialysate and serum was achieved. In detail, peak purity was assessed based on the absorbance and fluorescence spectra of the peak, confirming no co-elution of key analytes and high specificity of used HPLC method to separate CMW from other metabolites with no co-elution of contaminants in the peak. No decomposition of the CMW in samples was observed during the sample storage at 4 °C over 100 h, with peak areas being unchanged (relative standard deviation of peak areas < 0.93% based on samples of 3 patients).

Prior research has shown that average (± SD) plasma concentration of CMW in healthy control subjects (eGFR 104.01 ± 5.7 mL/min /1.73 m^2) was 0.26 ± 0.05 µmol/L in the Qatar Metabolomics Study on Diabetes[40], and 0.23 ± 0.05 µmol/L in serum of subjects (eGFR 114.1 ± 29.6 mL/min/1.73 m^2) in a Japanese study[26] focusing on diagnostic value of CMW concentration, respectively. In this analysis, the median (interquartile range) concentration of CMW in serum samples of ESKD patients was 2.78 (2.20–3.22) µmol/L prior to start of dialysis, which is presumably > 10 times higher than the average normal concentration in healthy controls. This is comparable to the estimated 13–16 fold increase of CMW in ESKD patients relative to healthy subjects reported by Tanaka et al. using relative amounts of metabolites[5]. Moreover, compared to CKD patients with eGFR of 50.9 ± 17.6 mL/min/1.73 m^2 and average CMW concentration 0.72 ± 0.28 µmol/L in plasma[40], CMW levels in dialysis patients in our study had raised further. As a limitation of this study, it was not possible to compare the relationships of CMW levels in ESKD patients and healthy individuals using the same method under identical conditions, as this study focused only on ESKD patients. In future studies, healthy subjects should be included as a control group to eliminate possible bias between the HPLC method of this study and methods used in prior research to improve the accuracy of the comparison of CMW levels in ESKD patients and healthy controls. However, to decrease the levels of CMW in ESKD patients, their intestinal and metabolic generation should be limited and extracorporeal removal enhanced like for other uremic solutes [41].

Our analysis shows that CMW is removed more efficiently during HD in relation to urea, a standard marker molecule of dialysis adequacy, (Fig. 2), with the RR of CMW being higher relative to RR of urea (> 6.7%) for all studied modalities ($p < 0.001$). Furthermore, hemodialytic removal of urea and CMW were considerably affected by treatment settings. In case of Low Flux HD with relatively low blood and dialysate flow rates, the average (± SD) RR was 66.4 ± 8.9% for CMW and 58.9 ± 7.0% for urea, which increased ($p < 0.001$) to 84.8 ± 6.1% and 78.1 ± 5.8% with the change to the most efficient HDF (High HDF), respectively (Supplementary Fig. S2). These results imply that removal characteristics of CMW are comparable to those of small water-soluble compounds, according to the classification proposed by EUTox in which uremic toxins are categorized into three groups: small water-soluble compounds, middle molecules and protein-bound solutes[4]. In contrast to the hydrophobic tryptophan, which is protein-bound solute[28], CMW is more water soluble due to the polar mannose residue, based on HPLC analysis (Fig. 1), which showed that retention time of CMW was 24% shorter than that of tryptophan using hydrophobic chromatography column. Efficient extracorporeal removal and renal filtration[25] of CMW may arise therefore from good water solubility of CMW. Besides, as the extent of post-dialytic rebound was in comparable magnitude for both CMW and urea ($p = 0.692$), CMW may have minimal resistance to intercompartmental shifts, similar to urea[42].

Traditionally, HD adequacy has been assessed by small water-soluble compounds clearance and quantified by Kt/V_{urea} or its simplified form (RR of urea), based on analysis of blood samples[43]. Whereas analysis of spent dialysate using measurement of UV absorption has been proven to be reliable, non-invasive alternative for Kt/V determination[37,44], which is used in haemodialysis machines for real-time dialysis adequacy monitoring on-line[45,46]. Also, optical methods have been developed for monitoring removal of characteristic biomarkers of uremic toxins with different physicochemical properties and dialytic removal patterns, such as protein bound indoxyl[29,47], middle molecule beta-2-microglobulin[47,48] and advanced glycation end product pentosidine[49] among others, which may facilitate personalizing HD prescriptions[50].

To estimate intradialytic removal and levels of CMW, an optics-based predictive model was created using stepwise linear regression in this study, which included three variables: fluorescence at Ex250Em380 and Ex260Em349, and UV absorbance at 295. A high accuracy (BIAS ± SE) and strong correlation between HPLC determined and model estimated CMW concentration in spent dialysate were achieved for both calibration

and validation group, 0.00 ± 0.07 µmol/L (r = 0.960, $p < 0.001$) and −0.02 ± 0.07 µmol/L (r = 0.939, $p < 0.001$), respectively. Although spent dialysate consists of individual fluorophores, which fluorescence spectra tend to partially overlap[29,51] with CMW (Supplementary Fig. S4), the results presented here (Fig. 4) suggest that it is possible to evaluate concentration of CMW with relatively high accuracy using combination of wavelengths of fluorescence and UV absorbance. Additionally, it can be deduced that fluorescence of spent dialysate at excitation of 280 nm and emission at 350 nm can be partly attributed to CMW, a specific region of fluorescence (left shoulder of the main fluorescence peak of spent dialysate) for which fluorophores causing the signal remained unidentified previously[29,51].

The developed model enabled to evaluate CMW-based dialysis adequacy parameters, such as RR, TRS and TAC non-invasively without blood sampling as CMW concentrations in blood can be determined from spent dialysate concentrations (Fig. 3). The results showed (Table 3) that optically assessed spent dialysate-based RRs of CMW were similar and strongly correlated to HPLC determined spent dialysate- and serum-based RRs (r = 0.958, and r = 0.939, respectively). While for TRS and TAC estimation, the correlation between the HPLC determined and optically estimated values were weaker (r = 0.792 ($p < 0.001$), and r = 0.717 ($p < 0.001$), respectively). The weaker correlation seen between blood and dialysate-based values can be partly attributed to the different sampling times of blood and spent dialysate samples in the beginning of treatments. Namely, spent dialysate samples were taken 7 min after the start of dialysis procedure and blood samples predialysis, which can cause divergence between serum and spent dialysate-based TAC values as described earlier[52] for solutes with double pool kinetics or small distribution volume that are removed rapidly. Moreover, it is expectable that RR was most precisely estimated clinical parameter, as RR is a relative measure, which is less influenced by the possible prediction error of the developed model caused by other fluorophores and chromophores as these can have similar removal efficiency[29,53]. In future, alternative data analysis approach could be used instead of stepwise linear regression to combine and transform available variables to develop a more precise model using larger cohort and dataset. Especially, considering that the developed multiparametric linear model can be sensitive to fluorescence peak shifting that is related to the composition of spent dialysate, which could alter the relationship between the excitation–emission wavelength and concentration of CMW.

Clinically, optical monitoring of CMW removal or TAC could be used to determine whether the previously seen relationship between CMW concentration and clinically relevant outcomes in earlier stages of CKD patients prior to ESKD, such as residual kidney function decline and mortality, remains valid in ESKD patients. The pathophysiological effect of CMW remains unidentified so far and additional experimental studies should be undertaken to elaborate whether CMW has causal role in CKD progression or if it is a non-toxic marker of solute retention, which concentration rises as residual kidney function declines[25]. Considering this, it would be interesting to investigate whether effective removal of CMW during HD improves clinical outcomes of ESKD patients and if CMW could be additional uremic solute marker to be monitored during HD[50]. Regardless of potential uremic toxicity of CMW, CMW has been shown to be strongly correlated to clinical outcomes and has a potential to improve management of CKD patients independently or in combination with other biomarkers, as biomarkers do not need to be causally involved in the disease process to predict the risk of future outcomes[7,13,14,54]. With this in mind, CMW may be useful as a marker for preserving and monitoring residual kidney function of ESKD patients, which remains a complicated task[55,56].

In summary, this study was set out to determine the levels of CMW in ESKD patients and its removal characteristics, assess the possibility for optical estimation of CMW concentrations in spent dialysate and dialysis adequacy parameters without blood sampling. We identified that CMW concentrations in ESKD patients may be over 10 times higher compared to CMW concentrations in healthy control subjects as reported in previous studies. The removal of CMW during HD is characteristic to small water-soluble uremic solutes and CMW is removed with higher efficiency compared to urea by dialysis treatment. The results show that the removal and levels of CMW can be monitored based on spectrophoto- and spectrofluorimetric analysis of spent dialysate, which makes it possible to evaluate CMW-based HD adequacy parameters, such as RR, TRS and TAC without blood sampling. To conclude, this study offers an alternative method for determination of CMW based on optical measurements, which has a potential to improve clinical management of ESKD patients.

Data availability

The data that support the findings of this study are available from Optofluid Technologies OÜ but restrictions apply to the availability of these data, which were used under license for the current study, and so are not publicly available. Data are however available from the corresponding author upon reasonable request and with permission of Optofluid Technologies OÜ.

Received: 4 October 2024; Accepted: 8 May 2025
Published online: 12 June 2025

References

1. Jager, K. J. et al. A single number for advocacy and communication—Worldwide more than 850 million individuals have kidney diseases. *Nephrol. Dial. Transplant.* **34**, 1803–1805. https://doi.org/10.1093/ndt/gfz174 (2019).
2. Meyer, T. W. & Hostetter, T. H. Approaches to uremia. *J. Am. Soc. Nephrol.* **25**, 2151–2158. https://doi.org/10.1681/ASN.2013121264 (2014).
3. Bello, A. K. et al. Epidemiology of haemodialysis outcomes. *Nat. Rev. Nephrol.* **18**, 378–395. https://doi.org/10.1038/s41581-022-00542-7 (2022).
4. Vanholder, R., Pletinck, A., Schepers, E. & Glorieux, G. Biochemical and clinical impact of organic uremic retention solutes: A comprehensive update. *Toxins* **10**, 33. https://doi.org/10.3390/toxins10010033 (2018).
5. Tanaka, H., Sirich, T. L., Plummer, N. S., Weaver, D. S. & Meyer, T. W. An enlarged profile of uremic solutes. *PLoS ONE* **10**, e0135657. https://doi.org/10.1371/journal.pone.0135657 (2015).

6. Zhang, W. R. & Parikh, C. R. Biomarkers of acute and chronic kidney disease. *Annu. Rev. Physiol.* **81**, 309–333. https://doi.org/10.1146/annurev-physiol-020518-114605 (2019).
7. Tesch, G. H. Review: Serum and urine biomarkers of kidney disease—A pathophysiological perspective. *Nephrology* **15**, 609–616. https://doi.org/10.1111/j.1440-1797.2010.01361.x (2010).
8. Breit, M. & Weinberger, K. M. Metabolic biomarkers for chronic kidney disease. *Arch. Biochem. Biophys.* **589**, 62–80. https://doi.org/10.1016/j.abb.2015.07.018 (2016).
9. Hocher, B. & Adamski, J. Metabolomics for clinical use and research in chronic kidney disease. *Nat. Rev. Nephrol.* **13**, 269–284. https://doi.org/10.1038/nrneph.2017.30 (2017).
10. Stevens, L. A., Coresh, J., Greene, T. & Levey, A. S. Assessing kidney function—Measured and estimated glomerular filtration rate. *N. Engl. J. Med.* **354**, 2473–2483. https://doi.org/10.1056/NEJMra054415 (2006).
11. Koppe, L., Fouque, D. & Soulage, C. O. The role of gut microbiota and diet on uremic retention solutes production in the context of chronic kidney disease. *Toxins* **10**, 155. https://doi.org/10.3390/toxins10040155 (2018).
12. Sekula, P. et al. A metabolome-wide association study of kidney function and disease in the general population. *J. Am. Soc. Nephrol.* **27**, 1175–1188. https://doi.org/10.1681/ASN.2014111099 (2016).
13. van der Burgh, A. C. et al. Circulating metabolites associated with kidney function decline and incident CKD: A multi-platform population-based study. *Clin. Kidney J.* https://doi.org/10.1093/ckj/sfad286 (2024).
14. Steinbrenner, I. et al. Urine metabolite levels, adverse kidney outcomes, and mortality in CKD patients: A metabolome-wide association study. *Am. J. Kidney Dis.* **78**, 669–677. https://doi.org/10.1053/j.ajkd.2021.01.018 (2021).
15. Denburg, M. R. et al. Metabolite biomarkers of ckd progression in children. *Clin. J. Am. Soc. Nephrol.* **16**, 1178–1189. https://doi.org/10.2215/CJN.00220121 (2021).
16. Minakata, S. et al. Monomeric c-mannosyl tryptophan is a degradation product of autophagy in cultured cells. *Glycoconj. J.* **37**, 635–645. https://doi.org/10.1007/s10719-020-09938-8 (2020).
17. Furmanek, A. & Hofsteenge, J. Protein c-mannosylation: Facts and questions. *Acta Biochim. Pol.* **47**, 781–789 (2000).
18. Minakata, S. et al. Protein c-mannosylation and c-mannosyl tryptophan in chemical biology and medicine. *Molecules* **26**, 5258. https://doi.org/10.3390/molecules26175258 (2021).
19. Schjoldager, K. T., Narimatsu, Y., Joshi, H. J. & Clausen, H. Global view of human protein glycosylation pathways and functions. *Nat. Rev. Mol. Cell Biol.* **21**, 729–749. https://doi.org/10.1038/s41580-020-00294-x (2020).
20. Qi, R. et al. Visible-light-promoted stereoselective c(sp 3)–h glycosylation for the synthesis of c-glycoamino acids and c-glycopeptides. *Angew. Chemie Int. Ed.* https://doi.org/10.1002/anie.202200822 (2022).
21. Julenius, K. NetCGlyc 1.0: prediction of mammalian c-mannosylation sites. *Glycobiology* **17**, 868–876. https://doi.org/10.1093/glycob/cwm050 (2007).
22. Bloch, J. S. et al. Structure, sequon recognition and mechanism of tryptophan c-mannosyltransferase. *Nat. Chem. Biol.* **19**, 575–584. https://doi.org/10.1038/s41589-022-01219-9 (2023).
23. Horiuchi, K. et al. A hydrophilic tetrahydro-β-carboline in human urine. *J. Biochem.* **115**, 362–366. https://doi.org/10.1093/oxfordjournals.jbchem.a124343 (1994).
24. Gutsche, B., Grun, C., Scheutzow, D. & Herderich, M. Tryptophan glycoconjugates in food and human urine. *Biochem. J.* **343**(Pt 1), 11–19 (1999).
25. Takahira, R. et al. Tryptophan glycoconjugate as a novel marker of renal function. *Am. J. Med.* **110**, 192–197. https://doi.org/10.1016/S0002-9343(00)00693-8 (2001).
26. Yonemura, K., Takahira, R., Yonekawa, O., Wada, N. & Hishida, A. The diagnostic value of serum concentrations of 2-(α-mannopyranosyl)-l-tryptophan for normal renal function. *Kidney Int.* **65**, 1395–1399. https://doi.org/10.1111/j.1523-1755.2004.00521.x (2004).
27. Niewczas, M. A. et al. Uremic solutes and risk of end-stage renal disease in type 2 diabetes: Metabolomic study. *Kidney Int.* **85**, 1214–1224. https://doi.org/10.1038/ki.2013.497 (2014).
28. Paats, J. et al. Serum levels and removal by haemodialysis and haemodiafiltration of tryptophan-derived uremic toxins in eskd patients. *Int. J. Mol. Sci.* **21**, 1522. https://doi.org/10.3390/ijms21041522 (2020).
29. Arund, J., Luman, M., Uhlin, F., Tanner, R. & Fridolin, I. Is fluorescence valid to monitor removal of protein bound uremic solutes in dialysis?. *PLoS ONE* **11**, e0156541. https://doi.org/10.1371/journal.pone.0156541 (2016).
30. Yamamoto, M., Pinto-Sanchez, M. I., Bercik, P. & Britz-McKibbin, P. Metabolomics reveals elevated urinary excretion of collagen degradation and epithelial cell turnover products in irritable bowel syndrome patients. *Metabolomics* **15**, 82. https://doi.org/10.1007/s11306-019-1543-0 (2019).
31. Fonin, A. V., Sulatskaya, A. I., Kuznetsova, I. M. & Turoverov, K. K. Fluorescence of dyes in solutions with high absorbance inner filter effect correction. *PLoS ONE* **9**, e103878. https://doi.org/10.1371/journal.pone.0103878 (2014).
32. Wang, T., Zeng, L.-H. & Li, D.-L. A review on the methods for correcting the fluorescence inner-filter effect of fluorescence spectrum. *Appl. Spectrosc. Rev.* **52**, 883–908. https://doi.org/10.1080/05704928.2017.1345758 (2017).
33. Uhlin, F., Fridolin, I., Magnusson, M. & Lindberg, L.-G. Dialysis dose (kt/v) and clearance variation sensitivity using measurement of ultraviolet-absorbance (on-line), blood urea, dialysate urea and ionic dialysance. *Nephrol. Dial. Transplant.* **21**, 2225–2231. https://doi.org/10.1093/ndt/gfl147 (2006).
34. Bland, J. M. & Altman, D. G. Statistical methods for assessing agreement between two methods of clinical measurement. *Lancet* **327**, 307–310. https://doi.org/10.1016/S0140-6736(86)90837-8 (1986).
35. Esbensen, K. *Multivariate data analysis—in practice. Introduction to multivariate data analysis and experimental design*. (CAMO Software, Oslo, 2009).
36. Eloot, S. et al. Kinetic behavior of urea is different from that of other water-soluble compounds: The case of the guanidino compounds. *Kidney Int.* **67**, 1566–1575. https://doi.org/10.1111/j.1523-1755.2005.00238.x (2005).
37. Fridolin, I., Magnusson, M. & Lindberg, L.-G. On-line monitoring of solutes in dialysate using absorption of ultraviolet radiation: Technique description. *Int. J. Artif. Organs* **25**, 748–761. https://doi.org/10.1177/039139880202500802 (2002).
38. Garred, L. J. Dialysate-based kinetic modeling. *Adv. Ren. Replace. Ther.* **2**, 305–318. https://doi.org/10.1016/S1073-4449(12)80029-X (1995).
39. Lim, P.-S. et al. Precise quantitative assessment of the clinical performances of two high-flux polysulfone hemodialyzers in hemodialysis: Validation of a blood-based simple kinetic model versus direct dialysis quantification. *Artif. Organs* **42**, E55–E66. https://doi.org/10.1111/aor.13011 (2018).
40. Sekula, P. et al. From discovery to translation: characterization of c-mannosyltryptophan and pseudouridine as markers of kidney function. *Sci. Rep.* **7**, 17400. https://doi.org/10.1038/s41598-017-17107-5 (2017).
41. Vanholder, R. C., Eloot, S. & Glorieux, G. L. R. L. Future avenues to decrease uremic toxin concentration. *Am. J. Kidney Dis.* **67**, 664–676. https://doi.org/10.1053/j.ajkd.2015.08.029 (2016).
42. Meyer, T. W., Sirich, T. L. & Hostetter, T. H. Dialysis cannot be dosed. *Semin. Dial.* **24**, 471–479. https://doi.org/10.1111/j.1525-139X.2011.00979.x (2011).
43. Steyaert, S., Holvoet, E., Nagler, E., Malfait, S. & Van Biesen, W. Reporting of "dialysis adequacy" as an outcome in randomised trials conducted in adults on haemodialysis. *PLoS ONE* **14**, e0207045. https://doi.org/10.1371/journal.pone.0207045 (2019).
44. Uhlin, F., Fridolin, I., Lindberg, L.-G. & Magnusson, M. Estimation of delivered dialysis dose by on-line monitoring of the ultraviolet absorbance in the spent dialysate. *Am. J. Kidney Dis.* **41**, 1026–1036. https://doi.org/10.1016/S0272-6386(03)00200-2 (2003).

45. Castellarnau, A., Werner, M., Günthner, R. & Jakob, M. Real-time kt/v determination by ultraviolet absorbance in spent dialysate: Technique validation. *Kidney Int.* **78**, 920–925. https://doi.org/10.1038/ki.2010.216 (2010).
46. Mohamed, A. & Davenport, A. Comparison of methods to estimate haemodialysis urea clearance. *Int. J. Artif. Organs* **41**, 371–377. https://doi.org/10.1177/0391398818766832 (2018).
47. Lauri, K. et al. Removal of urea, β2-microglobulin, and indoxyl sulfate assessed by absorbance and fluorescence in the spent dialysate during hemodialysis. *ASAIO J.* **66**, 698–705. https://doi.org/10.1097/MAT.0000000000001058 (2020).
48. Paats, J. et al. Optical method and biochemical source for the assessment of the middle-molecule uremic toxin β2-microglobulin in spent dialysate. *Toxins* **13**, 255. https://doi.org/10.3390/toxins13040255 (2021).
49. Kalle, S., Tanner, R., Luman, M. & Fridolin, I. Free pentosidine assessment based on fluorescence measurements in spent dialysate. *Blood Purif.* **47**, 85–93. https://doi.org/10.1159/000493522 (2019).
50. Rosner, M. H. et al. Classification of uremic toxins and their role in kidney failure. *Clin. J. Am. Soc. Nephrol.* **16**, 1918–1928. https://doi.org/10.2215/CJN.02660221 (2021).
51. Meibaum, J., Krause, S., Hillmer, H., Marcelli, D. & Strohhöfer, C. Identification and characterisation of fluorescent substances in spent dialysis fluid. *Int. J. Artif. Organs* **43**, 579–586. https://doi.org/10.1177/0391398820901826 (2020).
52. Paats, J. et al. Time-averaged concentration estimation of uraemic toxins with different removal kinetics: a novel approach based on intradialytic spent dialysate measurements. *Clin. Kidney J.* **16**, 735–744. https://doi.org/10.1093/ckj/sfac273 (2023).
53. Arund, J., Tanner, R., Uhlin, F. & Fridolin, I. Do only small uremic toxins, chromophores, contribute to the online dialysis dose monitoring by uv absorbance?. *Toxins* **4**, 849–861. https://doi.org/10.3390/toxins4100849 (2012).
54. Moons, K. G. M., Royston, P., Vergouwe, Y., Grobbee, D. E. & Altman, D. G. Prognosis and prognostic research: What, why, and how?. *BMJ* **338**, b375–b375. https://doi.org/10.1136/bmj.b375 (2009).
55. Shafi, T. & Levey, A. S. Measurement and estimation of residual kidney function in patients on dialysis. *Adv. Chronic Kidney Dis.* **25**, 93–104. https://doi.org/10.1053/j.ackd.2017.09.001 (2018).
56. Steubl, D. et al. Development and validation of residual kidney function estimating equations in dialysis patients. *Kidney Med.* **1**, 104–114. https://doi.org/10.1016/j.xkme.2019.04.002 (2019).

Acknowledgements

The authors thank dialysis patients who participated in the experiments, Rain Kattai and Deniss Karai for their skillful technical assistance; students Maris Alev and Relika Toome for helping with the data collection and analysis; nurses at the North Estonia Medical Centre for assistance during the clinical experiments.

Author contributions

Conceptualization I.F., M.L.; Methodology J.P., A.A., J.A., I.F., K.L., L.L., M.L., R.T.; investigation J.P., A.A., J.A., L.L; K.L.; data curation J.P., J.A., A.A., L.L., K.L.; validation J.P., J.A., I.F., K.L.; formal analysis J.P., J.A., I.F; visualization J.P; writing—original draft preparation J.P., R.T.; writing—review and editing J.P., A.A., J.A., J.H., I.F., K.L., L.L., M.L., J.P., K.P., R.T (all authors).;

Funding

The research was funded partly by the European Union through the European Regional Development Fund H2020-SMEINST-2-2017, OLDIAS2—On-line Dialysis Sensor Phase2 project with Grant Agreement nr 767572, the Estonian Centre of Excellence of Well-Being Sciences (EstWell) by grant TK218, and by Estonian Research Council grants PSG819 and PRG2643 funded from the Estonian Ministry of Education and Research

Declarations

Competing interests

Ivo Fridolin is CTO of Optofluid Technologies OÜ. Other authors have no conflict of interest to declare.

Additional information

Supplementary Information The online version contains supplementary material available at https://doi.org/10.1038/s41598-025-01844-z.

Correspondence and requests for materials should be addressed to J.P.

Curriculum vitae

Personal data

Name:	Joosep Paats
Date of birth:	26.05.1994
Place of birth:	Pärnu, Estonia
Citizenship:	Estonian

Contact data

E-mail:	joosep.paats@taltech.ee

Education

2020–…	Tallinn University of Technology, PhD program Physical Sciences, speciality Biomedical Engineering and Medical Physics, PhD studies
2018–2020	Tallinn University of Technology/University of Tartu, Biomedical Engineering and Medical Physics, MSc
2013–2016	University of Tartu, Gene Technology, BSc
2010–2013	Pärnu Sütevaka Humanitaargümnaasium, Secondary education

Language competence

Estonian	Native
English	Proficient
Russian	Beginner
French	Beginner

Professional employment

2021–2025	Tallinn University of Technology, junior researcher
2018–2021	Tallinn University of Technology, laboratory specialist

Elulookirjeldus

Isikuandmed

Nimi:	Joosep Paats
Sünniaeg:	26.05.1994
Sünnikoht:	Pärnu, Eesti
Kodakondsus:	Eesti

Kontaktandmed

E-post:	joosep.paats@taltech.ee

Hariduskäik

2020–…	Tallinna Tehnikaülikool, doktoriõppe kava Füüsikalised loodusteadused, peaeriala Biomeditsiinitehnoloogia, doktoriõpe
2018–2020	Tallinna Tehnikaülikool/Tartu Ülikool, Biomeditsiinitehnika ja meditsiinifüüsika, MSc
2013–2016	Tartu Ülikool, Geenitehnoloogia, BSc
2010–2013	Pärnu Sütevaka Humanitaargümnaasium, keskharidus

Keelteoskus

Eesti keel	Emakeel
Inglise keel	Kõrgtase
Vene keel	Algtase
Prantsuse keel	Algtase

Teenistuskäik

2021–2025	Tallinna Tehnikaülikool, nooremteadur
2018–2021	Tallinna Tehnikaülikool, labori spetsialist

ISSN 2585-6901 (PDF)
ISBN 978-9916-80-329-5 (PDF)